

## INFORMATION TO USERS

This manuscript has been reproduced from the microfilm master. UMI films the text directly from the original or copy submitted. Thus, some thesis and dissertation copies are in typewriter face, while others may be from any type of computer printer.

**The quality of this reproduction is dependent upon the quality of the copy submitted.** Broken or indistinct print, colored or poor quality illustrations and photographs, print bleedthrough, substandard margins, and improper alignment can adversely affect reproduction.

In the unlikely event that the author did not send UMI a complete manuscript and there are missing pages, these will be noted. Also, if unauthorized copyright material had to be removed, a note will indicate the deletion.

Oversize materials (e.g., maps, drawings, charts) are reproduced by sectioning the original, beginning at the upper left-hand corner and continuing from left to right in equal sections with small overlaps. Each original is also photographed in one exposure and is included in reduced form at the back of the book.

Photographs included in the original manuscript have been reproduced xerographically in this copy. Higher quality 6" x 9" black and white photographic prints are available for any photographs or illustrations appearing in this copy for an additional charge. Contact UMI directly to order.

# UMI

A Bell & Howell Information Company  
300 North Zeeb Road, Ann Arbor MI 48106-1346 USA  
313/761-4700 800/521-0600



**Permanganate Oxidations of Aromatic Hydrocarbons  
in Aqueous and Organic Solution**

by

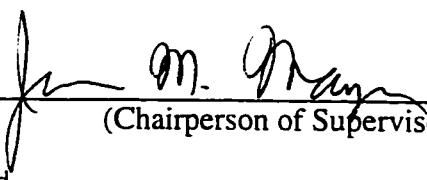
Kimberly A. Gardner

A Dissertation submitted in partial fulfillment  
of the requirements for the degree of

Doctor of Philosophy

University of Washington

1996

Approved by   
(Chairperson of Supervisory Committee)

Program Authorized  
to Offer Degree Department of Chemistry

Date June 19, 1996

**UMI Number: 9704494**

---

**UMI Microform 9704494**  
**Copyright 1996, by UMI Company. All rights reserved.**

**This microform edition is protected against unauthorized  
copying under Title 17, United States Code.**

---

**UMI**  
**300 North Zeeb Road**  
**Ann Arbor, MI 48103**

Doctoral Dissertation

In presenting this dissertation in partial fulfillment of the requirements for the Doctoral degree at the University of Washington, I agree that the Library shall make its copies freely available for inspection. I further agree that extensive copying of this dissertation is allowable only for scholarly purposes, consistent with "fair use" as prescribed in the U.S. Copyright Law. Requests for copying or reproduction of this dissertation may be referred to University Microfilms, 1490 Eisenhower Place, P.O. Box 975, Ann Arbor, MI 48106, to whom the author has granted "the right to reproduce and sell (a) copies of the manuscript in microform and/or (b) printed copies of the manuscript made from microform."

Signature Kimberly A. Spidner

Date June 19, 1996

University of Washington

Abstract

**Permanganate Oxidations of Aromatic Hydrocarbons  
in Aqueous and Organic Solution**

by Kimberly A. Gardner

Chairperson of the Supervisory Committee: Professor James M. Mayer  
Department of Chemistry

The oxidations of a select group of arylalkanes by permanganate have been studied in aqueous solution and in toluene. In water at pH 7, the reactions of toluene, ethylbenzene, and cumene with  $\text{KMnO}_4$  were studied. In toluene,  ${}^n\text{Bu}_4\text{NMnO}_4$  was used as the oxidant in the reactions of toluene, ethylbenzene, cumene, diphenylmethane, triphenylmethane, fluorene, 9,10-dihydroanthracene, and xanthene. The kinetics, which were monitored by UV/vis spectroscopy, show that the reactions, regardless of solvent, are first order with respect to both permanganate and substrate concentration, with no apparent induction periods. Despite these similarities, the reactions proceed by different mechanistic pathways, depending on the solvent.

The oxidation of neat toluene by  ${}^n\text{Bu}_4\text{NMnO}_4$  exhibits a significant isotope effect and the presence of  $\text{O}_2$  accelerates the disappearance of permanganate. Substitution at the *para* position of toluene has little effect on the rate of reaction. The products of toluene oxidation are benzoic acid with a trace of benzaldehyde. Permanganate is converted in all cases to colloidal  $\text{MnO}_2$  which was confirmed by an iodometric determination of the

oxidation state. In the reactions of dihydroanthracene and fluorene, the  $\text{MnO}_2$  is consumed in a subsequent reaction that appears to form a charge transfer complex. All of the data are consistent with rate limiting hydrogen atom transfer from the substrate to an oxo group of permanganate. The enthalpies of activation for the various substrates are shown to be directly proportional to the  $\Delta H^\circ$  of the hydrogen atom transfer step, over a range of 14 kcal/mol in C-H bond strength. This type of correlation is typical of organic radical reactions. Permanganate's ability to react by hydrogen atom transfer is rationalized on the basis of its ability to form a strong bond to  $\text{H}\cdot$ .

In neutral aqueous solution, toluene is oxidized by permanganate over three orders of magnitude faster than in neat toluene. The reaction rate shows no dependence on pH (over the range 6 to 11), buffer type, or the presence of  $\text{O}_2$ . Substitution in the *para* position has only a slight effect on the rate constant. Above pH 11, the reaction accelerates dramatically. There is a large primary isotope effect. As in the neat toluene reaction, the products are predominantly benzoic acid and colloidal  $\text{MnO}_2$ . Based on this evidence, a mechanism involving hydride transfer from the benzylic C-H to an oxo group of permanganate with stabilization of the incipient carbocation by the nucleophilic solvent is proposed. Studies of ethylbenzene and cumene under the same conditions, however, yield results which are difficult to rationalize with this mechanism. Specifically, these reactions show a dependence of the rate of permanganate disappearance on the presence of  $\text{O}_2$ . This has raised doubts about the generality, of the proposed mechanism. Possible explanations for the observations are discussed.

## Table of Contents

GENERAL INTRODUCTION.....	1
CHAPTER 1 .....	6
Introduction .....	7
Experimental .....	8
General.....	8
Materials .....	8
Kinetics .....	10
Data Analysis.....	12
Product Analyses .....	12
Manganese Oxidation State Determination.....	12
Organic Product Analyses .....	14
Experiments in the Presence of O <sub>2</sub> .....	16
Results.....	17
I. Oxidation of Toluene.....	17
II. Ethylbenzene, Cumene, Diphenylmethane, Triphenylmethane, 9,10-Dihydroanthracene, Xanthene, and Fluorene.....	24
III. Charge-Transfer Complexes.....	36
Discussion.....	40
I. Overview of the Reaction.....	40
II. Charge Transfer Complexes.....	40
III. The Rate Determining Step .....	43
IV. Understanding the Rate Constants: Bond Strengths and Linear Free Energy Correlations .....	48
Conclusions .....	57
CHAPTER 2.....	59
Introduction .....	60
Experimental .....	62
General.....	62

Materials .....	62
Kinetics .....	63
Data Analysis.....	63
Manganese Oxidation State Determinations .....	64
Organic Product Analyses .....	64
Experiments in the Presence of O <sub>2</sub> .....	66
Experiments with <sup>18</sup> O Labelling .....	67
Results .....	68
Discussion.....	82
Comparison with Reactions in Organic Solvent .....	82
The Rate Determining Step .....	84
Conclusions .....	92
REFERENCES .....	94
Appendix A: Analysis of Kinetic Data for Permanganate Reactions Monitored Spectroscopically .....	107
Appendix B: Spectroscopic Cell for Studying Aqueous Solutions of Hydrocarbons.....	116
Appendix C: Miscellaneous Related Reactions.....	121
Experimental .....	121
Results and Discussion .....	122
I. Reactions of Fluorene and Cumene with <sup>n</sup> Bu <sub>4</sub> NMnO <sub>4</sub> in Toluene .....	122
II. Reactions in Other Organic Solvents.....	124
Acetonitrile .....	124
Pyridine.....	128
III. Reactions of Possible Intermediates .....	128

## List of Figures

- Figure 1.** Overlay of UV/vis spectra from the reaction of  ${}^n\text{Bu}_4\text{NMnO}_4$  with toluene at 25 °C..... 13
- Figure 2.** A plot of  $\ln [\text{MnO}_4^-]$  vs. time for the reaction of toluene with  ${}^n\text{Bu}_4\text{NMnO}_4$  in toluene at 45 °C..... 15
- Figure 3.** An Eyring plot,  $\log (k_2/T)$  vs.  $1/T$ , for the reaction of  ${}^n\text{Bu}_4\text{NMnO}_4$  with toluene in toluene over the temperature range 25 to 65 °C..... 21
- Figure 4.** An Eyring plot,  $\log (k_2/T)$  vs.  $1/T$ , for the reaction of  ${}^n\text{Bu}_4\text{NMnO}_4$  with ethylbenzene in toluene over the temperature range 22 to 65 °C..... 30
- Figure 5.** An Eyring plot,  $\log (k_2/T)$  vs.  $1/T$ , for the reaction of  ${}^n\text{Bu}_4\text{NMnO}_4$  with diphenylmethane in toluene over the temperature range 22 to 65 °C..... 31
- Figure 6.** An Eyring plot,  $\log (k_2/T)$  vs.  $1/T$ , for the reaction of  ${}^n\text{Bu}_4\text{NMnO}_4$  with triphenylmethane in toluene over the temperature range 22 to 65 °C..... 32
- Figure 7.** An Eyring plot,  $\log (k_2/T)$  vs.  $1/T$ , for the reaction of  ${}^n\text{Bu}_4\text{NMnO}_4$  with 9,10-dihydroanthracene in toluene over the temperature range 22 to 65 °C. .... 33
- Figure 8.** An Eyring plot,  $\log (k_2/T)$  vs.  $1/T$ , for the reaction of  ${}^n\text{Bu}_4\text{NMnO}_4$  with xanthene in toluene over the temperature range 22 to 65 °C..... 34
- Figure 9.** Overlay of UV/vis spectra from the reaction of  ${}^n\text{Bu}_4\text{NMnO}_4$  with 9,10-dihydroanthracene in toluene at 25 °C. Inset plot of absorbance at 546 nm vs. time for the same reaction..... 37

<b>Figure 10.</b>	UV/vis spectrum of the solution at the end of the reaction of ${}^n\text{Bu}_4\text{NMnO}_4$ with 9,10-dihydroanthracene in toluene at 25 °C.....	38
<b>Figure 11.</b>	Plot of $\Delta H^\ddagger$ vs. $\Delta H^\circ$ for the hydrogen atom transfer step in reactions of ${}^n\text{Bu}_4\text{NMnO}_4$ with toluene, ethylbenzene, diphenylmethane, triphenylmethane, 9,10-dihydroanthracene, and xanthene.. ..	53
<b>Figure 12.</b>	Rate of hydrogen atom abstraction from toluene by $\text{HO}^\bullet$ , ${}^t\text{BuO}^\bullet$ , ${}^t\text{BuOO}^\bullet$ , and $\text{MnO}_4^-$ at 25-30 °C in toluene solvent vs. the strength of the O-H bond formed. ....	54
<b>Figure 13.</b>	Rate of hydrogen atom abstraction from ethylbenzene by $\text{HO}^\bullet$ , ${}^t\text{BuO}^\bullet$ , ${}^t\text{BuOO}^\bullet$ , and $\text{MnO}_4^-$ at 25-30 °C in toluene solvent vs. the strength of the O-H bond formed.....	55
<b>Figure 14.</b>	Rate of hydrogen atom abstraction from diphenylmethane by $\text{HO}^\bullet$ , ${}^t\text{BuO}^\bullet$ , ${}^t\text{BuOO}^\bullet$ , and $\text{MnO}_4^-$ at 25-30 °C in toluene solvent vs. the strength of the O-H bond formed.....	56
<b>Figure 15.</b>	Overlay of UV/vis spectra from the reaction of toluene with $\text{KMnO}_4$ in aqueous solution, pH 7, at 75 °C.....	65
<b>Figure 16.</b>	A plot of $\ln [\text{MnO}_4^-]$ vs. time for the reaction of toluene with $\text{KMnO}_4$ in aqueous solution, pH 7, at 75 °C.....	73
<b>Figure 17.</b>	An Eyring plot, $\log (k_2/T)$ vs. $1/T$ , for the reaction of toluene with $\text{KMnO}_4$ in aqueous solution, pH 7, over the temperature range 20 to 95 °C. ....	74
<b>Figure 18.</b>	An Eyring plot, $\log (k_2/T)$ vs. $1/T$ , for the reaction of ethylbenzene with $\text{KMnO}_4$ in aqueous solution, pH 7, over the temperature range 45 to 85 °C. ....	75

<b>Figure 19.</b>	A plot of $k_2$ vs. pH for the reaction of toluene with $\text{KMnO}_4$ in aqueous solution over the pH range 6 to 14.3. ....	77
<b>Figure 20.</b>	A plot of $\log k_2$ vs. $\sigma^+$ for a Hammett study of <i>para</i> -substituted toluenes reacting with $\text{KMnO}_4$ in aqueous solution, pH 7, at 75 °C.....	78
<b>Figure 21.</b>	UV/vis spectrum of the solution for the reaction of $\text{KMnO}_4$ and toluene in water after 2 half-lives. The small dots are the full UV/vis spectrum, the large squares are the segments used to model the $\text{MnO}_2$ , and the dashed line is the third order polynomial fit.....	109
<b>Figure 22.</b>	A plot of $\ln [\text{MnO}_4^-]$ vs. time for the reaction of triphenylmethane with ${}^n\text{Bu}_4\text{NMnO}_4$ in toluene at 55 °C. The curves arise from modelling the $\text{MnO}_2$ scattering/absorbance at 1200s (crosses), 1800s (filled circles), and 2100s (open circles).....	111
<b>Figure 23.</b>	A plot of $\ln [\text{MnO}_4^-]$ vs. time for the reaction of diphenylmethane with ${}^n\text{Bu}_4\text{NMnO}_4$ in toluene at 35 °C.....	113
<b>Figure 24.</b>	A plot of vapor pressure vs. mole fraction for an ideal solution of two volatile liquids. The solid line is the total vapor pressure, the dotted line is the vapor pressure of component A, and the dashed line is the vapor pressure of component B.....	117
<b>Figure 25.</b>	Cross-section of cuvette. ....	119

## List of Schemes

- Scheme 1.** Calculation of the O-H bond strength in  $\text{O}_3\text{MnO-H}^\cdot$  through a thermodynamic cycle involving addition of  $\text{H}^\cdot$  to  $\text{MnO}_4^-$ .....49
- Scheme 2.** Calculation of the enthalpy for transfer of  $\text{H}^\cdot$  from phenol through a thermodynamic cycle.....50
- Scheme 3.** [2+2] Addition of a C-H bond to a M=O bond with subsequent homolytic or heterolytic cleavage of the M-C bond.....90
- Scheme 4.** Proposed mechanistic pathway for the reaction of toluene with  $\text{MnO}_4^-$ , proceeding through the intermediates benzyl alcohol and benzaldehyde.....130

## List of Tables

<b>Table 1.</b>	Rate Constants for Reactions of Toluene and Substituted Toluenes with ${}^n\text{Bu}_4\text{NMnO}_4$ in Organic Solution.....	19
<b>Table 2.</b>	Rate Constants for Reactions of Ethylbenzene, Diphenylmethane, Triphenylmethane, 9,10-Dihydroanthracene, and Xanthene with ${}^n\text{Bu}_4\text{NMnO}_4$ in Organic Solution.....	26
<b>Table 3.</b>	Comparison of Rates, Activation Parameters, and C-H Bond Strengths for the Rate Determining Step of Reactions of ${}^n\text{Bu}_4\text{NMnO}_4$ with Various Hydrocarbons in Toluene. ....	29
<b>Table 4.</b>	Comparison of Charge Transfer Complexes of " $\text{MO}_x$ " Species with Arenes.....	42
<b>Table 5.</b>	Rate Constants for Reactions of Toluene, Ethylbenzene, and Related Substrates with $\text{KMnO}_4$ in Aqueous Solution.....	69
<b>Table 6.</b>	Comparison of Arylalkane Reactivity with $\text{MnO}_4^-$ in Water and Toluene. <sup>a</sup> .....	85
<b>Table 7.</b>	Rate Constants for the Reaction of Cumene with ${}^n\text{Bu}_4\text{NMnO}_4$ in Toluene. ....	123
<b>Table 8.</b>	Rate Constants for the Reaction of Fluorene with ${}^n\text{Bu}_4\text{NMnO}_4$ in Toluene. ....	125
<b>Table 9.</b>	Rate Constants for the Reaction of 9,10-Dihydroanthracene with $\text{KMnO}_4$ in Acetonitrile.....	127

<b>Table 10.</b>	<b>Rate Constants for Reactions with <math>\text{MnO}_4^-</math> of Species Related to</b>	
	<b>Substrates Studied.....</b>	<b>132</b>

## Acknowledgements

Very rarely is a project of any size completed by a person without help from others. The work which has gone into this dissertation is no exception and as such, I owe a huge debt of gratitude to a number of people. Foremost is my advisor, Professor James Mayer, who, for four years, has patiently taught me the art and science of chemistry. I will always be grateful for the privilege to learn from him. Technical advice and support were provided by Bob Morley and James Roe. During my time at the University of Washington, I was fortunate to work with a very supportive research group. I wish to thank Darin Du Mez, Tom Crevier, Brenda Woodward, and Drs. Seth Brown, Kun Wang, Steve McNeil, and Jerry Cook, who were always available to offer support and constructive criticism. In addition, I owe a special thanks to Linda Kuehnert, who gave me the chance to share my chemistry by allowing me to try to teach it to her. Some of her work is presented in this dissertation. This project relied on the gracious loan of equipment from a number of other research groups within the University of Washington chemistry department. Specifically, I wish to thank the Borden group for the use of their GC, the Sasaki group for the use of the HPLC and for helpful discussions about the inner workings of these instruments, and the Gouterman group for the unlimited use of their HPLC. Conversations about charge transfer complexes with Professor Jeanne McHale of the University of Idaho were invaluable and much appreciated.

Above all, I would like to thank my family who have supported me in all aspects of my life. My parents, James and Sandra Lott, encouraged me and nurtured in me a life long love of learning. Finally, I wish to acknowledge my husband, Jeff Gardner, whose love and support has helped me to reach this goal.

## **GENERAL INTRODUCTION**

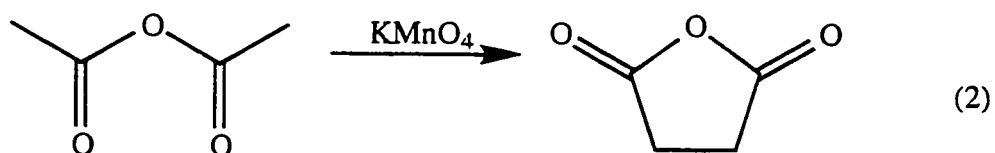
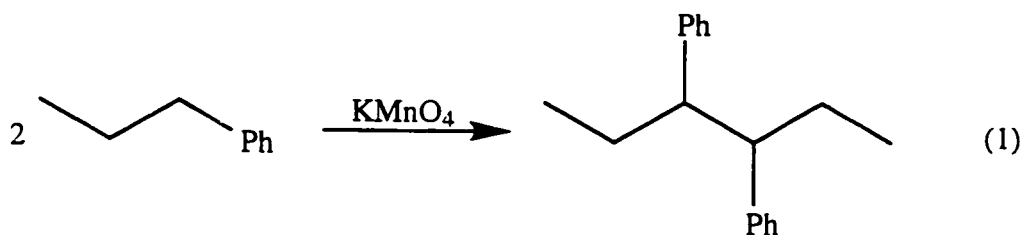
The selective oxidation of hydrocarbons is a fundamental transformation in chemistry, important in a wide range of areas from biological to industrial chemistry.<sup>1</sup> A recurrent theme in all of these fields is the use of metal-oxo species, both catalytically and stoichiometrically, as the active oxidants. Commercially, for example, a vanadium phosphorus oxide is used as a heterogeneous catalyst for the conversion of butane to maleic anhydride.<sup>2</sup> One of the most intensively studied metalloenzyme families, cytochrome P-450, utilizes a ferryl (FeO) group to selectively oxidize hydrocarbons to alcohols under mild conditions.<sup>3</sup> The classic examples of stoichiometric hydrocarbon oxidation by metal-oxo species come from the organic chemistry literature where permanganate, chromium(VI) reagents, and ruthenium tetroxide have been used, in some cases for over a century, to perform various oxidative transformations.<sup>1,4</sup> While these oxidants likely share some common features that enable them to attack C-H bonds, the proliferation of literature in all of these fields has made a comprehensive understanding of the chemistry a daunting task. Additionally, many of the systems which are most effective at selective hydrocarbon oxidation are also the most complex, involving either intricate biological systems, co-catalysts, or surface species on solid supports.

One approach to addressing the general reactivity of metal-oxo species with C-H bonds is to begin with the more simple and well-defined classic oxidants. By re-examining the reactivity of such oxidants as permanganate, we hope to gain a deeper understanding of oxidations of hydrocarbons by metal-oxo species in general. Earlier work studied reactions of hydrocarbons with chromyl chloride.<sup>5</sup> The focus of this dissertation is on reactions of permanganate with alkyl-aromatic hydrocarbons containing weak C-H bonds, from toluene to xanthene.<sup>6</sup>

Permanganate has been widely used as a strong, easily handled, readily available, and versatile oxidant, reacting with alcohols, alkenes, aldehydes, and saturated C-H bonds.<sup>7</sup> The lack of selectivity of permanganate is due, at least in part, to its ability to

react readily by either one-electron or two-electron pathways, and its conversion to potentially even stronger oxidants such as  $\text{Mn}^{3+}$ <sup>7</sup> and  $\text{MnO}_3^+$ .<sup>8</sup> The lowest energy reaction pathway can be determined by conditions such as solvent, pH, organic substrate, and other variables. While this flexibility has made permanganate a popular choice as an oxidant, it has also made a comprehensive understanding of its reactivity quite difficult.

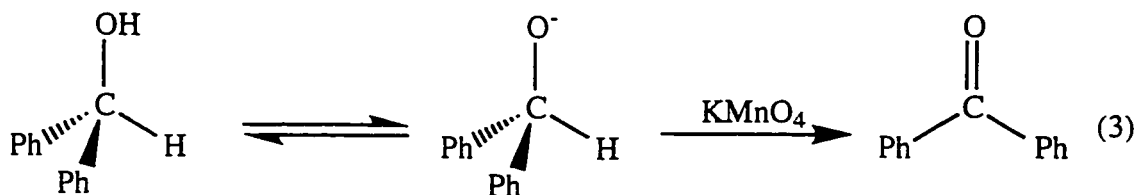
Most of the mechanistic studies of C-H bond oxidation by permanganate date from the 1950s and 1960s, as summarized in several reviews of the period.<sup>7a-d</sup> Organic radical intermediates feature prominently in many of the mechanistic proposals. For instance, the formation of 3,4-diphenylhexane from *n*-propylbenzene (eq 1) and formation of succinic anhydride from acetic anhydride (eq 2) have been cited as examples of reactions where radicals are very likely involved based on the products formed.<sup>7d</sup>



Radical mechanisms have also been invoked to explain the partial retention of stereochemistry observed in the oxidation of tertiary C-H bonds.<sup>9</sup> Studies of the permanganate oxidation of  $\gamma$ -valeric acids in aqueous basic solution by Brauman and Pandell<sup>9a</sup> and of 4-methylhexanoic acid and *p*-*sec*-butylbenzoic acid in neutral or basic solution by Wiberg and Fox<sup>9b</sup> demonstrated a 35-40% retention of stereochemistry at the

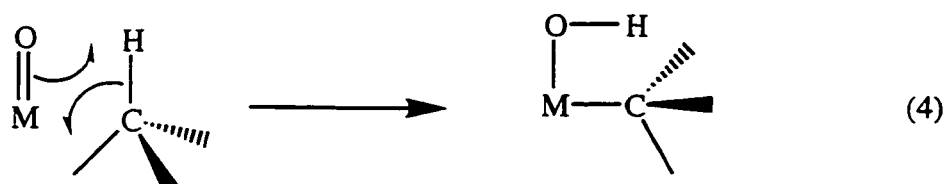
chiral carbon. In both cases, the researchers proposed mechanisms involving abstraction of a hydrogen atom followed by either collapse of the radical pair, leading to retention of configuration, or cage escape, leading to some racemization. However, in all of these examples, it is unclear how the organic radicals are formed. To quote from a 1958 review:<sup>7a</sup> "Ions derived from every valence state of manganese from VII to III, as well as the hydroxyl radical and other oxygenated species (e.g.,  $O^-$  and  $HO_2$ ) have been proposed as the active entities responsible for oxidation by permanganate." For instance, one study of toluene oxidation in aqueous acetic acid proposed that radicals were produced by  $Mn^{3+}$ , since addition of  $F^-$ , which strongly complexes  $Mn^{3+}$ , caused a severe inhibition of the reaction rate.<sup>10</sup> Curiously, these same researchers found that the oxidation of ethylbenzene under the same conditions was not inhibited by the addition of  $F^-$ !<sup>10c</sup>

While radical pathways have frequently been proposed for permanganate oxidations of C-H bonds, non-radical pathways have also been postulated. The oxidation of benzhydrol in neutral or basic aqueous solution, for example, proceeds by equilibrium deprotonation followed by hydride loss to permanganate to form benzophenone (eq 3).<sup>11</sup> The pre-equilibrium step is supported by a demonstrated dependence of the rate of reaction on the hydroxide ion concentration. The rate determining step, however, clearly involves C-H bond cleavage, probably with a linear transition state, as the reaction shows a significant primary isotope effect, 6.6.



Most recently, Lee has offered a sweeping proposal that all oxidations of C-H and O-H bonds by high valent metal-oxo species proceed by [2+2] addition of the C-H or O-H

Most recently, Lee has offered a sweeping proposal that all oxidations of C-H and O-H bonds by high valent metal-oxo species proceed by [2+2] addition of the C-H or O-H bond across the M=O  $\pi$  bond (eq 4, illustrated with a C-H bond)<sup>12</sup> and suggesting ". . .that none of the high-valent transition metal oxide oxidations involve either hydrogen atom or hydride transfer."<sup>12a</sup>



While this mechanism was first postulated on the basis of theoretical studies of  $\text{CrO}_2\text{Cl}_2$  oxidations,<sup>13</sup> there are now studies which have been published on permanganate,<sup>12b</sup> manganate,<sup>12a</sup> ruthenate,<sup>12c</sup> perruthenate,<sup>12c</sup> and ferrate<sup>12d</sup> oxidations of alcohols and hydrocarbons which Lee uses to substantiate his broad mechanistic proposal.

As this brief overview demonstrates, there is not a consensus in the literature on how permanganate is able to oxidize hydrocarbons. Presented here are studies of permanganate oxidations of alkyl-aromatic hydrocarbons with the goal of gaining a general understanding of this class of reactions. Chapter 1 examines the reactions of a wide range of hydrocarbon substrates reacting with permanganate in toluene through the use of the tetrabutylammonium salt of permanganate. More traditional permanganate reactions are examined in Chapter 2, devoted to hydrocarbon oxidations in aqueous solution. Permanganate has been used as a strong oxidant in organic chemistry for over a century, usually with little consideration to the complexity of its reactivity. This dissertation is further evidence that generalizations about the reactivity of permanganate are difficult, if not impossible, to make.

## CHAPTER 1<sup>14</sup>

## Introduction

Although permanganate has been used as an oxidant in organic chemistry for hydrocarbons, alcohols, ketones, and alkenes for over a century, such reactions have a fundamental problem. The common form of permanganate, its potassium salt, while cheap and readily available, is not soluble in most organic solvents. The organic solvents in which  $\text{KMnO}_4$  does dissolve--acetone, ethanol, pyridine, to name a few--are frequently as reactive as the target substrate, if not more so. The preferred solvent for  $\text{KMnO}_4$ --water--is not useful for most of the organic substrates of interest. The synthetic organic chemist has generally dealt with this problem by using two-phase systems, mixed solvent systems, or accepting a lower yield (based on permanganate) due to reaction with the solvent. While this circumvents the problem in terms of synthesis, such systems are not conducive to a mechanistic study. A more recent approach to permanganate oxidations of organic species has been to solubilize the permanganate by exchanging the counterion to a more organophilic cation,<sup>15</sup> such as  $\text{PPN}^+$  ( $\text{PPN}^+ = [(\text{Ph}_3\text{P})_2\text{N}]^+ =$  bis(triphenylphosphine)iminium)<sup>16</sup> or  ${}^n\text{Bu}_4\text{N}^+$  ( ${}^n\text{Bu} = \text{CH}_3\text{CH}_2\text{CH}_2\text{CH}_2 = n\text{-butyl}$ ),<sup>17</sup> or by encapsulating the counterion in a crown ether or similar cryptand.<sup>18</sup> Collectively, these forms of permanganate have become commonly known as "purple benzene".<sup>19</sup>

Permanganate oxidations in organic media are very appealing from a mechanistic standpoint as the system is greatly simplified. The substrate and the solvent can be the same if a permanganate salt can be found which is soluble in the desired organic compound. Oxidations in organic solvent also avoid some of the problems that are known to plague aqueous permanganate reactions, such as autocatalysis at high<sup>20</sup> and low pH<sup>10a</sup> and involvement of water in the reactions.<sup>21</sup> Mechanistic studies have been done on permanganate oxidations in organic media for more reactive substrates such as alkenes.<sup>22</sup> Hydrocarbons are more challenging as they tend to be less reactive with permanganate than other organic species. While there have been reports of alkane and arylalkane

oxidation by organic soluble permanganate salts,<sup>16,23,24</sup> only one of the studies has attempted to examine the mechanism by which these oxidations occur.<sup>24</sup> Presented here are the first broad mechanistic studies of permanganate oxidations of alkyl-aromatic hydrocarbons in organic solvents.

A variety of arylalkanes were selected to be studied, ranging in reactivity from toluene to xanthene and involving primary, secondary, and tertiary reactive sites. The permanganate salt used in this study, tetrabutylammonium permanganate,  ${}^n\text{Bu}_4\text{NMnO}_4$ , was chosen because of its solubility in toluene.<sup>15</sup> Toluene, as the least reactive substrate studied, was then used as the solvent for the other reactions. The results presented here suggest that permanganate reacts with these hydrocarbons directly, through a rate determining step common to all of the substrates, in which a hydrogen atom is transferred to permanganate, resulting in the formation of an organic radical. The reactivity is shown to be directly related to the strength of the bonds broken and formed in this rate determining step.

## Experimental

**General.** All reactions were done in the absence of air unless otherwise noted. Reactions were typically set up in a drybox dedicated to this oxidation project. It was found necessary to exclude all reductants other than alkanes and arylalkanes from this drybox.

**Materials.**  ${}^n\text{Bu}_4\text{NMnO}_4$  ( ${}^n\text{Bu} = n\text{-butyl}$ ,  $\text{CH}_3\text{CH}_2\text{CH}_2\text{CH}_2$ ) was prepared by a literature procedure.<sup>15</sup> Concentrated aqueous solutions of  ${}^n\text{Bu}_4\text{NBr}$  and  $\text{KMnO}_4$  were combined. The resulting precipitate was isolated on a frit, rinsed with water, and recrystallized from  $\text{CH}_2\text{Cl}_2$ /diethyl ether. The crystalline solid decomposes at room temperature over several days, so it was stored in a sealed container in the freezer. Each time the  ${}^n\text{Bu}_4\text{NMnO}_4$  was used, the container and its contents were warmed to room

temperature before unsealing the container to avoid condensing water onto the solid.

*CAUTION:  $n\text{Bu}_4\text{NMnO}_4$  is reported<sup>15</sup> to be prone to violent spontaneous decomposition. Care should be taken in handling the dry solid.*

Materials were purchased in the highest possible purity, purified immediately before use and/or were stored in the drybox. Solvents were purified by standard methods<sup>25</sup> except *d*<sub>8</sub>-toluene (100.0% by GCMS, Cambridge Isotope Laboratories) which was simply dried over sodium and vacuum transferred when needed. Toluene (100.0%, Baker), ethylbenzene (99.8%, Aldrich), and cumene (99%, Aldrich) were washed with ice-cold concentrated sulfuric acid, followed by water. They were washed with base (PhMe, 5% NaHCO<sub>3</sub> solution; PhCH<sub>2</sub>Me and PhCHMe<sub>2</sub>, 10% NaHCO<sub>3</sub> solution) and rinsed with water until the washings were neutral. Toluene was dried with CaSO<sub>4</sub> followed by sodium and was vacuum transferred just prior to use. Ethylbenzene was dried first with MgSO<sub>4</sub> and then sodium; it was vacuum transferred prior to use and found to be 100.0% by GC. Cumene was dried over Na<sub>2</sub>SO<sub>4</sub> and then Na or CaH<sub>2</sub> before being distilled under N<sub>2</sub>. The first fraction that distilled over was discarded and the second fraction was collected. Its purity by GC was found to be 99.96%. Cumene was degassed by freeze/pump/thaw cycles and stored in the glovebox (in an amber bottle, protected from light).

*ortho*-Dichlorobenzene was purified by shaking it with concentrated H<sub>2</sub>SO<sub>4</sub> until clear and washing with an equal portion water. After preliminary drying over CaCl<sub>2</sub>, it was refluxed over CaH<sub>2</sub> for three days and distilled from CaH<sub>2</sub>. In a fumehood, excluding all light except a red safelight, the solvent was run down a column of activated alumina, degassed, and stored into the drybox. The purity by GC was 99.9%. Immediately before each use, the solvent was further purified by running it down a 1 cm × 10 cm alumina column in the drybox. The alumina was activated by heating under vacuum at 190 °C for 7 hours and was stored in the glovebox.

*p*-Xylene (99.7%, Aldrich) was dried over sodium and vacuum transferred when needed. 4-Methylbenzophenone (99.8%, Aldrich) was used as received. *p*-Chlorotoluene (Aldrich) was refluxed over CaH<sub>2</sub> and distilled, collecting only the middle fraction (GC purity: 99.6%). Xanthene was used as received (99.4%, Aldrich). Fluorene (99%, Fluka) was used as received because purification techniques tended to concentrate the impurities. Others have reported similar purification difficulties with fluorene.<sup>26</sup> All other substrates were purified prior to use and their purity checked by GC. 9,10-Dihydroanthracene (99.97%, Aldrich) was purified by four consecutive recrystallizations from ethanol. Diphenylmethane (100.0%, Aldrich) was purified by sublimation. The purified material was a solid at room temperature.<sup>27</sup> Triphenylmethane (99.95%, Aldrich) was recrystallized from hot ethanol. *d*<sub>12</sub>-Dihydroanthracene was prepared by Tom Crevier by reduction of *d*<sub>10</sub>-anthracene by sodium in a solution of *d*<sub>1</sub>-ethanol. The isotopic purity was >98% as analyzed by GC and <sup>1</sup>H NMR.<sup>28</sup>

**Kinetics** All kinetics experiments were followed by optical spectroscopy, using a Hewlett Packard 8452A diode array spectrophotometer scanning over the range 400 to 640 nm. The temperature of the solution in the cuvette was held constant ( $\pm 0.1$  °C) using either a custom built aluminum block cell holder connected to a Peltier electronic control module or a Hewlett Packard water jacketed cell holder connected to a circulating water bath (Lauda model K-2/R).

<sup>n</sup>Bu<sub>4</sub>NMnO<sub>4</sub> is sparingly soluble in neat toluene, so a saturated or near-saturated solution is needed in order to follow the reaction kinetics. Solutions for kinetics experiments were prepared in the glovebox by adding toluene to an excess of <sup>n</sup>Bu<sub>4</sub>NMnO<sub>4</sub>. After stirring the mixture for several minutes, the undissolved solid was removed by filtration through a medium porosity frit. 2-3 mL of the solution were transferred to a 1 cm quartz cuvette sealed to a Teflon needle valve. Data collection was started immediately after the cuvette was placed in the cell holder. The initial MnO<sub>4</sub><sup>-</sup>

concentration was calculated from the first spectrum using the absorbance at 526 nm and the established<sup>15</sup> molar absorptivity of  $2530 \text{ M}^{-1}\text{cm}^{-1}$ , assuming that the solution was at approximately ambient temperature for this spectrum. For experiments above room temperature, the data collected in the first 5 minutes was discarded for the purposes of rate constant calculation to account for the time required to reach the desired temperature. Reactions of other substrates used a similar procedure, except that a known volume of the  ${}^n\text{Bu}_4\text{NMnO}_4$  solution in toluene was placed in the cuvette and a known quantity of substrate or concentrated solution of substrate was added. For example, reaction solutions for ethylbenzene oxidations were prepared by placing 1 mL of  ${}^n\text{Bu}_4\text{NMnO}_4$  in toluene solution and adding 1 mL of ethylbenzene. The cuvette was then sealed and shaken to insure mixing prior to data collection.

Xanthene reacts so quickly with  $\text{MnO}_4^-$  that an initial rate constant could not be obtained if the reaction solution was prepared in the glovebox and then equilibrated for 5 min in the cuvette holder. To insure that initial rate constants were obtained, experiments used a specially designed cuvette (described in Appendix B) which is sealable and injectable. In a typical procedure, an excess of  ${}^n\text{Bu}_4\text{NMnO}_4$  was added to toluene and stirred for several minutes in the glovebox. The undissolved solid was removed by passing the solution through a medium porosity frit. 2 mL of the solution was placed in the cuvette which was sealed and removed from the glovebox. The solution was equilibrated at  $10.0^\circ\text{C}$  by placing the cuvette in the thermostatted cell holder for 5 min. By syringe,  $15 \mu\text{L}$  of concentrated xanthene solution was added (101.4 mg xanthene in 5 mL of toluene). The cuvette was shaken to mix and data collection was started.

Reactions in *o*-dichlorobenzene solvent were assembled in the glove box. A typical experiment is described for *p*-chlorotoluene; other substrates were similar.  ${}^n\text{Bu}_4\text{NMnO}_4$  (~1.5 mg) was dissolved in 10 mL of freshly purified *o*-dichlorobenzene (see above) and 2.0 mL of this solution plus 1 mL *p*-chlorotoluene were added to a quartz

cuvette on which a needle valve had been fused. The cell was sealed, removed from the drybox, and data collection was started immediately. The initial permanganate concentration was determined from the absorbance at 526 nm in the first spectrum. For experiments above room temperature, the data were truncated to account for equilibration time. The solution changed color during the reaction from a light purple to burnt orange. The decomposition of  ${}^n\text{Bu}_4\text{NMnO}_4$  in *o*-dichlorobenzene in the absence of substrate was also studied in order to correct the observed rate constants for substrate oxidations. This procedure is described in detail in Appendix A. An Eyring plot was used to interpolate to the temperatures used in substrate oxidation.

**Data Analysis.** For all of the reactions, optical spectra in the range 400 to 640 nm show the disappearance of  $\text{MnO}_4^-$  and the appearance of a broad absorbance due to colloidal  $\text{MnO}_2$ . The presence of isosbestic points over the course of the reaction suggest that the colloid is well-behaved spectroscopically (Figure 1, the spectra are at 1, 5, 15, 30, 50, 75, and  $99 \times 10^3$  s). While this is in general true, analysis of the data is not straightforward and involves mathematical manipulations that are not directly relevant to the chemistry at hand. For this reason, the details of the data analysis have been placed in Appendix A.

The first order plots for most of the kinetics experiments are curved downward (*c.f.* Figure 2), so the rate constants reported are initial values only. The data analysis results in four observed rate constants for each kinetics experiment. The rate constants reported in Tables 1 and 2 are an average of the four values for each experiment, with the errors reflecting  $3\sigma$  of this average, given as a percentage of the average rate constant.

**Product Analyses. Manganese Oxidation State Determination.** For  $\text{MnO}_4^-$  reactions in organic solvents, traditional iodometric titrations are unreliable as a means of determining the average manganese oxidation state due to the interference of organic compounds with the starch indicator.<sup>29</sup> Instead, a spectroscopic technique

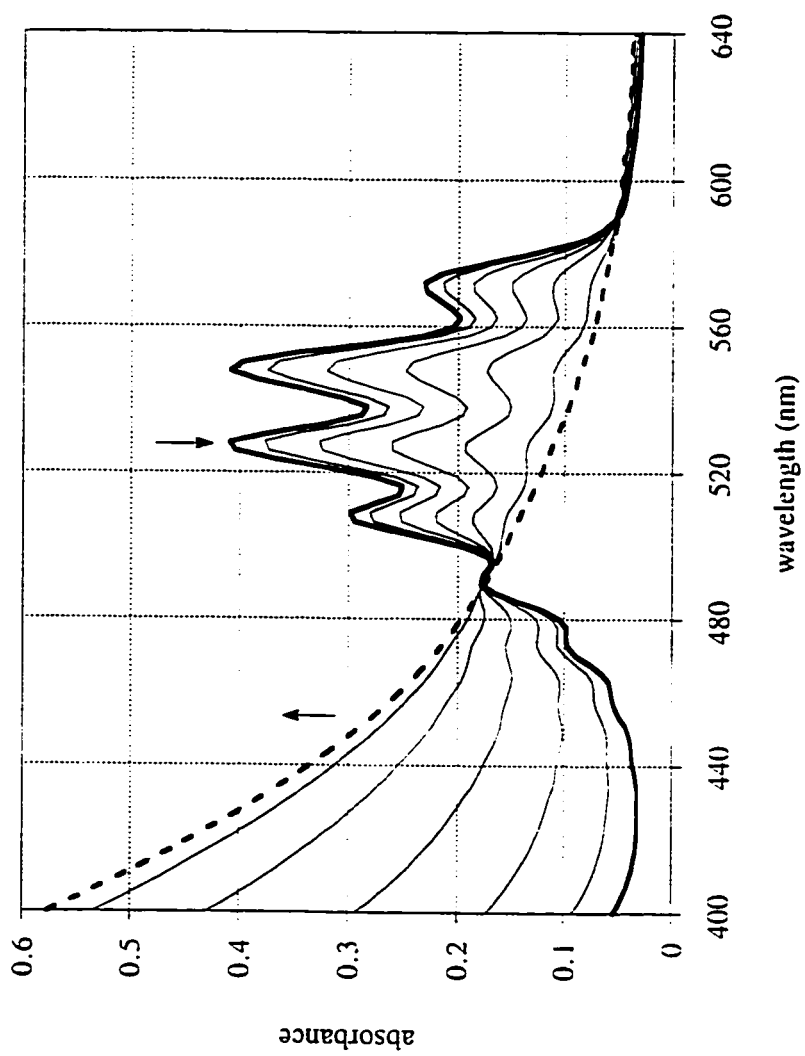


**Figure 1.** Overlay of UV/vis spectra from the reaction of  $n\text{Bu}_4\text{NMnO}_4$  with toluene at 25 °C.

developed by Lee<sup>22f</sup> was adapted. Promptly at the end of a kinetics experiment, a 1 mL aliquot of the reaction solution was placed in a 10 mL volumetric flask with 0.019 g of  $n\text{Pr}_4\text{NI}$  ( $n\text{Pr} = n\text{-propyl, CH}_3\text{CH}_2\text{CH}_2$ ). 1 mL of glacial acetic acid was added and  $\text{CH}_2\text{Cl}_2$  used to bring the total volume to 10.00 ( $\pm 0.02$ ) mL. After thorough mixing, an aliquot of the solution was promptly transferred to a cuvette and the visible spectrum recorded. The molar absorptivity of  $\text{I}_3^-$  at 365 nm is established to be  $26200 \text{ M}^{-1}\text{cm}^{-1}$ .<sup>22f</sup> From the absorbance of the solution at 365 nm (determined by interpolating between the absorbances at 364 and 366 nm), the concentration of  $\text{I}_3^-$  formed, and therefore, the average manganese oxidation state, was calculated.

**Organic Product Analyses.** Organic products in permanganate oxidation reactions are known to be bound in and/or on the colloidal particles of  $\text{MnO}_2$ ,<sup>30</sup> so the  $\text{MnO}_2$  must be destroyed prior to quantitative analysis. Destruction of  $\text{MnO}_2$  particles suspended in organic solvents used an acidic aqueous solution, resulting in a two phase system. If the reaction products might include an organic acid such as benzoic acid, the aqueous layer was made basic to extract the acidic organic products prior to separation of the layers. Products in the aqueous layer were identified and quantified by HPLC, comparing their retention times with authentic samples and comparing their integral versus a calibration curve using potassium hydrogen phthalate (KHP) as an internal standard. HPLC analyses were performed on a Hitachi system consisting of a L-6200 pump connected to a L-4250 UV/vis detector interfaced to a D-2500 integrator.<sup>31</sup> A Beckman Ultrasphere ODS (25 cm/4.6 mm) reverse phase column was employed for the separations. All analyses were performed under isocratic conditions with a solvent consisting of 80% Millipore water, 20% acetonitrile, and 0.1% trifluoroacetic acid. The organic layer was analyzed by GC and the organic products identified by comparison of their retention times with authentic samples. Quantification of the products relied on a one point calibration using an internal standard, typically benzyl alcohol. GC analyses were

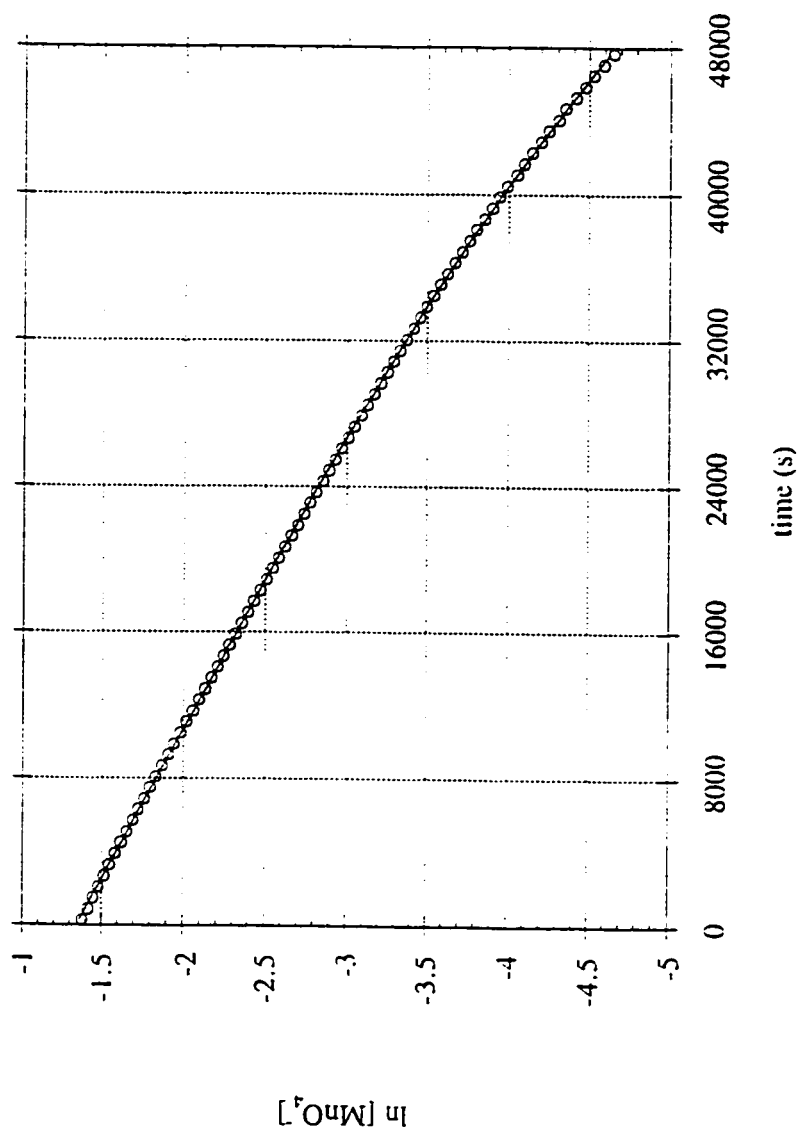


**Figure 2.** A plot of  $\ln [\text{MnO}_4^-]$  vs. time for the reaction of toluene with  $n\text{Bu}_4\text{NMnO}_4$  in toluene at  $45^\circ\text{C}$ .

performed on a Hewlett Packard 5890 Series II gas chromatograph with a 30 m HP-5 fused silica capillary column and an FID detector. The GC was interfaced to a Gateway 2000 486 computer running HP GC ChemStation software to perform data manipulations.

In a typical procedure for toluene, an excess of  $n\text{Bu}_4\text{NMnO}_4$  was added to toluene, stirred for several minutes, and filtered through a medium porosity frit to remove any undissolved solids. A 2 - 3 mL aliquot of the (roughly saturated) solution was set aside. A 20 mL aliquot was transferred to a greaseless Pyrex vessel with a Teflon needle valve, which was sealed and heated in a thermostatted water bath at 57 °C for five hours. The small aliquot was transferred to a cuvette, and a UV/vis spectrum was recorded. The concentration of permanganate was calculated from the absorbance at 526 nm, assuming a molar absorptivity of  $2.53 \times 10^3 \text{ M}^{-1} \text{ cm}^{-1}$ .<sup>32</sup> At the end of the reaction, the vessel was cooled to room temperature and 5 mL of 0.02 M  $\text{NaHSO}_3$  solution was added to reduce the colloidal  $\text{MnO}_2$  to  $\text{Mn}^{2+}$ . The layers were shaken until colorless. Solid  $\text{NaHCO}_3$  was added until the solution pH was approximately 9, to insure that any benzoic acid was converted to benzoate and partitioned into the aqueous layer.<sup>33</sup> The aqueous and organic layers were separated. The organic layer was analyzed by GC. The aqueous layer was prepared for HPLC analysis by combining 1.2 mL of the aqueous layer, 0.2 mL of 0.989 mM KHP solution, and 40  $\mu\text{L}$  of concentrated HCl. A similar procedure was used for ethylbenzene.

For reactions where the products were not expected to be carboxylic acids, the solutions were prepared for product analysis by adding 3-4 drops of concentrated aqueous  $\text{NaHSO}_3$  solution to a reaction mixture from a kinetic experiment to destroy the  $\text{MnO}_2$ . Benzyl alcohol was added as an internal standard and the organic layer was separated. Analysis of the organic layer was by GC; the small aqueous layer was not analyzed.

**Experiments in the Presence of  $\text{O}_2$ .** These experiments were performed by setting up identical reactions side by side, with and without  $\text{O}_2$ . For instance, toluene was

added to an excess of  ${}^n\text{Bu}_4\text{NMnO}_4$  in the glovebox and stirred until the solution was saturated. The solution was filtered and equal amounts were placed into two reaction vessels, which were removed from the box and cooled to  $-78\text{ }^\circ\text{C}$ . The headspace of one vessel was evacuated on the vacuum line and backfilled with  $\text{O}_2$ . The reactions were monitored visually in a room temperature ( $24\text{ }^\circ\text{C}$ ) water bath by the disappearance of the permanganate purple color and appearance of the orange color of the colloid.

## Results

The oxidations of alkyl-aromatic compounds containing weak C-H bonds by  ${}^n\text{Bu}_4\text{NMnO}_4$  have been studied in organic solvents.  ${}^n\text{Bu}_4\text{NMnO}_4$  has a slight but significant solubility in toluene, a saturated solution having a concentration of approximately  $0.3\text{ mM}$ . This is ideal for following the kinetics by optical spectroscopy, monitoring the disappearance of permanganate and the growth of  $\text{MnO}_2$ . However, the solubility of the permanganate is substantially lower in ethylbenzene generally making reactions in this solvent impractical. As a result, oxidations of ethylbenzene, diphenylmethane, triphenylmethane, fluorene, 9,10-dihydroanthracene, and xanthene used toluene as the solvent. The reactions of *para*-substituted toluenes were run in *o*-dichlorobenzene, in which  ${}^n\text{Bu}_4\text{NMnO}_4$  is very soluble. Neither *o*-dichlorobenzene nor toluene is an ideal solvent for these reactions, as both are reactive with permanganate, but under these conditions alternative solvents were either more reactive ( $\text{CH}_2\text{Cl}_2$ ,  $\text{CH}_3\text{CN}$ , pyridine) or showed insufficient solubility (benzene).<sup>35</sup> The reactions were found to be sensitive to trace impurities in solvents and substrates, so much effort was spent purifying materials and establishing a drybox with no extraneous reductants.

**I. Oxidation of Toluene.**  ${}^n\text{Bu}_4\text{NMnO}_4$  decays in toluene solvent over a week at ambient temperatures. The kinetics were monitored by visible spectroscopy (Figure 1), with the structured permanganate absorbance changing to the broad, sloping

absorbance due to  $\text{MnO}_2$  (see below). Under most of the reaction conditions, the colloid is fairly well-behaved optically, obeying Beer's law closely enough to show isosbestic points (as has been observed in related studies<sup>22</sup>). Analysis of the optical data required modeling of the  $\text{MnO}_2$  absorbance, as described in the Experimental section and Appendix A, which generated four values for the rate constant from each data set. The rate constants reported in Table 1 are the average of the four values, and the reported errors are  $3\sigma$  of the distribution of the four values (as a percentage of the average rate constant). The rate constants are reproducible to ca.  $\pm 10\%$  (see Table 1), which is somewhat larger than the error associated with the data analysis from one kinetic experiment.

None of the kinetic runs showed an induction period. The first order plots are all slightly curved downward, corresponding to as much as a doubling of the observed rate constant over the course of the reaction (Figure 2). Initial rates are therefore used. The exact shape of the first-order plots is sensitive to the way the colloidal  $\text{MnO}_2$  spectrum is modelled (see Appendix A), but the initial rates are not significantly affected. At  $45\text{ }^\circ\text{C}$ , the same initial rate constant was obtained from experiments with more than a factor of 2 difference in initial  ${}^n\text{Bu}_4\text{NMnO}_4$  concentration, demonstrating that the reaction is first order with respect to this concentration. The dependence on toluene concentration could not be examined since the reactions were done in neat toluene. It is assumed that this dependence is first order by analogy to toluene oxidation in *o*-dichlorobenzene<sup>37</sup> and the oxidation of other hydrocarbons in toluene (see below). As shown by the data in Table 1, there is good reproducibility of the rate constants. An Eyring plot (Figure 3) was generated from the average rate constant at each temperature studied. The activation parameters, calculated from rate data from  $25\text{ }^\circ\text{C}$  to  $65\text{ }^\circ\text{C}$ , are  $\Delta H^\ddagger = 21.0 (\pm 1.0)$  kcal/mol and  $\Delta S^\ddagger = -16 (\pm 3)$  e.u. Oxidation of *d*<sub>8</sub>-toluene is significantly slower, with  $k_{\text{H}}/k_{\text{D}} = 6 (\pm 1)$  at  $45\text{ }^\circ\text{C}$ . The colloidal  $\text{MnO}_2$  is not well behaved in the *d*<sub>8</sub>-toluene reactions, precluding accurate determination of the rate constant.

**Table 1.** Rate Constants for Reactions of Toluene and Substituted Toluenes with  ${}^n\text{Bu}_4\text{NMnO}_4$  in Organic Solution.

$[\text{MnO}_4^-]$ (mM)	substrate concentration (M)	T (°C)	$k_2$ ( $\text{M}^{-1}\text{s}^{-1}$ )	data analysis error <sup>a</sup>	solvent <sup>b</sup>
<i>Toluene</i>					
0.269	9.37	25.0	$8.26 \times 10^{-7}$	3.8%	toluene
0.336	9.21	40.0	$5.91 \times 10^{-6}$	6.4%	toluene
0.208	9.15	45.0	$1.07 \times 10^{-5}$	4.8%	toluene
0.196	9.15	45.0	$1.27 \times 10^{-5}$	5.5%	toluene
0.216	9.15	45.0	$1.14 \times 10^{-5}$	12%	toluene
0.0890	9.15	45.0	$1.18 \times 10^{-5}$	3.8%	toluene
0.264	9.15 ( <i>d</i> <sub>g</sub> -toluene)	45.0	$1.80 \times 10^{-6}$	4.6%	<i>d</i> <sub>g</sub> -toluene
0.207	9.15 ( <i>d</i> <sub>g</sub> -toluene)	45.0	$2.08 \times 10^{-6}$	1.3%	<i>d</i> <sub>g</sub> -toluene
0.217	9.04	55.0	$2.36 \times 10^{-5}$	22%	toluene
0.213	9.04	55.0	$2.47 \times 10^{-5}$	3.1%	toluene
0.209	9.04	55.0	$2.66 \times 10^{-5}$	1.7%	toluene
0.251	8.93	65.0	$6.36 \times 10^{-5}$	7.7%	toluene
0.214	8.93	65.0	$7.60 \times 10^{-5}$	2.6%	toluene
0.202	8.93	65.0	$6.77 \times 10^{-5}$	4.3%	toluene

**Table 1.** (continued)*Substituted toluenes*

0.480	2.75 CH <sub>3</sub> C <sub>6</sub> H <sub>4</sub> CH <sub>3</sub>	55.0	$8.37 \times 10^{-5}$	9.5%	C <sub>6</sub> H <sub>4</sub> Cl <sub>2</sub> <sup>b</sup>
0.268	1.8 <sup>c</sup> CH <sub>3</sub> C <sub>6</sub> H <sub>4</sub> C(O)Ph	55.0	$2.4 \times 10^{-4}$	11%	C <sub>6</sub> H <sub>4</sub> Cl <sub>2</sub>
0.310	2.76 CH <sub>3</sub> C <sub>6</sub> H <sub>4</sub> Cl	55.0	$2.02 \times 10^{-4}$	7.6%	C <sub>6</sub> H <sub>4</sub> Cl <sub>2</sub>

---

<sup>a</sup> Range of four rate constants derived from analysis of the single kinetics run (see Experimental Section and Appendix A). <sup>b</sup> C<sub>6</sub>H<sub>4</sub>Cl<sub>2</sub> is *o*-dichlorobenzene. <sup>c</sup> This value is estimated. Please see footnote 36 for details.

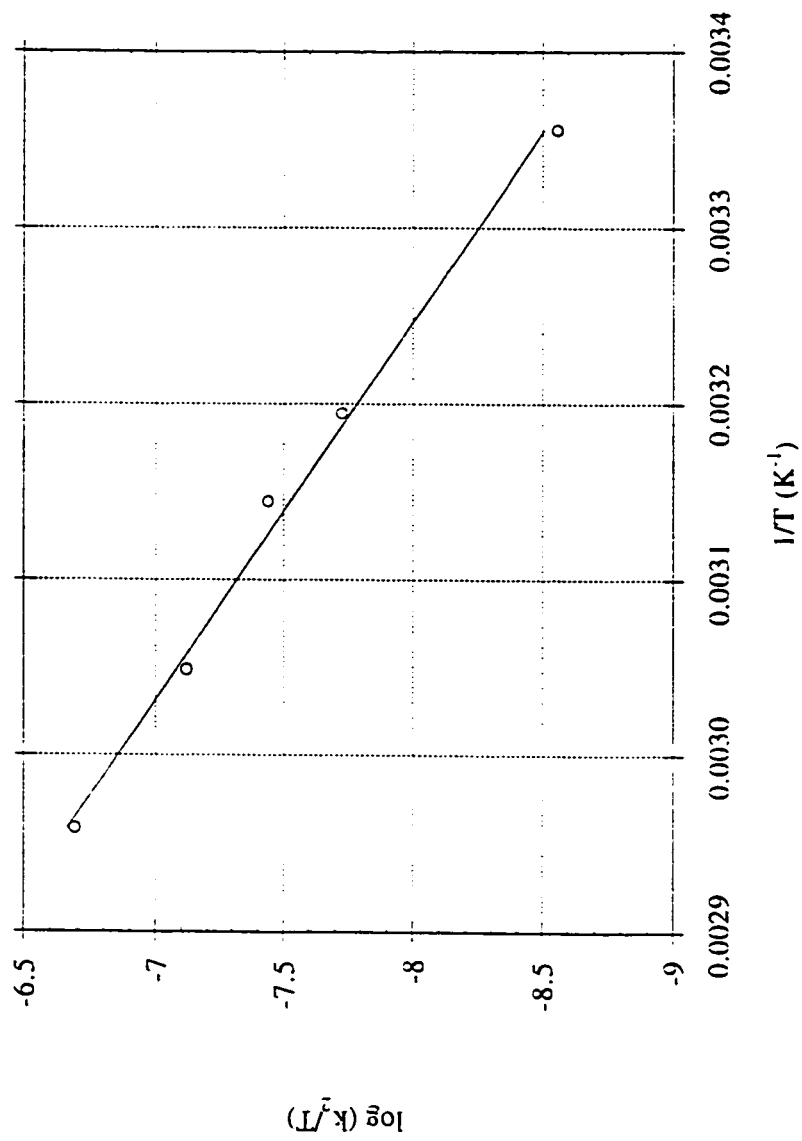


**Figure 3.** An Eyring plot,  $\log(k_2/T)$  vs.  $1/T$ , for the reaction of  $\text{Bu}_4\text{NMnO}_4$  with toluene in toluene over the temperature range 25 to 65 °C.

As a test for the intermediacy of radicals, a reaction was run in the presence of oxygen gas; all other reactions were performed with careful exclusion of air. More common radical traps such as  $\text{CBrCl}_3$  are problematic in this system as the expected products (*i.e.*, benzyl bromide) are subject to further oxidation by permanganate and/or are reactive with the aqueous acidic work up needed to destroy the colloidal  $\text{MnO}_2$  (benzyl bromide is converted to benzyl alcohol). Reductive traps, such as  ${}^n\text{Bu}_3\text{SnH}$ , are not compatible with permanganate. Oxygen is known to react with radicals at near the diffusion limit,<sup>38</sup> as does permanganate.<sup>39</sup>  $\text{O}_2$  should compete with  $\text{MnO}_4^-$  in reacting with any radicals present, thus having an effect on the kinetics. It is unclear whether the presence of  $\text{O}_2$  should accelerate or decelerate the disappearance of  $\text{MnO}_4^-$  if benzyl radicals are generated, but it is highly unlikely that there would be no effect. The concentration of dissolved oxygen in toluene under 1 atm pressure of oxygen at 20 °C is 5.7 mM,<sup>40</sup> more than an order of magnitude larger than the permanganate concentration. Visually monitored, the reaction containing oxygen showed complete loss of permanganate in one day compared to almost a week for an identical reaction under nitrogen. This result suggests the intermediacy of radicals in the oxidation.

The manganese product of the reaction is colloidal  $\text{MnO}_2$ , as indicated by its characteristic sloping optical spectrum.<sup>41</sup> In addition, the average manganese oxidation state of the product was determined to be 4.05 ( $\pm 0.08$ ) using a spectroscopic iodometric technique. The predominant organic product is benzoic acid, with a trace of benzaldehyde observed. These two products account for 62% of the permanganate oxidizing equivalents consumed. Any benzaldehyde left behind in the organic layer upon workup would have been below the detection limits by GC (< 50% yield of benzaldehyde). Based on oxidizing equivalents of permanganate being converted to manganese dioxide, the yield of benzaldehyde would have had to have been < 50%, which is not possible. All other GC detections limits reported in this paper will be in this format, given in terms of the product

yield based on the experiment performed. Benzyl alcohol was not detected, perhaps because a yield below 20% would be below the detection limits by HPLC and GC. The low solubility of  $n\text{Bu}_4\text{NMnO}_4$  in toluene means that the organic products are formed in very small amounts. Some of the “missing” oxidative equivalents may be consumed in complete oxidation of toluene (or an impurity) to  $\text{CO}_2$  and  $\text{H}_2\text{O}$ , as has been observed in other systems.<sup>10a</sup> Because of the large number of oxidative equivalents needed for this oxidation (36 for complete toluene oxidation), a small amount of material can consume a large quantity of permanganate. It is also likely that there is some oxidation of the  $n\text{Bu}_4\text{N}^+$  counterion.  $n\text{Bu}_4\text{NMnO}_4$  is tightly ion paired in toluene,<sup>42</sup> giving a high local concentration of butyl C-H bonds. The reaction of  $n\text{Bu}_4\text{NMnO}_4$  in benzene with benzyltributylammonium bromide ( $n\text{Bu}_3\text{NCH}_2\text{Ph}^+\text{Br}^-$ ) gives large amounts of benzoic acid, showing that counterion oxidation can be a facile process. Attempts to use  $\text{PPN}^+\text{MnO}_4^-$ ,<sup>16</sup> in which cation oxidation should be less facile, were prevented by its lack of solubility in toluene.

A Hammett study was done in *o*-dichlorobenzene solvent, measuring the rates of oxidation of *p*-xylene, *p*-chlorotoluene, and 4-methylbenzophenone (toluene with a *p*-C(O)Ph group). This comparison cannot be done using the substrates as neat solvents because of their different solvent properties. The oxidation of toluene by  $n\text{Bu}_4\text{NMnO}_4$  was shown to be the same in *o*-dichlorobenzene as in toluene.<sup>34</sup> The reaction is first order in both  $\text{MnO}_4^-$  and toluene concentrations, accelerates upon addition of  $\text{O}_2$ , and has similar rate constants. The error associated with reproducibility of the rate constants is much larger than for the reactions in toluene, as a result of solvent purity complications.<sup>43</sup> For a Hammett study, the range of substituents is very limited by the high reactivity of permanganate: for instance, *p*-nitrotoluene was found to react autocatalytically with  $n\text{Bu}_4\text{NMnO}_4$  in *o*-dichlorobenzene. The substituent has only a small effect on the oxidation rate constant (Table 1), with increases in rate constants observed for both

electron donating ( $\text{CH}_3$ ) and electron withdrawing substituents ( $\text{Cl}$ ,  $\text{C}(\text{O})\text{Ph}$ ). The relative rate constants at  $55\text{ }^\circ\text{C}$  are (after the statistical adjustment for the number of methyl groups in *p*-xylene): *p*-xylene, 3.3; toluene, 1; *p*-chlorotoluene, 8.1; 4-methylbenzophenone, 9.6. The lack of correlation with either  $\sigma$  or  $\sigma^+$  values<sup>44</sup> precludes determination of a  $\rho$  value. This lack of a Hammett correlation is frequently observed in the case of radical reactions.<sup>45</sup>

For all of the oxidations in *o*-dichlorobenzene, the manganese containing product is colloidal  $\text{MnO}_2$ , as indicated by its optical spectrum. The only organic product found in the toluene oxidation was benzoic acid, although the presence or absence of benzyl alcohol could not be determined in the presence of a huge excess of *o*-dichlorobenzene. Running the reaction of toluene with  ${}^n\text{Bu}_4\text{NMnO}_4$  in *o*-dichlorobenzene at ambient temperatures under an atmosphere of  $\text{O}_2$  resulted in a slight increase in the apparent rate of permanganate disappearance, suggesting that, as for the reaction in neat toluene, radicals are formed during the course of the reaction. Under these conditions, the concentration of dissolved oxygen is probably comparable to the permanganate concentration.<sup>46</sup>

**II. Ethylbenzene, Cumene, Diphenylmethane, Triphenylmethane, 9,10-Dihydroanthracene, Xanthene, and Fluorene.** Typically, kinetic experiments were performed in toluene under pseudo-first order conditions with an excess of substrate. First order plots, as in the reaction of toluene, are curved downward. Initial rates are calculated in all cases and fairly good reproducibility is observed, with variation of less than 25%. None of the first order plots shows an induction period, although an initial fast reaction was sometimes observed (~5% of the reaction for all substrates except diphenylmethane), likely due to oxidation of an impurity; this portion was not included in the determination of the initial rates. In all of the reactions studied, the initial rate constants show a first order dependence on both substrate and permanganate concentration, indicating a bimolecular rate determining step.

The rate constants for all of the substrates studied are summarized in Table 2. These values are reported as measured experimentally and have not been corrected to account for either the number of hydrogens oxidized or the reaction stoichiometry. At room temperature, reactivity increases in the order *t*-butylbenzene<sup>47</sup> << toluene < ethylbenzene < diphenylmethane < triphenylmethane < fluorene < dihydroanthracene < xanthene. This order corresponds to a decrease in the C-H bond strength (see Discussion). Fluorene can only be placed tentatively on this list because kinetic experiments showed poor reproducibility, with rate constants for initial rates of ca.  $6 \times 10^{-2} \text{ M}^{-1}\text{s}^{-1}$  at 25 °C. Most of the reactions were examined over a 30 to 40 °C temperature range to derive activation parameters (Table 3). In order for the rate constants and entropies of activation to be comparable, the values in Table 3 have been divided by the number of reactive hydrogen atoms in each substrate and for the idealized stoichiometry of the reactions. In toluene oxidation, for example, there are three reactive hydrogens and the idealized stoichiometry is that two equivalents of  $\text{MnO}_4^-$  are consumed for every toluene molecule that is activated (assuming 100% yield of benzoic acid).<sup>48</sup> The Eyring plots are all quite linear over the temperature ranges studied (Figure 4: ethylbenzene; Figure 5: diphenylmethane; Figure 6: triphenylmethane; Figure 7: dihydroanthracene; Figure 8: xanthene). As seen for toluene oxidation, a primary isotope effect is observed on comparison of the oxidations of dihydroanthracene and its *d*<sub>12</sub>-isotopomer, with an apparent  $k_{\text{H}12}/k_{\text{D}12}$  of 3.0 at 25 °C, as determined kinetically. This value is much smaller than reported for related oxidations, although the reason for this is not clear.<sup>24</sup> Fluorene and dihydroanthracene also showed some unusual features in the later stages of their reactions with <sup>n</sup>Bu<sub>4</sub>NMnO<sub>4</sub>, as described in part III below.

The manganese product of these oxidations is MnO<sub>2</sub>, as indicated by its characteristic final visible spectrum.<sup>41</sup> The average manganese oxidation state was also confirmed for the reaction of ethylbenzene to be 3.96 (± 0.08), in agreement with the

**Table 2.** Rate Constants for Reactions of Ethylbenzene, Diphenylmethane, Triphenylmethane, 9,10-Dihydroanthracene, and Xanthene with  ${}^n\text{Bu}_4\text{NMnO}_4$  in Toluene.

[MnO <sub>4</sub> <sup>-</sup> ] (mM)	substrate concentration (M)	T (°C)	k <sub>2</sub> (M <sup>-1</sup> s <sup>-1</sup> )	data analysis error <sup>a</sup>
<i>Ethylbenzene</i>				
0.0529	8.15 <sup>b</sup>	22.0	6.11 × 10 <sup>-6</sup>	8.8%
0.183	2.72	25.0	8.79 × 10 <sup>-6</sup>	2.4%
0.222	2.65	35.0	2.07 × 10 <sup>-5</sup>	4.2%
0.142	6.41	35.0	2.97 × 10 <sup>-5</sup>	20%
0.179	2.72	45.0	5.31 × 10 <sup>-5</sup>	2.3%
0.132	3.99	45.0	8.80 × 10 <sup>-5</sup>	2.6%
0.137	3.99	45.0	7.31 × 10 <sup>-5</sup>	2.1%
0.130	3.99	45.0	7.92 × 10 <sup>-5</sup>	4.0%
0.126	3.99	45.0	7.97 × 10 <sup>-5</sup>	3.2%
0.120	3.94	55.0	2.70 × 10 <sup>-4</sup>	2.5%
0.150	3.89	65.0	5.98 × 10 <sup>-4</sup>	5.0%
0.137	3.89	65.0	7.10 × 10 <sup>-4</sup>	3.6%
<i>Diphenylmethane</i>				
0.166	0.302	15.0	6.40 × 10 <sup>-5</sup>	5.7%
0.305	0.498	25.0	1.57 × 10 <sup>-4</sup>	1.1%
0.185	0.381	25.0	1.86 × 10 <sup>-4</sup>	0.8%
0.187	0.382	35.0	4.56 × 10 <sup>-4</sup>	1.1%
0.262	0.332	45.0	1.12 × 10 <sup>-3</sup>	1.8%

**Table 2.** (continued)

0.343	0.155	45.0	$1.19 \times 10^{-3}$	1.9%
<i>Triphenylmethane</i>				
0.178	0.0687	25.0	$2.06 \times 10^{-3}$	3.0%
0.240	0.0269	25.0	$1.61 \times 10^{-3}$	3.3%
0.187	0.0271	35.0	$4.50 \times 10^{-3}$	14%
0.0941	0.0268	45.0	$1.20 \times 10^{-2}$	9.7%
0.128	0.0265	55.0	$2.15 \times 10^{-2}$	11%
0.164	0.0265	55.0	$3.05 \times 10^{-2}$	1.8%
0.137	0.0265	55.0	$2.40 \times 10^{-2}$	1.8%
<i>9,10-Dihydroanthracene</i>				
0.188	0.00255	10.0	$9.57 \times 10^{-2}$	11%
0.209	0.00251	20.0	$1.81 \times 10^{-1}$	11%
0.280	0.00251	25.0	$3.17 \times 10^{-1}$	0.9%
0.124	0.00129	25.0	$3.43 \times 10^{-1}$	1.0%
0.200	0.00251	25.0	$2.79 \times 10^{-1}$	11%
0.0944	0.00249	25.0	$3.24 \times 10^{-1}$	10%
0.279	0.00273 ( <i>d</i> <sub>12</sub> -DHA <sup>c</sup> )	25.0	$1.06 \times 10^{-1}$ ( <i>d</i> <sub>12</sub> -DHA <sup>c</sup> )	10%
0.111	0.00128	30.0	$5.52 \times 10^{-1}$	17%
0.126	0.00128	35.0	$6.82 \times 10^{-1}$	3.6%
<i>Xanthene</i>				
0.113	0.000843	10.0	$4.18 \times 10^{-1}$	3.5%
0.0687	0.000838	15.0	$8.17 \times 10^{-1}$	0.3%

**Table 2.** (continued)

0.0676	0.00109	20.0	1.23	11%
0.141	0.00475	25.0	1.63	13%
0.0640	0.00109	25.0	1.44	5.6%
0.141	0.00109	25.0	1.37	3.7%
0.0524	0.000819	35.0	2.72	7.8%

---

---

<sup>a</sup> Range of four rate constants derived from analysis of the single kinetics run (see Experimental Section and Appendix A). <sup>b</sup> Experiment in neat ethylbenzene. <sup>c</sup> DHA is 9,10-dihydroanthracene.

**Table 3.** Comparison of Rates, Activation Parameters, and C-H Bond Strengths for the Rate Determining Step of Reactions of  ${}^n\text{Bu}_4\text{NMnO}_4$  with Various Hydrocarbons in Toluene.

substrate	$k$ ( $\text{M}^{-1}\text{s}^{-1}$ ) at 298K per H <sup>a</sup>	$\Delta\text{H}^\ddagger$ (kcal/mol)	$\Delta\text{S}^\ddagger$ (e.u.) <sup>b</sup>	$\Delta\text{G}^\ddagger$ (kcal/mol) <sup>b</sup>	C-H BDE (kcal/mol) <sup>c</sup>
PhCH <sub>3</sub>	$1.4 \times 10^{-7}$	21.0 ( $\pm 1.0$ )	-18 ( $\pm 3$ )	26 ( $\pm 1$ )	88.0
PhCH <sub>2</sub> CH <sub>3</sub>	$3.3 \times 10^{-6}$	20.8 ( $\pm 0.6$ )	-13 ( $\pm 3$ )	25 ( $\pm 1$ )	85.4
Ph <sub>2</sub> CH <sub>2</sub>	$6.5 \times 10^{-5}$	17.1 ( $\pm 0.5$ )	-20 ( $\pm 3$ )	23 ( $\pm 1$ )	84
Ph <sub>3</sub> CH	$2.7 \times 10^{-3}$	16.5 ( $\pm 0.8$ )	-16 ( $\pm 5$ )	21 ( $\pm 2$ )	81
DHA <sup>d</sup>	$1.2 \times 10^{-1}$	13.8 ( $\pm 1.0$ )	-17 ( $\pm 7$ )	19 ( $\pm 2$ )	78
xanthene	$5.6 \times 10^{-1}$	11.7 ( $\pm 1.2$ )	-20 ( $\pm 8$ )	18 ( $\pm 3$ )	75.5

<sup>a</sup> Extrapolated from best fit straight line of Eyring plot. A correction has also been made to account for the idealized reaction stoichiometry. <sup>b</sup> Values are at 298K, per H. <sup>c</sup> Bond strengths are discussed in reference 83. <sup>d</sup> DHA is 9,10-dihydroanthracene.

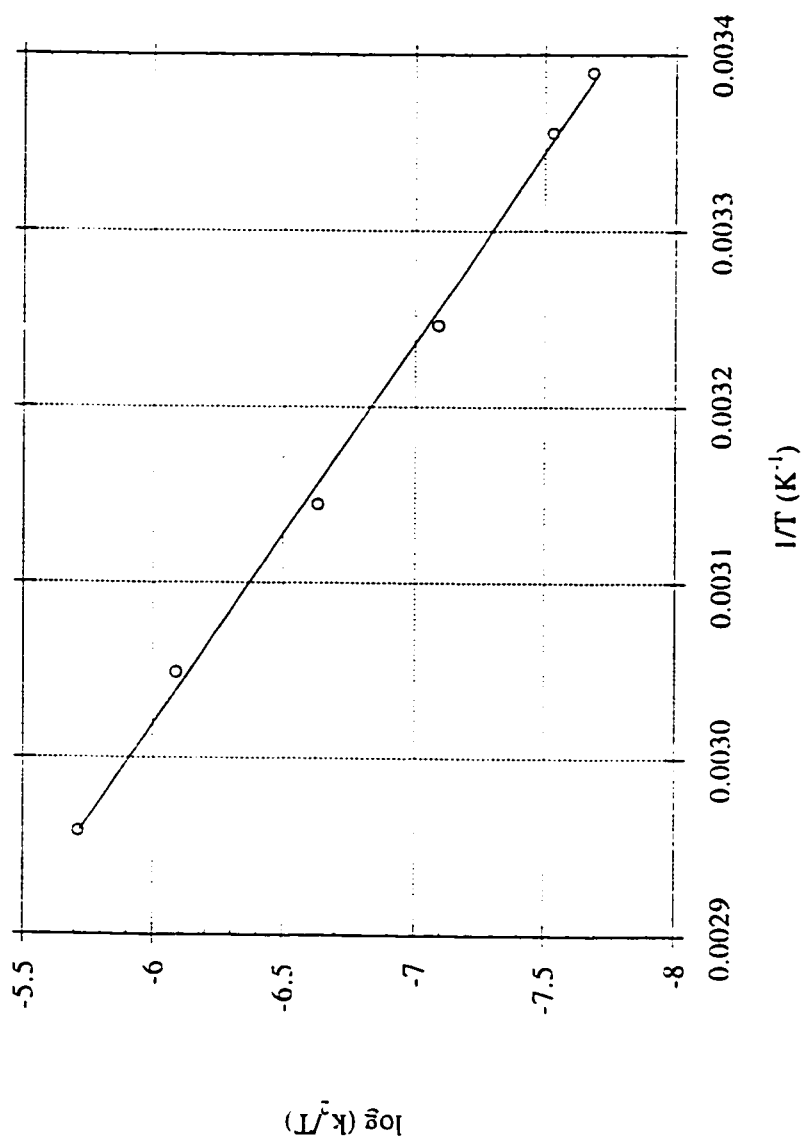


**Figure 4.** An Eyring plot,  $\log(k_2/T)$  vs.  $1/T$ , for the reaction of  $n\text{Bu}_4\text{NMnO}_4$  with ethylbenzene in toluene over the temperature range 22 to 65 °C.

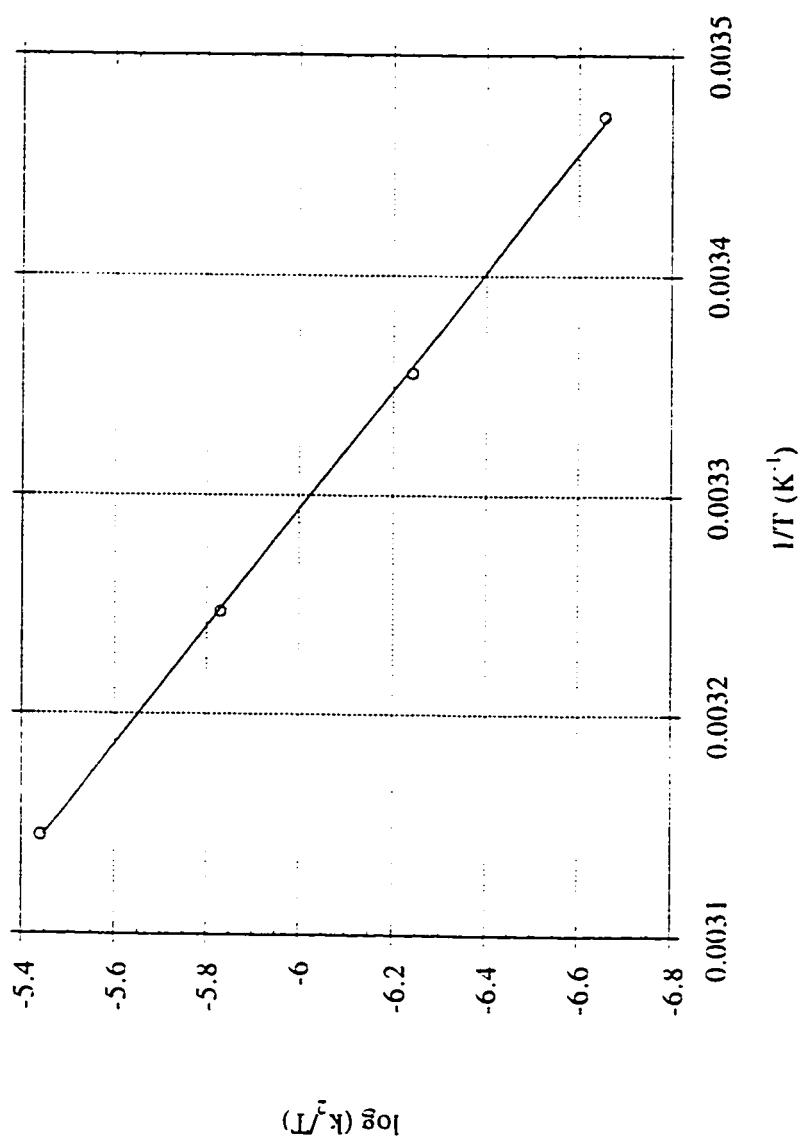


**Figure 5.** An Eyring plot,  $\log(k_2/T)$  vs.  $1/T$ , for the reaction of  $n\text{Bu}_4\text{NMnO}_4$  with diphenylmethane in toluene over the temperature range 15 to 45 °C.

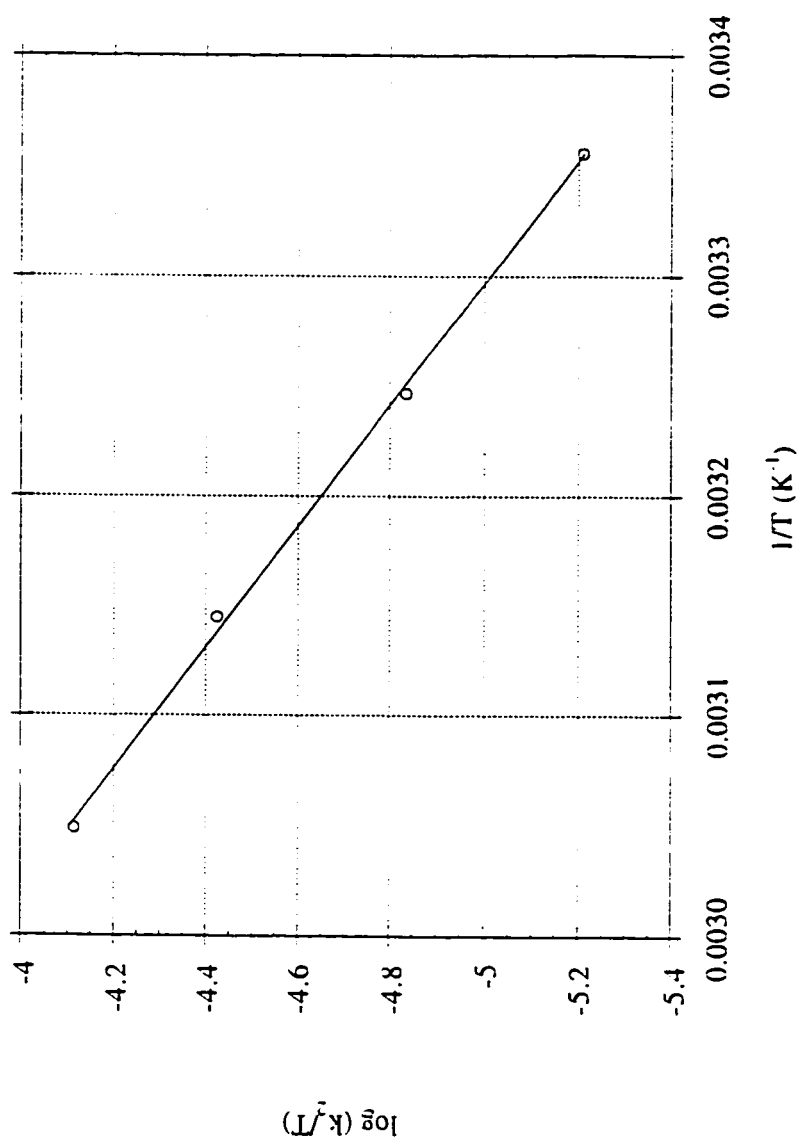


**Figure 6.** An Eyring plot,  $\log(k_2/T)$  vs.  $1/T$ , for the reaction of  $n\text{Bu}_4\text{NMnO}_4$  with triphenylmethane in toluene over the temperature range 25 to 55 °C.

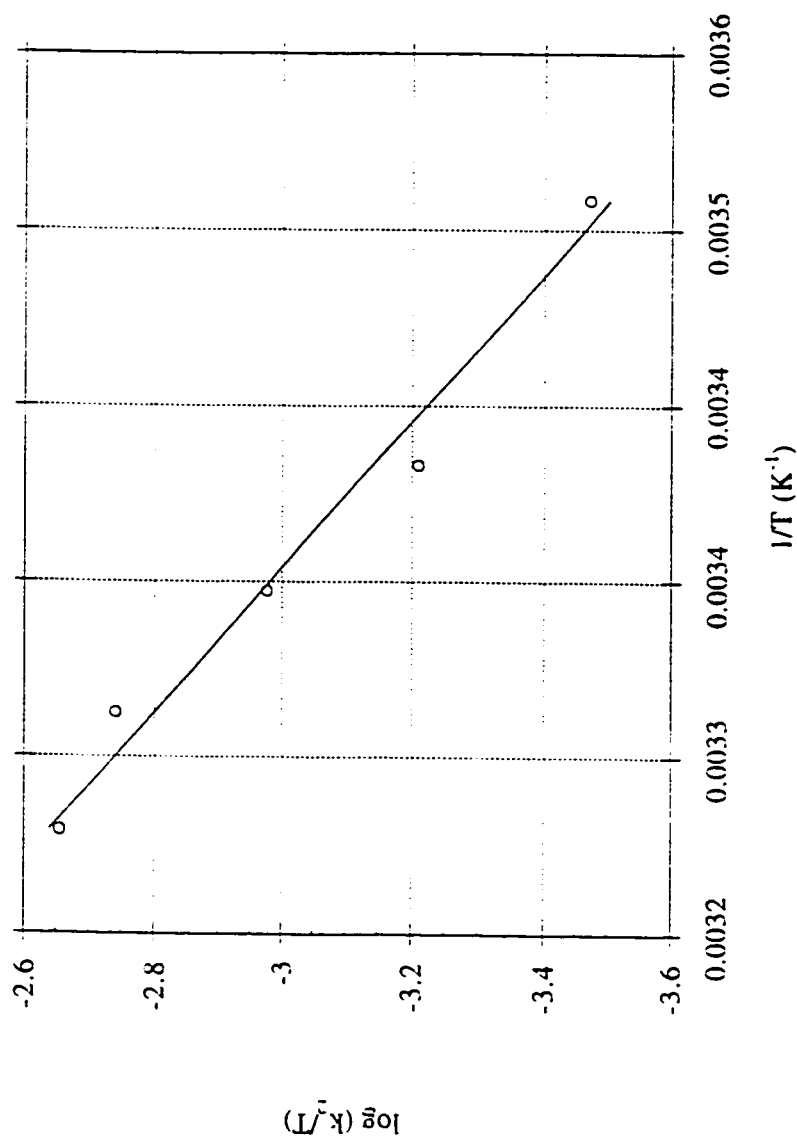


**Figure 7.** An Eyring plot,  $\log(k_2/T)$  vs.  $1/T$ , for the reaction of  $n\text{Bu}_4\text{NMnO}_4$  with 9,10-dihydroanthracene in toluene over the temperature range 10 to 35 °C.

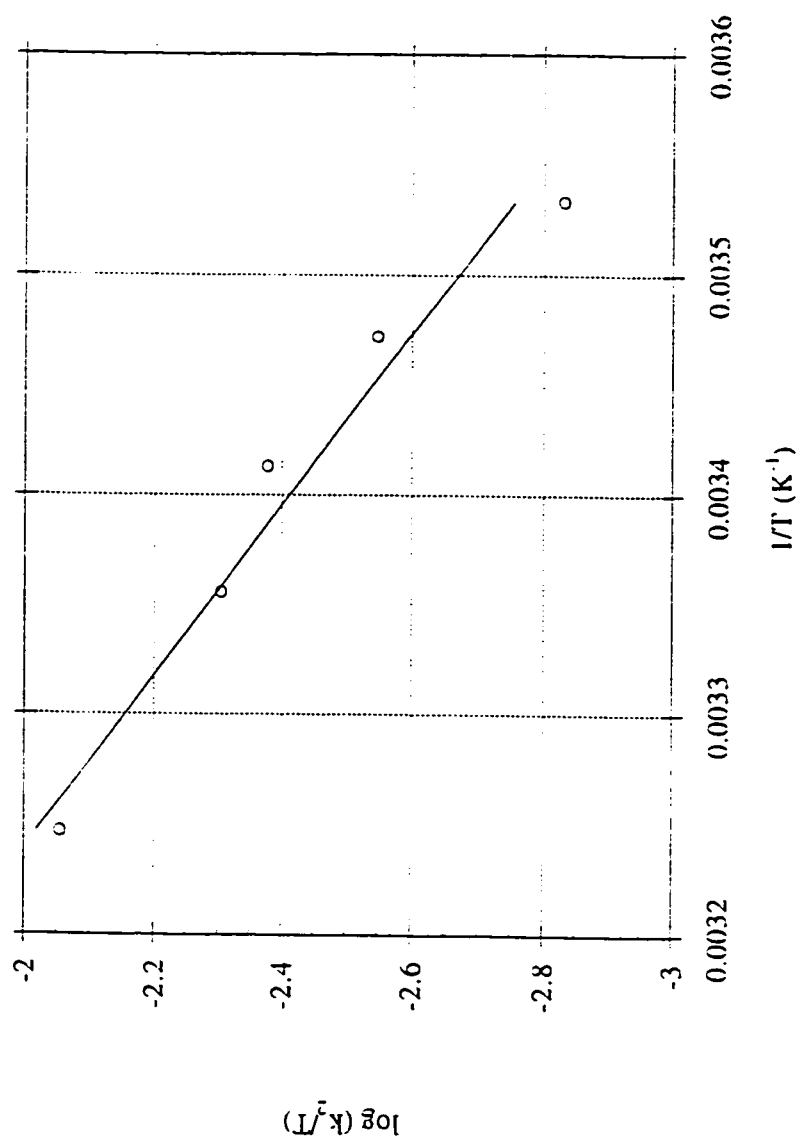


**Figure 8.** An Eyring plot,  $\log(k_2/T)$  vs.  $1/T$ , for the reaction of  ${}^n\text{Bu}_4\text{NMnO}_4$  with xanthenes in toluene over the temperature range 10 to 35 °C.

results of the toluene experiments. Quantification of the organic products in these reactions is difficult because the low solubility of  $n\text{Bu}_4\text{NMnO}_4$  means that very little of the products is formed, typically a micromole or less. In addition, an aqueous acidic workup is needed to destroy the colloidal  $\text{MnO}_2$  on which some of the products are bound and this results in a two phase system (see Experimental section). Analysis of the organic products from the reaction of ethylbenzene was performed on a reaction solution of neat ethylbenzene since ethylbenzene and toluene reportedly both form benzoic acid when oxidized by permanganate.<sup>49</sup> The aqueous layer contained acetophenone, accounting for approximately 30% of the oxidizing equivalents of permanganate. Within the detection limits, benzoic acid (< 5% yield) and *sec*-phenethylalcohol (< 10% yield) were absent in the aqueous layer. The remaining oxidizing equivalents were likely in the form of acetophenone left in the organic layer, as acetophenone has little water solubility and any acetophenone in the organic layer would have been below the GC detection limits (< 10% yield of acetophenone).

The other oxidations give the expected products. Xanthene is oxidized to xanthone by  $n\text{Bu}_4\text{NMnO}_4$  in toluene. No other organic products are observed by GC. The yield of xanthone is ~80% based on the oxidizing equivalents of permanganate consumed. Diphenylmethane forms benzophenone with a yield of 44% based on permanganate oxidizing equivalents consumed. These yields were determined by GC of the organic layer after destruction of the  $\text{MnO}_2$  colloid; any products that partition into the aqueous layer were not observed. Determination of the product(s) from triphenylmethane oxidation is particularly problematic because the expected product,  $\text{Ph}_3\text{COH}$ , is unstable under the necessary acid work up. Some  $\text{Ph}_3\text{COH}$  was observed by GC when a solution was analyzed without destruction of the colloid, but this accounted for only 9% of the oxidizing equivalents of permanganate. No other organic species were found to be present, but organic products are known to be bound in or on the colloidal particles.<sup>30</sup>

When the  $\text{MnO}_2$  was reduced with a very slightly acidic solution (pH 5), the yield of  $\text{Ph}_3\text{COH}$  increased to 19%. Dihydroanthracene gives anthracene as the only apparent organic reaction product, in approximately 65% yield based on the anthracene absorbance at 380 nm.<sup>50</sup> No other organic products were detected either by GC of the reaction solution or by  $^1\text{H}$  NMR of the solids left after solvent removal.

Despite repeated efforts, the reaction of cumene with  $^n\text{Bu}_4\text{NMnO}_4$  in toluene gave irreproducible kinetic results. The details are given in Appendix C. The same reaction in *o*-dichlorobenzene was plagued by similar problems.<sup>52</sup> Experiments in neat cumene were not feasible as  $^n\text{Bu}_4\text{NMnO}_4$  is essentially insoluble in cumene. The reason for this erratic behavior is unclear. Some of the reactions were slower than might have been expected given the results of the toluene and ethylbenzene experiments, suggesting that the problems were not the result of oxidation of an impurity.<sup>53</sup>

**III. Charge-Transfer Complexes.** The reaction of dihydroanthracene with  $^n\text{Bu}_4\text{NMnO}_4$  in toluene at 25 °C proceeds initially as described above, with a roughly first order decay until all of the  $\text{MnO}_4^-$  is gone and  $\text{MnO}_2$  has formed, based on the visible spectra. At that point, a second, very fast reaction occurs, leading to the disappearance of all of the  $\text{MnO}_2$  and the formation of a new species. After requiring 2000 seconds for complete consumption of the permanganate (at 25 °C), all of the  $\text{MnO}_2$  is consumed within another 200 seconds. An overlay of spectra from a representative reaction and a trace of the absorbance at 546 nm vs. time are shown in Figure 9.

The new species formed has a very strong absorbance in the visible region with maxima at 524 and 560 nm, and with extinction coefficients comparable to those of the permanganate starting material. There is a vibrational progression between 300 and 400 nm which partially overlaps the vibrational progression of anthracene, but is shifted to longer wavelength (Figure 10). The spacing of the bands in the progression is lower in energy than free anthracene, approximately  $1100\text{ cm}^{-1}$  for the new species compared to

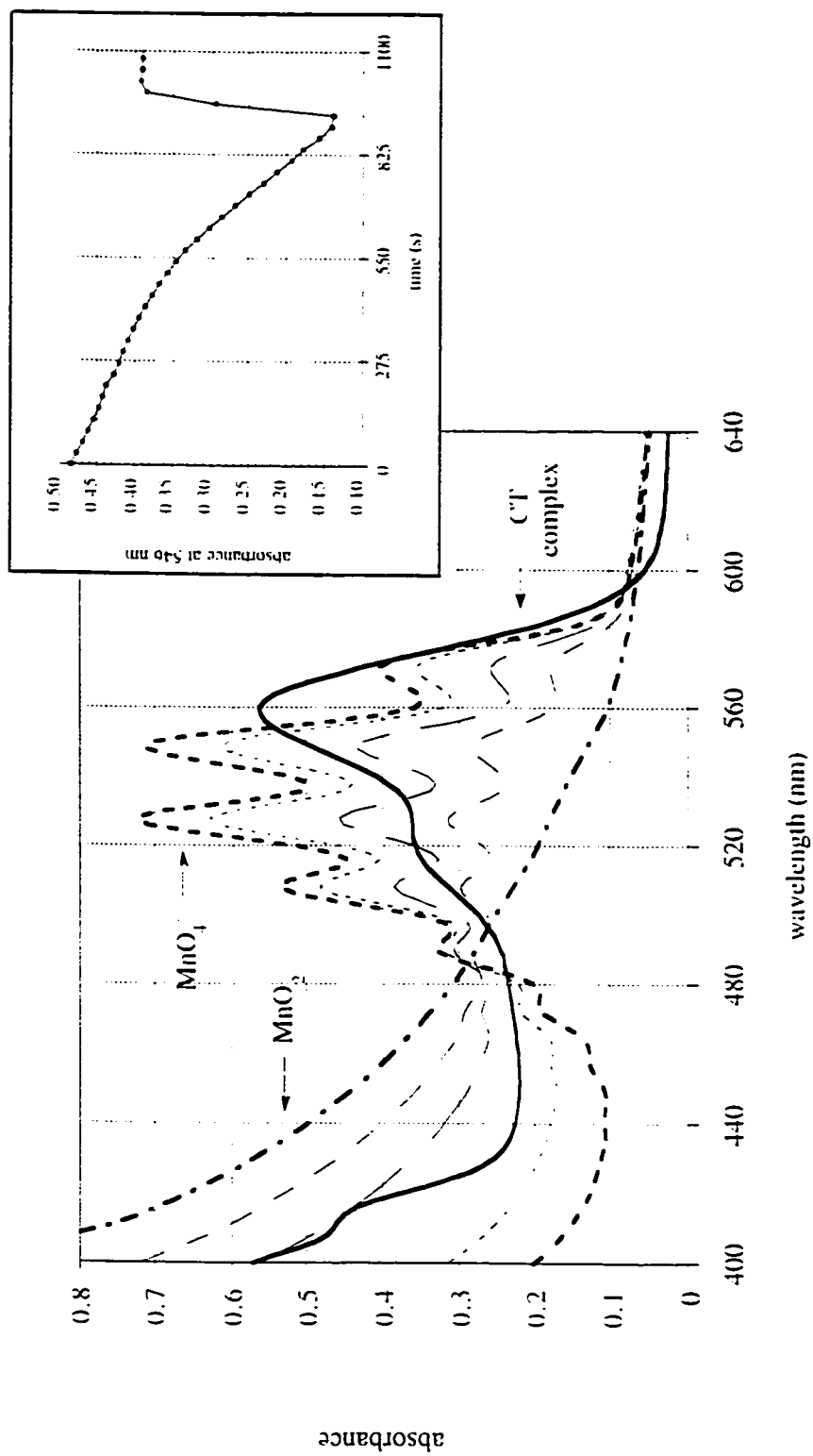


**Figure 9.** Overlay of UV/vis spectra from the reaction of  $n\text{Bu}_4\text{NMnO}_4$  with 9,10-dihydroanthracene in toluene at 25 °C. Inset plot of absorbance at 546 nm vs. time for the same reaction.

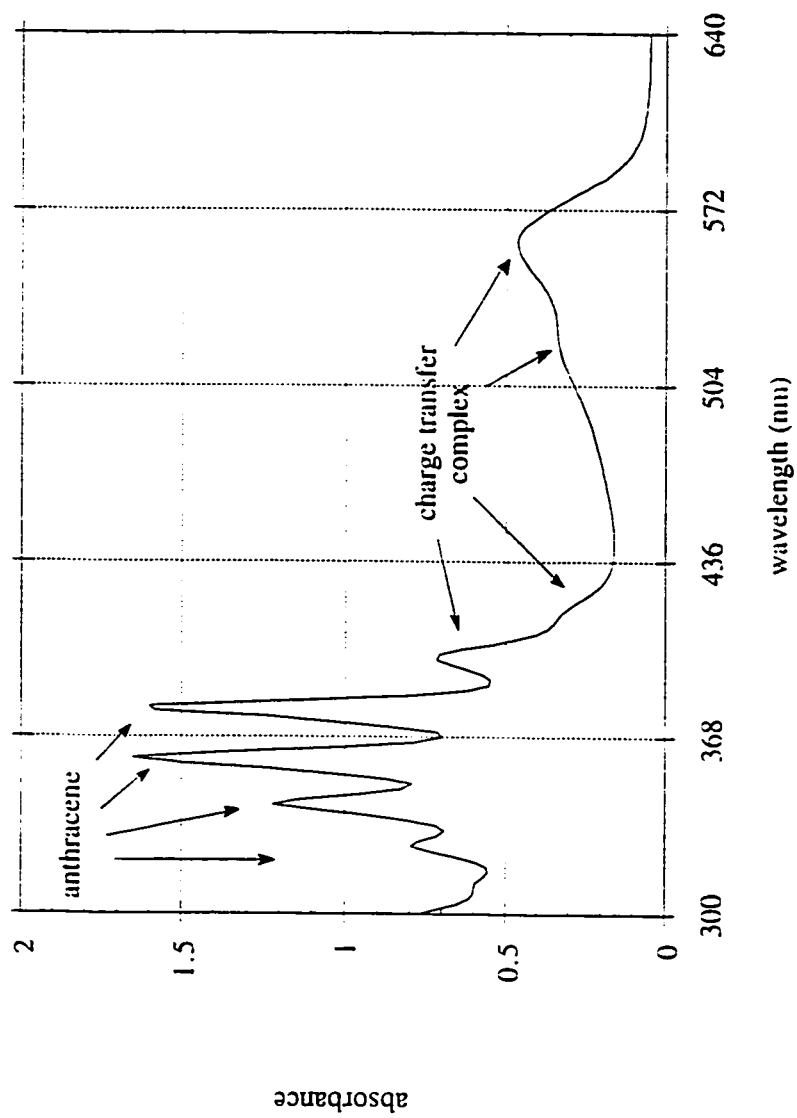


**Figure 10.** UV/vis spectrum of the solution at the end of the reaction of  $n\text{Bu}_4\text{NMnO}_4$  with 9,10-dihydroanthracene in toluene at 25 °C.

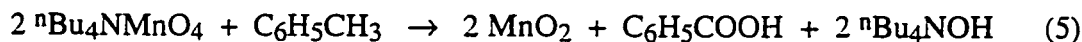
1400  $\text{cm}^{-1}$  for anthracene. The new product is purple in solution and is unstable to air and light, with exposure to either resulting in a colorless solution. Removal of the solvent leads to a pale pink residue, unexpected considering the intense color of the species in solution. Similar behavior is observed on reaction of  ${}^n\text{Bu}_4\text{NMnO}_4$  and dihydroanthracene in acetonitrile, but the new product absorbances are blue-shifted by 30 nm, with maxima at 494 and 530 nm.

The characteristics of the new product are all indicative of a charge transfer complex.<sup>54</sup> High extinction coefficients, sensitivity to light, and difficulty in isolation are typical of these weakly bound complexes. It is likely that the charge-transfer complex involves anthracene and some manganese-oxo species, but attempts to form it by other routes have failed. Colloidal  $\text{MnO}_2$ , formed by reaction of  ${}^n\text{Bu}_4\text{NMnO}_4$  with toluene, does not form a charge transfer complex with dihydroanthracene, anthracene, or both. Anthracene interacting directly with  ${}^n\text{Bu}_4\text{NMnO}_4$  in toluene also does not result in formation of the complex. The inability to produce the charge transfer complex under other conditions may be due to formation of the complex on the surface of the colloid. This idea is supported by the variability of the rate of the fast reaction, possibly related to the character of the colloid.

The reaction of fluorene with  ${}^n\text{Bu}_4\text{NMnO}_4$  in toluene also forms a charge-transfer complex, an air sensitive species with intense absorption bands at 454 and 374 nm. Unlike the reaction of dihydroanthracene, in this case the permanganate does not need to be consumed prior to formation of the charge-transfer complex. This reaction is quite variable. Some of the time the fluorene oxidation resembles a clock reaction, proceeding smoothly until a point at which there is rapid consumption of  $\text{MnO}_4^-$  and formation of the new species. In other cases, with identical batches of  ${}^n\text{Bu}_4\text{NMnO}_4$ , fluorene, and vacuum-transferred toluene, reaction takes place immediately without any initial slower portion or the charge transfer species does not form over an extended period.

## Discussion

**I. Overview of the Reactions.** Permanganate is a versatile multi-electron oxidant, able to oxidize a variety of substrates in one- or two-electron steps.<sup>7</sup> In the reactions studied here, manganese undergoes a three-electron change from Mn(VII) to Mn(IV) and the substrates are oxidized by 2, 4, or 6 electrons. For instance, 9,10-dihydroanthracene to anthracene is a two-electron oxidation, ethylbenzene to acetophenone is a four-electron oxidation, and toluene to benzoic acid is a six-electron oxidation. Thus, two molecules of permanganate are consumed in the production of one molecule of benzoic acid, according to the stoichiometry of eq 5. Eq 5 could be equivalently written to produce  ${}^n\text{Bu}_4\text{N}^+\text{C}_6\text{H}_5\text{CO}_2^- + \text{H}_2\text{O}$ ; all of products appear to be associated with the colloidal  $\text{MnO}_2$ .



The primary information concerning these reactions is their kinetic behavior. No induction periods are observed for any of the substrates. In some reactions, there is a rapid loss of a small amount of permanganate, which we have interpreted as the oxidation of an impurity and ignored in the data analysis. The reactions closely follow the second order kinetics rate law of eq 6 roughly over the first half-life, as indicated by the linear dependence of the pseudo-first order  $k_{obs}$  on substrate concentrations and the lack of a dependence of  $k_{obs}$  on the starting  ${}^n\text{Bu}_4\text{NMnO}_4$  concentration.

$$\frac{d[\text{MnO}_4^-]}{dt} = -k_2 [{}^n\text{Bu}_4\text{NMnO}_4][\text{substrate}] \quad (6)$$

**II. Charge Transfer Complexes.** The formation of charge transfer complexes at the end of the anthracene and fluorene reactions is without precedent in

permanganate chemistry. There are, however, well documented charge transfer complexes of aromatic hydrocarbons with other metal-oxo species, such as  $\text{CrO}_2\text{Cl}_2$ <sup>55</sup> and  $\text{OsO}_4$ .<sup>54a</sup> The assignment of the new species in the permanganate reactions as charge transfer complexes is based on several experimental observations. The strength of the absorbance band, the sensitivity of the product to light, and the difficulties encountered in isolation are all common characteristics of charge transfer complexes.<sup>54</sup> The complex derived from reaction of  ${}^n\text{Bu}_4\text{NMnO}_4$  and dihydroanthracene in acetonitrile has its absorption maxima 30 nm shifted to the blue from that in toluene, a shift that is similar those observed by Wallis and Kochi<sup>54a</sup> for anthracene/ $\text{OsO}_4$  complexes in polar vs. non-polar solvents (see Table 4). Table 4 also shows that for both these and the  $\text{OsO}_4$  charge transfer complexes, the energy of the optical transition is related to the ionization potential of the aromatic donor, as is typical of charge transfer absorbances.<sup>54</sup> The comparison between the manganese and osmium systems cannot be made directly as Wallis and Kochi did not study fluorene, but mesitylene and fluorene have similar ionization potentials and show the same trend.

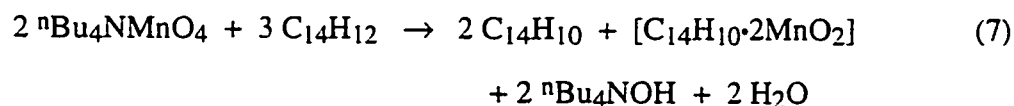
While attempts to isolate this complex or to form it by other means have been unsuccessful, the spectroscopic data contain a number of clues about the nature of the complex. In the dihydroanthracene reaction, the donor species is very likely anthracene based on the observed vibrational progression between 300 and 400 nm due to the anthracene ring-breathing mode. The lower frequency of this mode in the charge transfer complex vs. free anthracene is seen in known anthracene charge transfer complexes.<sup>54c</sup> The acceptor portion of the complexes is undoubtedly a manganese-oxo species. The evidence strongly suggests, in fact, that the species may be the colloid surface. Upon formation of the charge transfer complex, the optical spectrum of  $\text{MnO}_2$  in the 400 to 600 nm region disappears. There are two possible explanations for this phenomenon. The  $\text{MnO}_2$  spectrum in this region is due to absorbance of light by the surface of the colloid.<sup>41</sup>

**Table 4.** Comparison of Charge Transfer Complexes of "MO<sub>x</sub>" Species with Arenes

arene	IP (eV) <sup>c</sup>	$\lambda_{\text{max}}$ (nm) / solvents			
		complexes with OsO <sub>4</sub> <sup>a</sup>		complexes with "MnO <sub>x</sub> " <sup>b</sup>	
		<i>n</i> -C <sub>6</sub> H <sub>14</sub>	CH <sub>2</sub> Cl <sub>2</sub>	toluene	CH <sub>3</sub> CN
mesitylene	8.39	390	--	--	--
fluorene	8.63	--	--	454/374	--
anthracene	7.23	520	510	560/524	530/494

<sup>a</sup> Values taken from reference 54a. <sup>b</sup> Values from this work. <sup>c</sup> Values taken from reference 7f.

Reduction of the  $\text{MnO}_2$  units on the surface of the colloid to  $\text{Mn}^{2+}$  is known to cause the  $\text{MnO}_2$  spectrum to change and decrease in intensity in this region.<sup>41</sup> Complex formation which results in the reduction of the colloid surface could account for these observations. Alternatively, the absence of  $\text{MnO}_2$  absorbance may be an indication that the complex is tightly bound to the surface of the colloid. Particularly in the fluorene reaction, the duration of the slow reaction does not correlate with any known reaction variable, possibly because charge transfer complex formation is related to the nature of the colloid. In the dihydroanthracene reaction, the final optical spectra indicate a yield of one mole of free anthracene per mole of permanganate consumed, suggesting the reaction stoichiometry of eq 7 (dihydroanthracene =  $\text{C}_{14}\text{H}_{12}$ ; anthracene =  $\text{C}_{14}\text{H}_{10}$ ). The water and hydroxide formed are likely associated with the manganese product, whose detailed nature remains unclear.<sup>56</sup>



**III. The Rate Determining Step.** All of the evidence implies that the rate determining step of these reactions is bimolecular attack of permanganate on a C–H bond of a substrate. No induction periods are observed, second-order kinetics are obeyed (initially, until oxidation products accumulate or data analysis problems arise), and there are significant primary isotope effects in the toluene and dihydroanthracene oxidations. There is no support for the suggestion that other manganese species are involved in the initial hydrocarbon activation step. Similar conclusions were reached by Brauman and Pandell in their study of oxidation of  $\gamma$ -phenylvaleric acid in concentrated aqueous base and by Wiberg and Fox in their studies of *p*-*sec*-butylbenzoic acid and 4-methylhexanoic acid in neutral and basic aqueous solution.<sup>9</sup> All of the substrates studied here react with

permanganate through a common rate determining step, as will be shown below. Since toluene has been most thoroughly studied, our discussion is focused on this substrate, although the results are general for this group of arylalkanes.

The isotope effect for the rate limiting step in the toluene and dihydroanthracene oxidations may not be quite the same as the ratio of observed rate constants,  $k_H/k_D$ . This is due to potentially different stoichiometries in the reactions of protio vs. deuterio substrates. The slower activation of the deuterated materials means that more permanganate is consumed in side reactions such as counterion oxidation and/or overoxidation of products. As such, these isotope effects should be taken as the lower limit. Ideally, more accurate values for the isotope effects could be obtained by comparing the product yields from reactions of protio and deuterio substrates. There are many problems associated with product analysis for these reactions, however, including the formation of charge transfer complexes and the very small amounts of products generated. These problems preclude a more accurate determination of the isotope effects.

A variety of mechanistic pathways are conceivable for permanganate oxidations because of its ability to act as a one- or two-electron oxidant. Outersphere electron transfer is a well documented pathway for permanganate reactions,<sup>7</sup> not surprising given its reduction potential of +0.56 V (in H<sub>2</sub>O vs. NHE).<sup>57</sup> This has not been proposed as a mechanism for hydrocarbon oxidation by permanganate but it has been discussed in OsO<sub>4</sub><sup>53a</sup> and cytochrome P-450 reactions.<sup>58</sup> However, transfer of an electron from the arylalkane to permanganate (eq 8) is ruled out as a mechanism for these reactions for the following reasons.



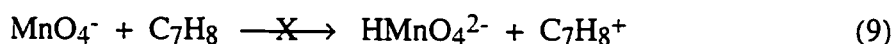
First, the small substituent effects are inconsistent with electron transfer. *p*-Xylene reacts only about twice as fast as toluene despite being 0.4 V easier to oxidize:  $E^\circ_{\text{ox}} = 1.54$  V for

*p*-xylene vs. 1.96 V for toluene (in MeCN, vs. Ag<sup>+</sup>/AgNO<sub>3</sub>).<sup>59</sup> If the reaction were proceeding by electron transfer, this 0.4 V difference in oxidation potential would be expected to manifest itself in a difference of reactivity of several orders of magnitude.<sup>60</sup> Furthermore, forming the radical cation of 4-methylbenzophenone should be much more difficult than that of toluene, yet this substrate is oxidized faster than toluene. Second, outersphere electron transfer is an unlikely process in non-polar media such as toluene because of the difficulty in stabilizing the charged species which result. Permanganate should have a less positive redox potential in toluene than in water (i.e. less than 0.56 V),<sup>57</sup> and formation of the toluene radical cation would be less favorable in toluene solvent than in acetonitrile (i.e. greater than 1.96 V).<sup>7f</sup> Therefore, based on the aqueous and MeCN potentials, outersphere electron transfer is at least 1.4 V uphill, which corresponds to an equilibrium constant of  $<10^{-24}$ . Since the forward reaction proceeds at  $10^{-6} \text{ M}^{-1}\text{s}^{-1}$ , the reverse reaction (back electron transfer) would have to proceed at the impossible bimolecular rate of  $10^{18} \text{ M}^{-1}\text{s}^{-1}$ . This rules out electron transfer as either the rate limiting step or as a pre-equilibrium step in the reaction.

The primary isotope effect,  $k_{\text{H}}/k_{\text{D}} = 6$  for toluene, shows that the rate limiting step involves C-H bond cleavage. C-H bond cleavage could occur by proton, hydrogen atom, or hydride transfer to a permanganate oxo group or by [2+2] addition across a Mn-O bond. Proton transfer is not reasonable given the very low acidity of toluene and the low basicity of permanganate. [2+2] addition to metal oxo bonds has been suggested based on *ab initio* calculations of CrO<sub>2</sub>Cl<sub>2</sub> reactions<sup>13</sup> and based on experimental studies of permanganate<sup>12b</sup> and manganate reactions.<sup>12a</sup> The analogous addition across a metal-imido linkage is well preceded for early transition metal systems.<sup>61</sup> [2+2] addition of a toluene C-H bond across an Mn=O bond would generate a five-coordinate benzyl-manganese-trioxo-hydroxide, [Mn(CH<sub>2</sub>C<sub>6</sub>H<sub>5</sub>)(O)<sub>3</sub>OH]. However, there is little evidence for such an expansion of coordination number in the chemistry of permanganate. This

mechanism would therefore predict a sizable steric effect, with particular difficulty in formation of a manganese-tertiary alkyl complex. As shown below, no such effect is observed: the rates of oxidation depend on the strength of the C–H bond being cleaved and not whether the hydrogen is 1°, 2°, or 3°. Similarly, the entropies of activation reported here ( $\Delta S^\ddagger = -16$  e.u. for toluene oxidation) are not as negative as expected for a constrained [2+2] transition state.<sup>12a</sup>

Hydride transfer from organic substrates to permanganate is well preceded, most clearly in the oxidation of alcohols.<sup>7,11,62</sup> A similar mechanism has also been invoked in the oxidation of hydrocarbons by the high valent metal-oxo species, (trpy)(bpy)RuO<sup>2+</sup>.<sup>63</sup> Hydride transfer has recently been proposed for the permanganate oxidation of toluene in water,<sup>6</sup> but is unlikely as a mechanism in organic solvents based on the substituent effects observed. Abstraction of H<sup>•</sup> from toluene would form HMnO<sub>4</sub><sup>2-</sup> and benzyl cation (eq 9). The formation of benzyl cation would be very sensitive to substituent effects, much like electron transfer. *p*-Xylene should be much more reactive while an acceleration of only 3 times is observed. Furthermore, *p*-chlorotoluene and 4-methylbenzophenone should react substantially more slowly by this mechanism while rate accelerations occur. In addition, the formation of higher charged species, such as benzyl cation, is unfavorable in such a non-polar solution.

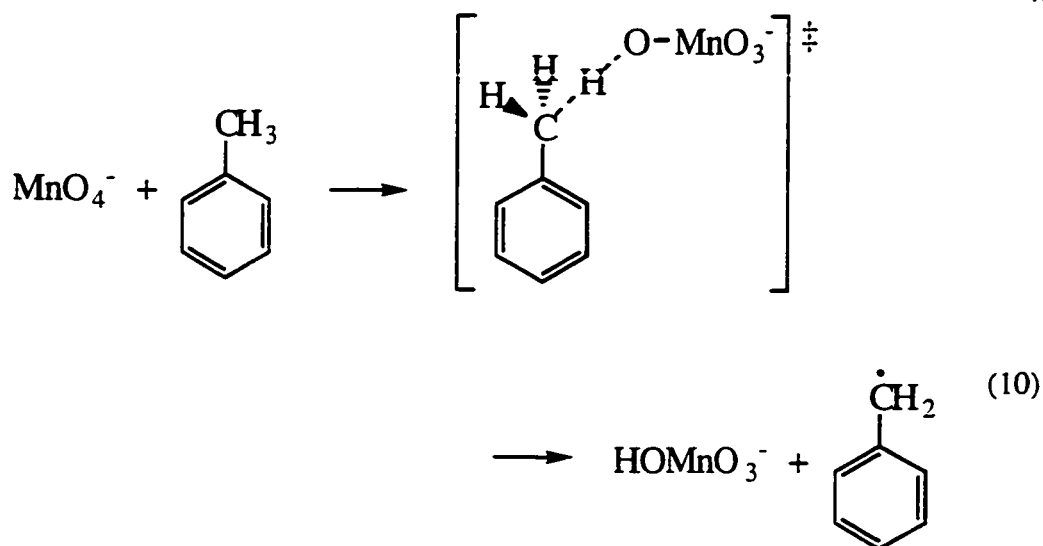


Rate limiting hydrogen atom transfer from the substrate (eq 10) to a permanganate oxo group is consistent with all of the experimental evidence. This is probably the most commonly proposed mechanism for permanganate oxidations of C–H bonds.<sup>7-11</sup> This proposal is consistent with the primary isotope effects, the activation parameters, and the relative rates of oxidation of the different substrates (see below). The lack of a solvent effect -- similar rates in toluene and *o*-dichlorobenzene solvents -- is characteristic of

radical reactions<sup>64</sup> and is not consistent with mechanisms involving polar transition states or products. The observed influence of added O<sub>2</sub> is a classic indicator of radical intermediates. Oxygen is known to trap radicals at near the diffusion limit and would be expected to compete with permanganate in reacting with any radicals present.<sup>38, 39</sup>

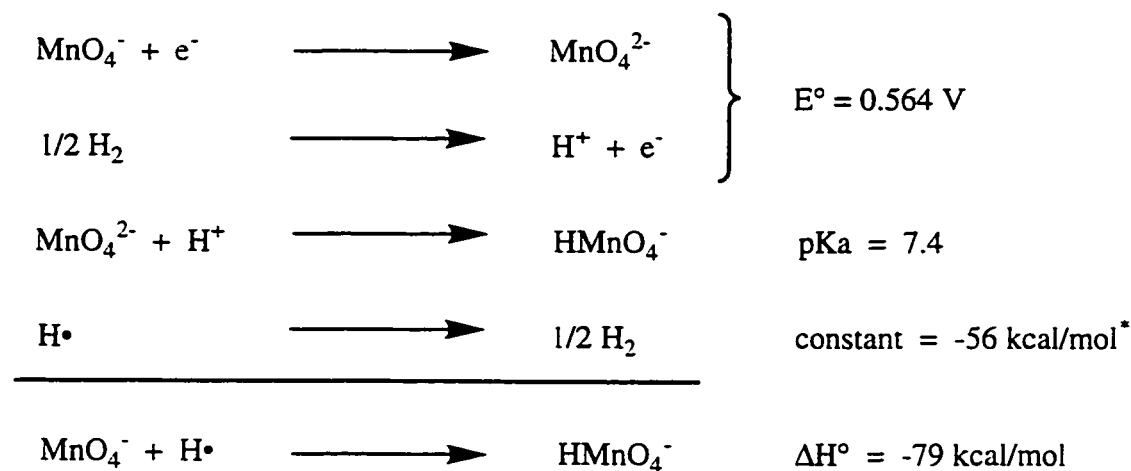
Hydrogen atom abstraction reactions exhibit small substituent effects and often do not show a linear Hammett correlation.<sup>12b,c,45</sup> Previous studies of permanganate oxidation of toluenes in aqueous acetic acid, which proceed much faster than the reactions described here, have suggested Hammett  $\rho$  values of -1.5<sup>7c,10</sup> and -2.8.<sup>65</sup> A more valuable comparison is with hydrogen atom abstraction with <sup>t</sup>BuOO•, where the relative rates are (after the statistical adjustment for the number of methyl groups in *p*-xylene): *p*-xylene, 1.8; toluene, 1; *p*-chlorotoluene, 1; 4-methylacetophenone, 0.3.<sup>66</sup> The analogous values for <sup>n</sup>Bu<sub>4</sub>NMnO<sub>4</sub> are 3.3 : 1 : 8.1 : 9.6 (the last for 4-methylbenzophenone).

Permanganate is a slower and more selective hydrogen atom abstractor than <sup>t</sup>BuOO• (see below), so larger substituent effects are observed. The faster oxidation of electron-deficient toluenes by permanganate is surprising, both in light of the <sup>t</sup>BuOO• rates and the common pattern that electron withdrawing groups usually make molecules harder to oxidize. Perhaps the permanganate negative charge interacts a little more strongly with the more positive hydrogens of *p*-chlorotoluene and 4-methylbenzophenone.



**IV. Understanding the Rate Constants: Bond Strengths and Linear Free Energy Correlations.** We have proposed that the reason that permanganate and related oxidants can abstract hydrogen atoms ( $\text{H}\cdot$ ) from organic substrates is because of the strong bond they form on addition of  $\text{H}\cdot$ .<sup>5,6</sup> The data reported here provide strong support for this hypothesis. Our perspective based on bond strengths and enthalpy changes contrasts with the standard chemical intuition that an oxidant needs to be a radical in order to perform hydrogen atom abstraction. This intuition is an implicit assumption in many mechanistic proposals for hydrocarbon oxidation, not only with homogeneous reagents such as permanganate but also regarding metalloenzymes and industrial heterogeneous catalysts.<sup>67</sup> Permanganate does not fit with this intuition because it is a closed-shell, diamagnetic species, and there is no evidence from spectroscopic studies<sup>68</sup> for a thermally accessible triplet state. It should be noted that it is spin-allowed for two diamagnetic species to react and form a singlet radical pair, as in eq 10. An organic example of  $\text{H}\cdot$  transfer between diamagnetic molecules is provided by the reactions of  $\alpha$ -methylstyrene with dihydroanthracene and xanthene at 300 °C<sup>69</sup> (and it is not clear that the need for a spin change leads to an extra activation barrier in transition metal complexes<sup>70</sup>).

The enthalpy for addition of  $\text{H}\cdot$  to permanganate, which is the magnitude of the O–H bond strength in  $\text{HMnO}_4^-$ , can be calculated from the thermochemical cycle in Scheme 1. Such cycles have been used by Bordwell and others to determine bond strengths to hydrogen in many organic and organometallic compounds.<sup>71</sup> Because enthalpies are path independent, the affinity of  $\text{MnO}_4^-$  for  $\text{H}\cdot$  is equivalent to its affinity for an electron (its redox potential,  $E^\circ$ ) and a proton (the acid dissociation constant,  $K_a$  of  $\text{HMnO}_4^-$ ). Scheme 1 is slightly different from those we have reported previously,<sup>5,6</sup> in part because a recent pulse radiolysis study provides a new value for the  $\text{pK}_a$  of  $\text{HMnO}_4^-$ .



$$^* \text{ constant} = \Delta H^\circ\{\text{H}\cdot(\text{g}) \rightarrow 1/2 \text{H}_2(\text{g})\} - \Delta H^\circ\{\text{H}\cdot(\text{g}) \rightarrow \text{H}\cdot(\text{aq})\} - 1/2 \text{TS}^\circ\{\text{H}_2(\text{g})\}$$

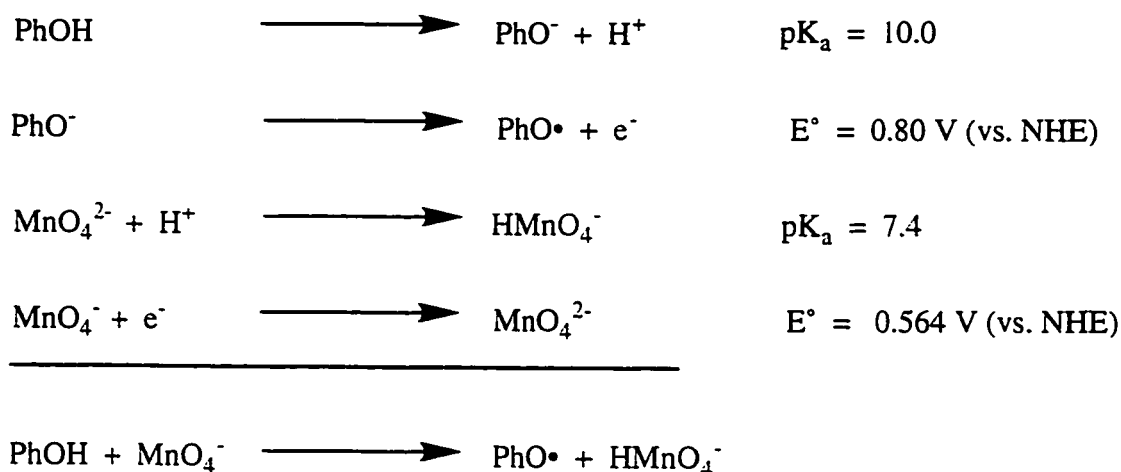
**Scheme 1.** Calculation of the O–H bond strength in  $\text{O}_3\text{MnO-H}\cdot$  through a thermodynamic cycle involving addition of  $\text{H}\cdot$  to  $\text{MnO}_4^-$ .

kcal/mol. The constant  $C$  can be calculated from standard values, with the assumptions that the entropies of  $\text{MnO}_4^-$  and  $\text{HMnO}_4^-$  are equal and that the solvation of  $\text{H}\cdot$  is well approximated by the solvation of  $\text{H}_2$ .<sup>75</sup>

$$\text{BDE}(\text{H-OMnO}_3^-) = 23.06E^\circ + 1.37\text{p}K_a - C \quad (11)$$

$$\text{where } C = \Delta H^\circ\{\text{H}\cdot(\text{g}) \rightarrow 1/2\text{H}_2(\text{g})\} - \Delta H^\circ\{\text{H}\cdot(\text{g}) \rightarrow \text{H}\cdot(\text{aq})\} - 1/2\text{TS}^\circ\{\text{H}_2(\text{g})\}$$

Alternatively, the constant is not needed if relative bond strengths are calculated from a thermodynamic cycle where the hydrogen atom is transferred from another species, HA (HA = PhOH or PhNH<sub>2</sub>), as in Scheme 2 where phenol is used. The standard free energy  $\Delta G^\circ$  is calculated from the known  $E^\circ$  and  $K_a$  values<sup>78</sup> and is taken to be equal to  $\Delta H^\circ$  because  $\Delta S^\circ \cong 0$ .



**Scheme 2.** Calculation of the Enthalpy for Transfer of  $\text{H}\cdot$  from Phenol Through a Thermodynamic Cycle.

The derived  $\Delta H^\circ$  is the difference between the H–OMnO<sub>3</sub><sup>-</sup> and H–A bond strengths. This calculation is expressed algebraically in eq 12. Calculations with either phenol or aniline as the hydrogen atom donor give 79 kcal/mol for the H–OMnO<sub>3</sub><sup>-</sup> bond strength.

$$\begin{aligned} \Delta H^\circ &= \text{BDE (H-A)} - \text{BDE (H-OMnO}_3^-) \\ &= 23.06 [E^\circ(\text{A}\cdot) - E^\circ(\text{MnO}_4^-)] + 1.37 [\text{pK}_a(\text{HA}) - \text{pK}_a(\text{HMnO}_4^-)] \end{aligned} \quad (12)$$

The O–H bond strength of 79 kcal/mol in HMnO<sub>4</sub><sup>-</sup> is 10 kcal/mol weaker than the O–H bond in <sup>t</sup>BuOOH (89 kcal/mol)<sup>79</sup> and is in between the H–Br and H–I bond strengths of 87 and 71 kcal/mol. Thermodynamically, permanganate is a less potent version of <sup>t</sup>BuOO• or Br• -- with the important difference that permanganate is a stable species that can be put in a bottle, not a short lived intermediate. Since <sup>t</sup>BuOO• or Br• readily abstract H• from alkylaromatic compounds, it is not surprising that permanganate does as well. This qualitative perspective -- that hydrogen atom abstracting reactivity depends on bond strengths -- is a valuable insight into the reactivity of permanganate. The bond strengths are critical because  $\Delta H^\circ$  for a hydrogen atom transfer reaction is the difference between the strength of the bond being broken and that being formed. An oxidant or active site must have enough thermodynamic affinity for H• so that the reaction is not too enthalpically uphill, since  $\Delta H^\ddagger$  is always greater than  $\Delta H^\circ$ . The permanganate reactions discussed here vary from 10 kcal/mol uphill for H• abstraction from toluene to 5 kcal/mol downhill for abstraction from xanthene (Table 3).

Formation of a strong bond to a hydrogen atom is not only a *necessary* condition for H• transfer -- the data suggest that it is a *sufficient* condition as well. It is well established that rates of hydrogen atom abstraction by main-group radicals are directly related to bond strengths. OH• reacts with almost all organic compounds at close to the diffusion limit<sup>80</sup> because it forms such a strong bond to H• (119 kcal/mol<sup>76</sup>) while <sup>t</sup>BuOO• is a much less reactive oxidant<sup>81</sup> because it forms a weaker O–H bond of 89 kcal/mol.<sup>76</sup>

Evans and Polanyi suggested (in 1936) a linear relationship between activation energies and net enthalpy change in hydrogen atom transfer reactions (eq 13), and this correlation works quite well over a narrow range of  $\Delta H^\circ$  for similar radicals and substrates.<sup>82</sup> Over a wider range,  $\alpha \rightarrow 0$  as the reactions get very exothermic and  $\alpha \rightarrow 1$  as the reactions get very endothermic.

$$E_a = \beta + \alpha(\Delta H), \quad \text{or } \log k \propto \Delta G^\ddagger = \beta + \alpha(\Delta H) \quad (13)$$

The data reported here fit the Polanyi equation well, in two different ways. First, enthalpies of activation for oxidation of the different arylalkanes by  ${}^n\text{Bu}_4\text{NMnO}_4$  are directly proportional to  $\Delta H^\circ$  (Figure 11). The linearity of this relation over the 15 kcal/mol range of  $\Delta H^\circ$  is very good, especially given the large uncertainties in some of the C–H bond strengths. The slope of the best fit straight line,  $\alpha$ , is 0.69. In terms of reactivity, this translates into a 0.69 kcal/mol increase in activation barrier for every 1 kcal/mol increase in C–H bond strength. For reactions that are fairly close to thermoneutral, as these are, a  $\alpha$  value of 0.69 is in agreement with predictions from the Hammond postulate. An equivalent correlation is seen between  $\Delta G^\ddagger$  (or  $\log k_2$ ) and  $\Delta H^\circ$ , because the entropies of activation are essentially constant. These correlations of rate constants and activation parameters with C–H bond strengths strongly support the assignment of the rate-determining step as hydrogen atom transfer from carbon to an oxo group. If there were any manganese-carbon bond formation, as in a [2+2] mechanism for instance, significant steric effects would be observed. Rather, rates of abstraction from primary, secondary, and tertiary C–H bonds all fit on the same line.

The rate of hydrogen atom transfer from toluene to  ${}^n\text{Bu}_4\text{NMnO}_4$  also correlates with rates of abstraction by  $\text{OH}\cdot$ ,  ${}^t\text{BuO}\cdot$ , and  ${}^t\text{BuOO}\cdot$  (Figure 12). Similar relations are observed for ethylbenzene and diphenylmethane, where sufficient data exist (Figures 13

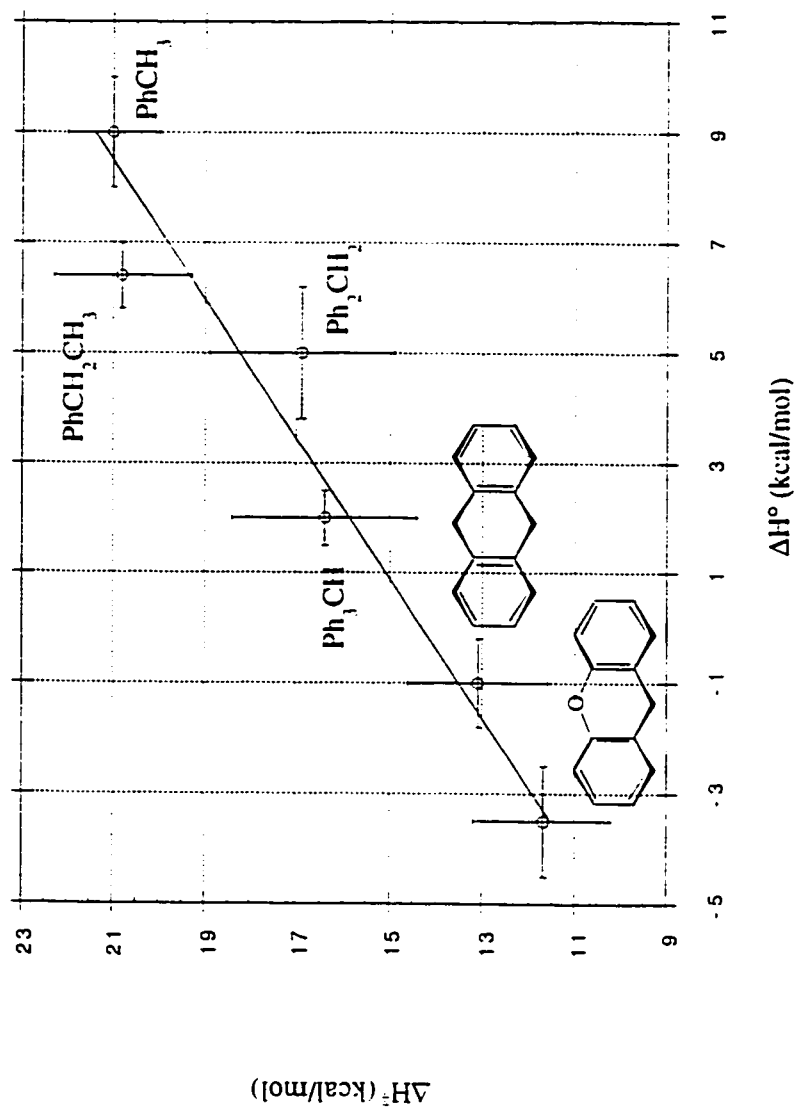


**Figure 11.** Plot of  $\Delta H^\ddagger$  vs.  $\Delta H^\circ$  for the hydrogen atom transfer step in reactions of  $n\text{Bu}_4\text{NMnO}_4$  with toluene, ethylbenzene, diphenylmethane, triphenylmethane, 9,10-dihydroanthracene, and xanthene.

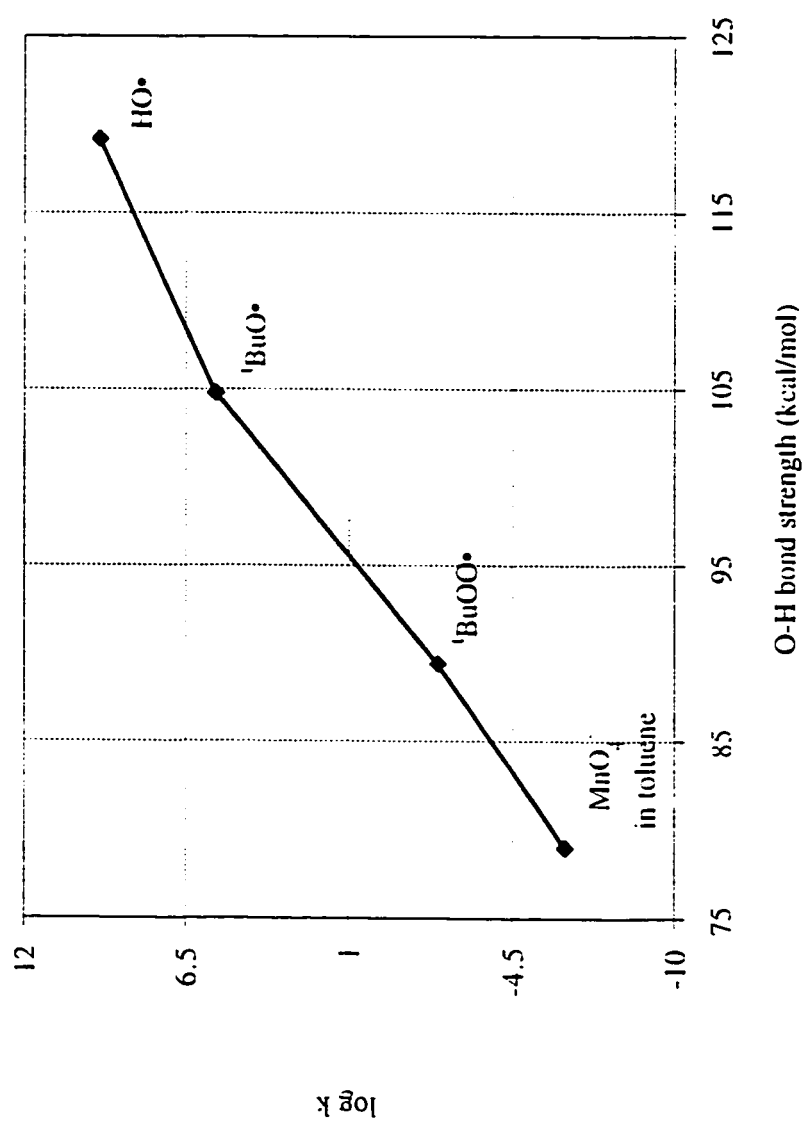


**Figure 12.** Rate of hydrogen atom abstraction from toluene by HO•, tBuO•, tBuOO•, and MnO<sub>4</sub><sup>-</sup> at 25-30 °C in toluene solvent vs. the strength of the O-H bond formed.

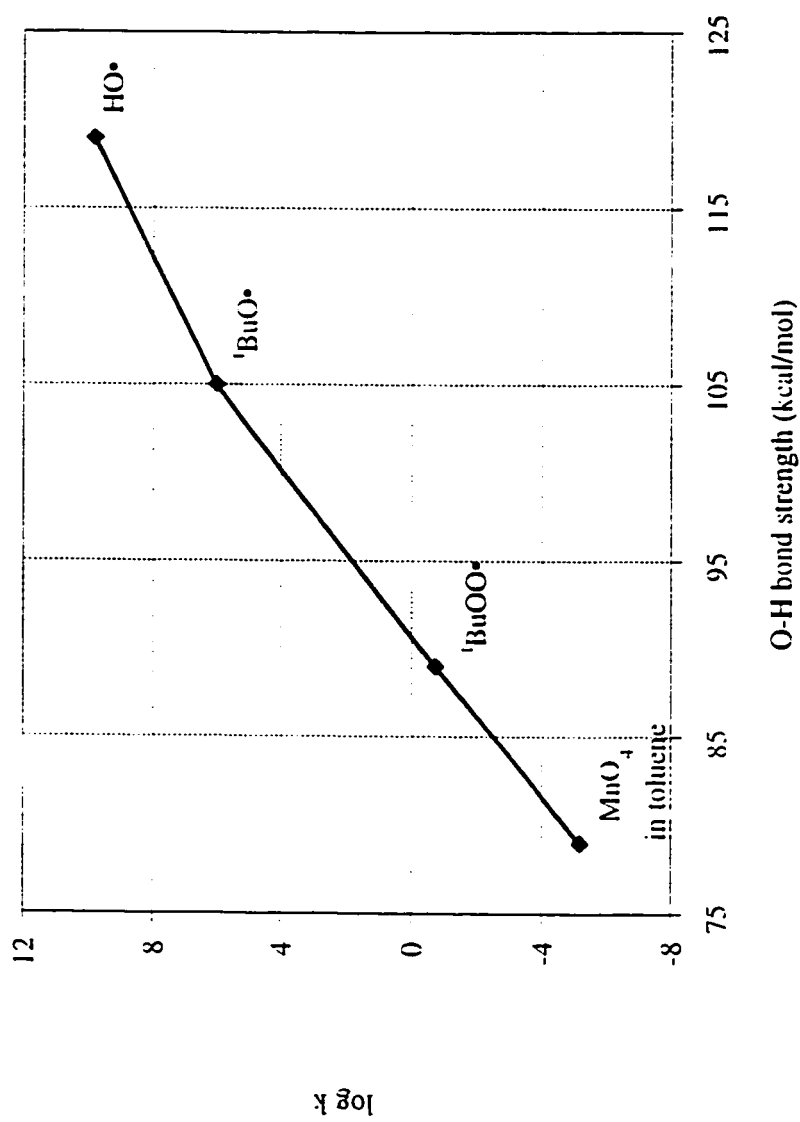


**Figure 13.** Rate of hydrogen atom abstraction from ethylbenzene by  $\text{HO}\cdot$ ,  $t\text{BuO}\cdot$ ,  $t\text{BuOO}\cdot$ , and  $\text{MnO}_4^-$  at 25-30 °C in toluene solvent vs. the strength of the O-H bond formed.

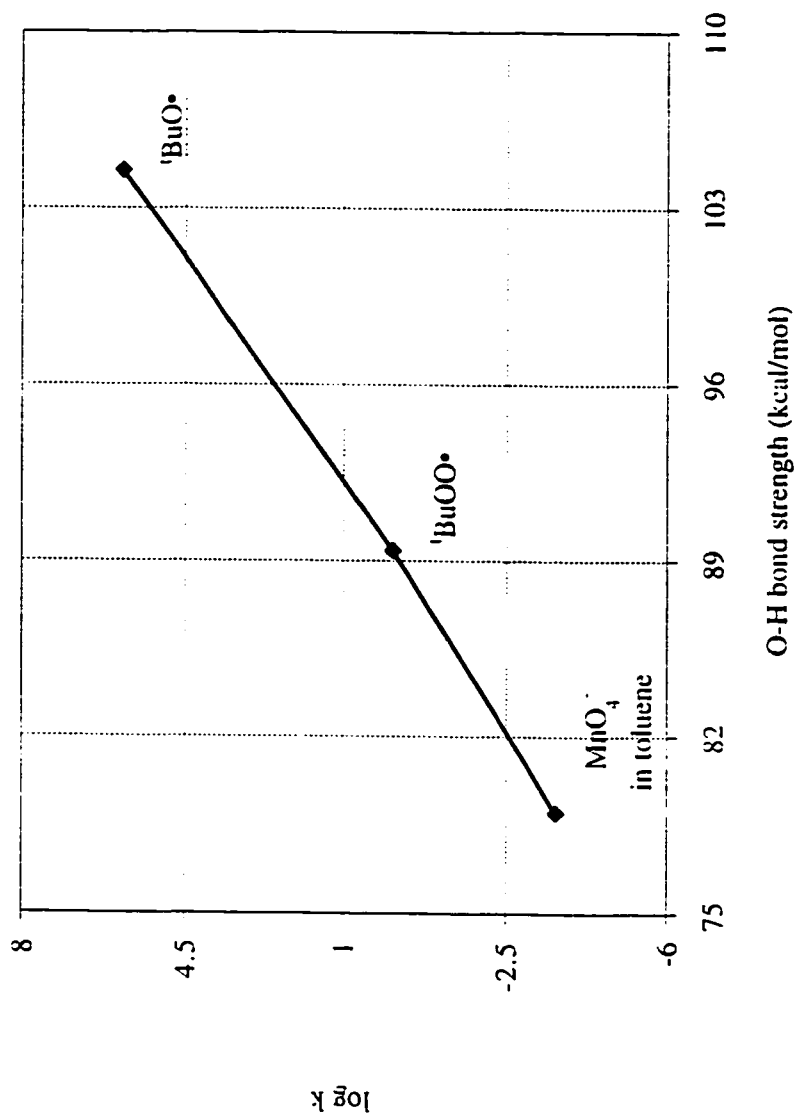


**Figure 14.** Rate of hydrogen atom abstraction from diphenylmethane by  $t\text{BuO}\cdot$ ,  $t\text{BuOO}\cdot$ , and  $\text{MnO}_4^-$  at 25-30 °C in toluene solvent vs. the strength of the O-H bond formed.

and 14). This is the second kind of Polanyi correlation, for reactions of one substrate with a range of oxidants. These correlations are not precise, with uncertainties of at least an order of magnitude over the ca.  $10^{16}$  range of rate constants plotted. But the permanganate reactions fit right on the lines. Thus *permanganate acts just as one would predict for an oxygen radical that makes a 79 kcal/mol bond to a hydrogen atom*. The similarity of permanganate to oxygen radicals is remarkable given that permanganate is a diamagnetic, closed shell species. The frontier orbitals of the hydrogen atom transfer reaction are different in the radical vs. the closed-shell case, as discussed elsewhere.<sup>5c</sup> These data indicate that, at least for metal-oxo species such as permanganate, the primary determinant of hydrogen atom abstraction reactivity is the strength of the O–H bond formed, rather than details of the electronic structure of the oxidant. These conclusions should apply equally well to metal-oxo species in enzyme active sites and on the surface of a heterogeneous catalyst. Preliminary studies of  $\mu$ -oxo compounds and coordination complexes are qualitatively supportive of these ideas.<sup>88</sup>

## Conclusions

In toluene solvent,  ${}^n\text{Bu}_4\text{NMnO}_4$  oxidizes arylalkanes with weak C–H bonds by dehydrogenation and/or oxygenation. For instance, toluene is converted mostly to benzoic acid, xanthene to xanthone, and dihydroanthracene to anthracene. For all of the substrates examined, the initial reactions are first order with respect to the concentration of both  ${}^n\text{Bu}_4\text{NMnO}_4$  and substrate with no apparent induction periods. Significant primary isotope effects are observed for the reactions of toluene and dihydroanthracene. The addition of  $\text{O}_2$  to a solution of  ${}^n\text{Bu}_4\text{NMnO}_4$  in toluene accelerates the disappearance of permanganate, indicating that organic radicals are formed during the course of the reaction.  ${}^n\text{Bu}_4\text{NMnO}_4$  oxidizes all of the substrates through a common rate determining step in which a hydrogen atom is transferred from the substrate to a manganese-oxo group. The

enthalpies of activation correlate with the strength of the C–H bond being cleaved, as is typical of hydrogen atom abstraction by main group radicals such as  ${}^t\text{BuOO}\cdot$ . This correlation includes primary, secondary, and tertiary C–H bonds, with no evidence of steric effects that should accompany formation of a metal-carbon bond.

Permanganate can abstract a hydrogen atom from organic substrates because it has a high thermodynamic affinity for  $\text{H}\cdot$ . The  $\Delta\text{H}^\circ$  for addition of  $\text{H}\cdot$  to  $\text{MnO}_4^-$  to give  $\text{HMnO}_4^-$  in aqueous solution is calculated to be  $-79$  kcal/mol using a thermochemical cycle. Using this value, the rates of  ${}^n\text{Bu}_4\text{NMnO}_4$  oxidation of toluene, ethylbenzene, and diphenylmethane are shown to correlate with the rates of hydrogen atom abstraction by the oxygen radicals  $\text{OH}\cdot$ ,  ${}^t\text{BuO}\cdot$ , and  ${}^t\text{BuOO}\cdot$ . Thus permanganate reacts just as one would predict for an oxygen radical that makes a  $79$  kcal/mol bond with a hydrogen atom. This behavior is in spite of the fact that permanganate is a diamagnetic, closed shell species, with no radical character. It is concluded that *for metal-oxo oxidants, a high thermodynamic affinity for  $\text{H}\cdot$  is necessary and sufficient for hydrogen atom-abstrating reactivity.*

## **CHAPTER 2**

## Introduction

Traditionally, mechanistic studies of permanganate oxidations have been performed in aqueous solution, most often strongly acidic or basic solution.<sup>7</sup> The reason for the use of water as a solvent is that the most readily available form of permanganate, its potassium salt, is highly soluble in water and stable in the absence of a substrate. For oxidations of hydrocarbons, an aqueous solvent is somewhat problematic, as most hydrocarbons have limited solubility in water, at best. Toluene is an arylalkane which is amenable to study under these conditions. In water, toluene has a slight solubility, approximately 5 mM at room temperature. Additionally, permanganate is reactive enough with toluene that the kinetics of the reaction can be examined on a reasonable time scale.

In Chapter 1, the reaction of toluene with permanganate was examined in neat toluene and established to proceed by a one electron pathway, hydrogen atom transfer. A single study under a specific set of conditions is not definitive for permanganate reacting with a given substrate, however. The literature of permanganate oxidations of organic compounds contains many examples of reactions where slight changes in reaction conditions cause dramatic differences in reactivity or reaction pathway. Reactions with toluene perhaps best illustrate this point.

Four mechanistic studies have been published on the oxidation of toluene by permanganate in aqueous acidic solution. The first study, reported in 1955,<sup>10a</sup> found that the reaction produced benzoic acid, accelerated as the pH decreased, and was inhibited upon addition of  $F^-$  which is known to complex  $Mn^{3+}$ . Cullis and Ladbury concluded that the active oxidant was  $Mn^{3+}$  and the mechanism went through radical intermediates. Under almost identical conditions, Radhakrishnamurti and Mahapatro<sup>65</sup> observed faster rates, no inhibition with addition of  $F^-$ , and significant substituent effects ( $\rho^+ = -2.4$  for a Hammett study of various substituted toluenes). They also favored a radical reaction pathway, but concluded that permanganate was the active oxidant. In stark contrast to

these studies is the work of Stewart and Spitzer,<sup>8</sup> who examined the oxidation of toluene in aqueous trifluoroacetic acid. Although the acid concentration was comparable to that in the aqueous acetic acid studies, trifluoroacetic acid apparently converted permanganate to  $\text{MnO}_3^+$ , a much stronger oxidant. Ring attack was the dominant reaction pathway and the reaction accelerated as the pH was decreased.

The most recent study of toluene oxidation by permanganate in aqueous solution was published while the work presented in this Chapter was in progress.<sup>89</sup> It is also the most relevant to the study reported in here. Over the pH range 5 to 7, in the presence of perchlorate, the oxidation of benzene, toluene, ethylbenzene, cumene, and several other arylalkanes was examined. Lobachev and Rudakov concluded that the reaction proceeded by attack of permanganate on the benzylic C-H bond to produce radicals, similar to the mechanism proposed by Brauman and Pandell in their study of the oxidation of a tertiary C-H bond by permanganate.<sup>9a</sup>

These four studies show how seemingly small changes, such as pH, buffering species, or substrate, can affect the reaction pathway that permanganate chooses. In toluene, the reaction of permanganate with toluene was demonstrated (in Chapter 1) to proceed by hydrogen atom transfer. The literature discussed above suggests a radical pathway in acidic water as well,<sup>10a,65,89</sup> although the details of the mechanism or mechanisms are unclear. Our re-examination of this reaction in water focuses on a regime not studied previously--aqueous solution at pH 7 and higher. Toluene was examined in detail and a mechanism for the rate determining step proposed on the basis of those results.<sup>6</sup> Subsequent studies of ethylbenzene and cumene reactions under the same conditions have raised doubts about the mechanism or at least its generality in this series of substrates. This Chapter presents all of the results, evaluates the possible mechanistic pathways in light of the experimental evidence, and proposes experiments, where practical, to further elucidate the mechanism.

## Experimental

**General.** All reactions were done in the absence of air unless otherwise noted. All aqueous solutions were purged of oxygen by bubbling Ar or N<sub>2</sub> through the solution for 15 minutes just prior to use. The pH of the buffer solutions was measured using a Corning 220 pH meter and a Corning general purpose combination electrode.

**Materials.** KMnO<sub>4</sub> (99.3%, Baker) was recrystallized twice from water and stored in the dark. Millipore water was used in the preparation of all aqueous solutions. KH<sub>2</sub>PO<sub>4</sub> ('Baker Analyzed': 101.2%), K<sub>2</sub>HPO<sub>4</sub> ('Baker Analyzed': 99.0%), NaHCO<sub>3</sub> ('Baker Analyzed': 100.2%), Na<sub>2</sub>CO<sub>3</sub> (Mallinckrodt), and NaOH ('Baker Analyzed': 98.5%) were used as received in the preparation of buffer solutions.

Toluene (100.0%, Baker), ethylbenzene (99.8%, Aldrich), cumene (99%, Aldrich) and *d*<sub>8</sub>-toluene (100.0%, Cambridge Isotope Laboratories) were used as received. Substituted toluenes for aqueous studies--*p*-nitrotoluene (Matheson), *p*-toluic acid (Eastman), *p*-chlorotoluene (98%, Aldrich), *p*-xylene (99+%, Aldrich), *p*-toluenesulfonic acid (99%, Baker) and *d*<sub>8</sub>-toluene (Cambridge Isotope Laboratories) were used as received.

<sup>18</sup>O labelled KMnO<sub>4</sub> was prepared according to a literature procedure by placing KMnO<sub>4</sub> and 20% <sup>18</sup>O labelled water (Cambridge Isotope Laboratories) in a sealed vessel and heating to 90 °C for 24 hours. The water was removed under vacuum. To purify the enriched KMnO<sub>4</sub>, it was dissolved in unlabelled water at room temperature, filtered through a fine frit to separate the MnO<sub>2</sub>, and the water removed under vacuum. The <sup>18</sup>O enrichment was determined to be 10% by negative ion electrospray mass spectrometry,<sup>90</sup> recently demonstrated to be a valid mass spectrometric technique for analyzing permanganate.<sup>91</sup> The <sup>18</sup>O labelled water used as a solvent for experiments designed to

determine the origin of the oxygen in the organic product was 70% enriched (Cambridge Isotope Laboratories).

**Kinetics** All kinetics experiments were followed by optical spectroscopy, using a Hewlett Packard 8452A diode array spectrophotometer scanning over the range 400 to 640 nm. The temperature of the solution in the cuvette was held constant ( $\pm 0.1$  °C) using either a custom built aluminum block cell holder connected to a Peltier electronic control module or a Hewlett Packard water jacketed cell holder connected to a circulating water bath (Lauda model K-2/R).

Reactions in aqueous solutions were monitored using a cuvette built to minimize head space and allow injections. This cell and the special considerations required for studying these solutions are described in detail in Appendix B. In a typical kinetics experiment,  $3.2 (\pm 0.2)$  mL of degassed  $3.97$  mM  $K_2HPO_4/4.00$  mM  $KH_2PO_4$  solution was placed in the cuvette which had been flushed with  $N_2$  for 5 minutes. Toluene ( $2.4 \pm 0.2$   $\mu$ L) was added and the cuvette was sealed. The toluene was dissolved by heating the cuvette in the cell holder for 30 minutes at  $75.0$  °C: note that the compact cuvette design allows all of the solution and head space to be within the heated volume. A background scan was taken of this solution. A concentrated  $KMnO_4$  solution,  $80.0 (\pm 0.1)$  mg of  $KMnO_4$  in  $10.00 (\pm 0.02)$  mL of phosphate buffer, was filtered through a fine frit to remove any  $MnO_2$  and  $25.0 (\pm 0.3)$   $\mu$ L was injected into the sealed cuvette. The cuvette was removed from the cell holder, shaken, replaced, and data collection was started. A similar technique was used to prepare the solutions for the Hammett study. For substrates which were solids, the appropriate amounts were weighed out and added directly to the  $N_2$  flushed cuvette before addition of the degassed buffer solution.

**Data Analysis.** For all of the reactions, the disappearance of  $MnO_4^-$  and corresponding appearance of  $MnO_2$  were followed by optical spectroscopy, over the range 400 to 640 nm. The  $MnO_2$  which forms is colloidal, but fairly stable to coagulation.

apparently as a result of a buildup of negative charge on the surface of the particles.<sup>15,56</sup> Under these conditions then, while the product is a colloid, it is well-behaved spectroscopically, as evidenced by the formation of isosbestic points (Figure 15). This allows the kinetic data to be analyzed, although this procedure is not straightforward. The data analysis is described in detail in Appendix A. The method results in the calculation of four observed rate constants calculated for each kinetics experiment. The rate constants reported in Table 5 are the average of the four values with the errors reflecting  $3\sigma$ , as a percentage of the average rate constant.

**Manganese Oxidation State Determinations.** The final average manganese oxidation state for aqueous reactions of  $\text{MnO}_4^-$  was determined by iodometric titration, a well established technique for  $\text{MnO}_2$ .<sup>92</sup> The reaction mixture to be analyzed was prepared by degassing 25.00 ( $\pm 0.03$ ) mL of 4.00 mM  $\text{KH}_2\text{PO}_4$ /3.98 mM  $\text{K}_2\text{HPO}_4$  in a glass vessel by bubbling Ar through the solution for 15 minutes. By syringe, 13.0 ( $\pm 0.3$ )  $\mu\text{L}$  of toluene and 250 ( $\pm 2$ )  $\mu\text{L}$  of 61.6 mM  $\text{KMnO}_4$  solution were added. The vessel was sealed with a Teflon stopcock and placed in a 75 °C stirred water bath for 5 hours. The contents were cooled to room temperature and quantitatively transferred to an Erlenmeyer flask. The flask was purged with a flow of  $\text{N}_2$  for 5 minutes. Concentrated HCl (1 mL) and KI solution (3.6 mL,  $9.2 \times 10^{-2}$  M) were added and the mixture allowed to stand for 5 minutes to insure complete formation of  $\text{I}_3^-$ . The  $\text{I}_3^-$  was backtitrated with  $3.13 (\pm 0.02) \times 10^{-2}$  M  $\text{Na}_2\text{S}_2\text{O}_3$  solution (concentration determined by titration against  $\text{K}_2\text{Cr}_2\text{O}_7$  primary standard the same day) by rapid addition until the yellow color began to fade. Starch indicator solution (0.5 mL; prepared by dissolving soluble starch in boiling water) was then added and the titration completed as indicated by the disappearance of the blue starch- $\text{I}_3^-$  complex. A total of 0.98 mL of  $\text{Na}_2\text{S}_2\text{O}_3$  solution was used.

**Organic Product Analyses.** For the aqueous reactions, the organic products were identified by comparison of their HPLC retention times with authentic

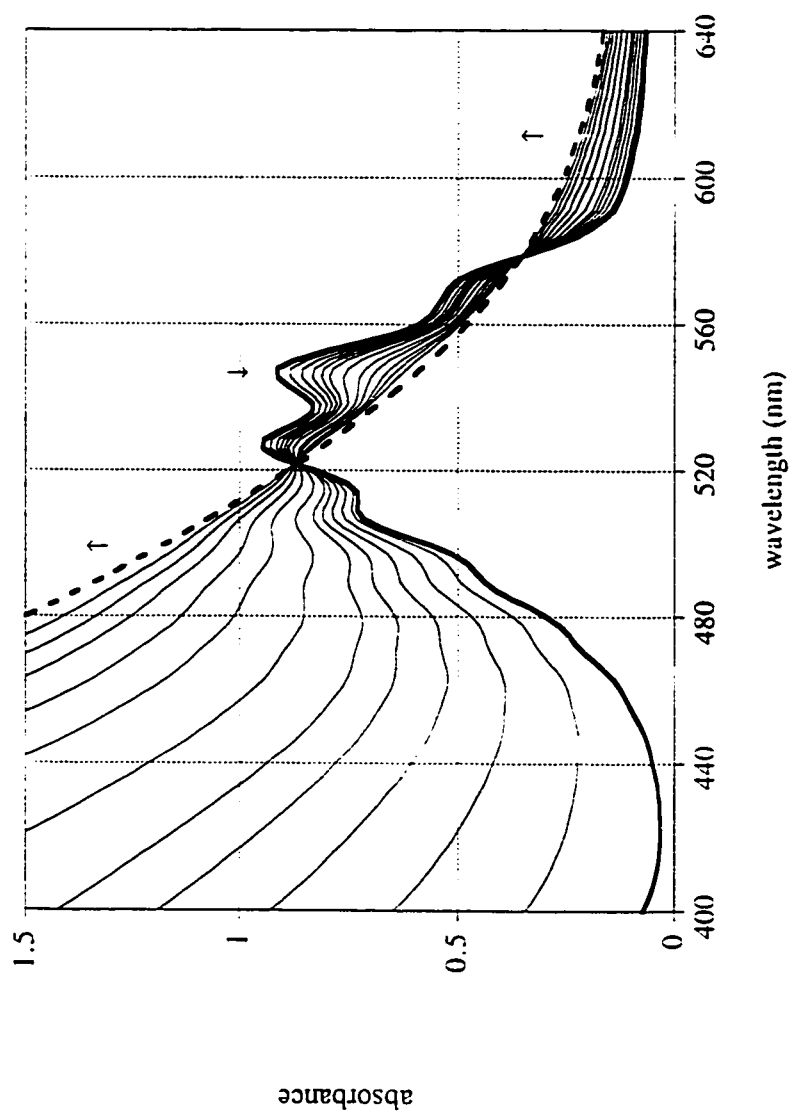


**Figure 15.** Overlay of UV/vis spectra from the reaction of toluene with  $\text{KMnO}_4$  in aqueous solution, pH 7, at 75 °C.

samples. Quantification of the oxidation products relied on HPLC, using potassium hydrogen phthalate (KHP) as an internal standard to generate a calibration curve. HPLC analyses were performed on a Hitachi system consisting of a L-6200 pump connected to a L-4250 UV/vis detector interfaced to a D-2500 integrator. A Beckman Ultrasphere ODS (25 cm/4.6 mm) reverse phase column was employed for the separations. All analyses were performed under isocratic conditions with a solvent consisting of 80% Millipore water, 20% acetonitrile, and 0.1% TFA.

In a typical procedure, a greaseless Pyrex vessel sealed with a Teflon valve was loaded sequentially with  $20.00 \pm 0.03$  mL of degassed phosphate buffer (4 mM  $\text{KH}_2\text{PO}_4$ /4 mM  $\text{K}_2\text{HPO}_4$ ),  $25.0 \pm 0.3$   $\mu\text{L}$  of ethylbenzene, and  $200 \pm 2$   $\mu\text{L}$  aliquot of a concentrated  $\text{KMnO}_4$  solution ( $65.1 \pm 0.1$  mg of  $\text{KMnO}_4$  in  $5.00 \pm 0.02$  mL of phosphate buffer). The sealed vessel was heated to  $75.0 (\pm 0.1)$  °C for 90 min, then rapidly cooled to room temperature. The Teflon valve was opened and 0.1 - 0.2 g of solid KI and 200  $\mu\text{L}$  of concentrated HCl were added to destroy the colloidal  $\text{MnO}_2$  (necessary because some of the oxidation products are bound to the colloid<sup>30</sup>). Alternatively, the  $\text{MnO}_2$  was reduced by addition of solid  $\text{NaHSO}_3$ . A solution was prepared for HPLC analysis by combining 200  $\mu\text{L}$  of the reaction solution and 200  $\mu\text{L}$  of 0.989 mM KHP solution.

**Experiments in the Presence of  $\text{O}_2$ .** Since the headspace size has an influence on the toluene concentration in the reaction mixture and the toluene concentration is related to the reaction rate, this experiment was done in the special cuvette and followed spectrophotometrically to compare to  $\text{O}_2$ -free reactions. The pH 7 phosphate buffer solution was sparged with  $\text{O}_2$  for 15 minutes. The cuvette was filled with  $3.2 (\pm 0.2)$  mL of the  $\text{O}_2$  saturated solution,  $2.4 (\pm 0.2)$   $\mu\text{L}$  of toluene, and sealed. The cuvette was heated to 75 °C in the Peltier cell holder and used to take a background scan. A concentrated  $\text{KMnO}_4$  solution was prepared by dissolving  $41.2 (\pm 0.1)$  mg of  $\text{KMnO}_4$  in  $5.00 (\pm 0.02)$  mL of phosphate buffer solution and filtering it through a fine frit to remove

any  $\text{MnO}_2$ . After the solution in the cuvette was equilibrated,  $25.0 (\pm 0.2) \mu\text{L}$  of the  $\text{KMnO}_4$  solution was injected and kinetics data collection was started.

**Experiments with  $^{18}\text{O}$  Labelling.** The origin of the oxygen incorporated in the organic product from the reaction of cumene was examined by a series of product analysis experiments using  $^{18}\text{O}$  labelled solvent (70%  $^{18}\text{O}$  labelled  $\text{H}_2\text{O}$ ) or  $\text{MnO}_4^-$  (10%  $^{18}\text{O}$  labelled  $\text{KMnO}_4$ ). The reactions were done in sealed containers maintained at room temperature ( $24^\circ\text{C}$ ) in a stirred water bath. The amount of  $^{18}\text{O}$  present in the product was determined by analyzing the reaction solution by GCMS. The instrument used for the analyses was a Hewlett Packard 5890/5971 gas chromatograph-mass spectrometer.

Three experiments were performed. The solution to determine if the oxygen in cumyl alcohol exchanged with the oxygen in water was prepared by saturating  $^{18}\text{O}$  labelled  $\text{H}_2\text{O}$  with cumyl alcohol. The undissolved cumyl alcohol was left in the solution. A solution of cumene with  $^{18}\text{O}$  labelled  $\text{KMnO}_4$  in unlabelled water was prepared by degassing a portion of ordinary buffered solution by passing  $\text{N}_2$  through it for 15 minutes, placing it in a cuvette, and adding cumene and a small amount of solid 10%  $^{18}\text{O}$  labelled  $\text{KMnO}_4$ . The analogous solution using  $^{18}\text{O}$  labelled  $\text{H}_2\text{O}$  and unlabelled  $\text{KMnO}_4$  was prepared by placing approximately 1 mg each  $\text{KH}_2\text{PO}_4$  and  $\text{K}_2\text{HPO}_4$  in a small reaction vessel. To this,  $50 \mu\text{L}$  of  $^{18}\text{O}$  labelled  $\text{H}_2\text{O}$  (70%) was added and the solution was degassed by two freeze/pump/thaw cycles. The reaction vessel was filled with  $\text{N}_2$  and cumyl alcohol and a small amount of solid  $\text{KMnO}_4$  were added.

Ordinarily, the colloidal  $\text{MnO}_2$  must be destroyed in order to analyze the organic products as they are bound in and/or on the colloid. Reduction of the colloid requires acidic conditions, which might accelerate exchange of the oxygen atoms in the cumyl alcohol product with the solvent. To determine if this was occurring, each reaction solution was analyzed twice--before reduction of the colloid and after reduction of the colloid. The colloid was destroyed by adding a small amount of solid  $\text{NaHSO}_3$ .

## Results

Reactions of  $\text{KMnO}_4$  with toluene and ethylbenzene have been studied in aqueous buffered solutions. Under these conditions, the permanganate is stable in the absence of organic substrate, showing less than 2% decay over 4 hr at 65 °C. The organic substrate is always present in excess (pseudo-first order conditions), which is permitted by their small but significant solubility in water ( $\geq 1$  mM).<sup>40</sup> These solutions show a positive deviation from Raoult's law. There is a much higher vapor pressure of the organic substrate than would be predicted by its mole fraction. A special cuvette was constructed with minimal head space to insure that most of the substrate placed in the cell is in solution. The cell is described in Appendix B. The entire cuvette can be heated within the cell holder in the spectrometer to minimize temperature gradients. The kinetics of the reactions were monitored in this cuvette by visible spectroscopy (Figure 15), with the structured permanganate absorbance in the spectral region 400 to 640 nm changing to the sloping absorbance due to colloidal  $\text{MnO}_2$  (see below). The colloid is, in most cases, optically well behaved and obeys Beer's law, as indicated by the presence of isosbestic points (this has been observed previously<sup>12,41</sup>). Analysis of the optical data required modeling of the  $\text{MnO}_2$  absorbance, resulting in four rate constants for each data set. This is discussed in great detail in Appendix A. The rate constants given in Table 5 are the average of the four values. The associated errors are  $3\sigma$ , reported as a percentage of the average rate constant. For these aqueous studies, the error associated with a given kinetic experiment is typically the same as the error (defined as  $3\sigma$ ) between different experiments, typically 15-20%.

Toluene is slowly oxidized by potassium permanganate at room temperature in aqueous phosphate buffer (pH 7), taking nearly a week for the reaction to approach completion. First order plots are linear over 3 half-lives with no induction period (Figure

**Table 5.** Rate constants for reactions of toluene, ethylbenzene, and related substrates with  $\text{KMnO}_4$  in aqueous solution.

$[\text{MnO}_4^-]$ (mM)	substrate concentration (mM)	T (°C)	$k_2$ ( $\text{M}^{-1}\text{s}^{-1}$ )	data analysis error <sup>a</sup>	pH
<i>Toluene</i>					
0.418	4.11	20	$7.34 \times 10^{-4}$	46%	6.87
0.302	4.11	21.1	$7.01 \times 10^{-4}$	25%	6.87
0.392	4.07	55.0	$8.14 \times 10^{-3}$	10%	6.87
0.392	4.07	65.0	$1.51 \times 10^{-2}$	15%	6.87
0.385	4.07	65.0	$1.52 \times 10^{-2}$	15%	6.87
0.392	6.98	75.0	$2.59 \times 10^{-2}$	18%	6.87
0.392	6.98	75.0	$3.13 \times 10^{-2}$	21%	6.87
0.392	3.49	75.0	$2.86 \times 10^{-2}$	16%	6.87
0.237	7.01	75.0	$2.82 \times 10^{-2}$	22%	6.87
0.404	6.98	75.0	$2.43 \times 10^{-2}$	19%	6.87
	$\text{O}_2$ saturated <sup>c</sup>				
0.394	6.98	85.0	$4.09 \times 10^{-2}$	18%	6.87
0.385	6.98	85.0	$3.87 \times 10^{-2}$	20%	6.87
0.395	6.98	95.0	$7.05 \times 10^{-2}$	86%	6.87
0.385	6.98	95.0	$7.85 \times 10^{-2}$	27%	6.87
0.418	4.11 ( <i>d</i> <sub>8</sub> -toluene)	20	$7.16 \times 10^{-5}$	10%	6.87
0.392	6.98	75.0	$2.72 \times 10^{-2}$	13%	7.81
0.390	6.98	75.0	$2.87 \times 10^{-2}$	23%	7.81

**Table 5.** (continued)

0.390	6.98	75.0	$2.31 \times 10^{-2}$	32%	5.83
0.392	6.98	75.0	$2.66 \times 10^{-2}$	14%	5.83
0.395	6.98	75.0	$2.77 \times 10^{-2}$	23%	8.83
0.392	6.98	75.0	$2.80 \times 10^{-2}$	26%	8.83
0.405	6.69	75.0	$2.65 \times 10^{-2}$	14%	10.80
0.401	6.69	75.0	$8.1 \times 10^{-2} d$	18%	13 <sup>e</sup>
0.401	4.46	75.0	$3.4 \times 10^{-1} d$	7.5%	14 <sup>e</sup>
0.399	2.97	75.0	$9.2 \times 10^{-1} d$	2.7%	14.3 <sup>e</sup>
0.389	6.69	75.0	$2.68 \times 10^{-2}$	27%	pD = 7 <sup>f</sup>
<i>Substituted toluenes</i>					
0.381	2.9 CH <sub>3</sub> C <sub>6</sub> H <sub>4</sub> CO <sub>2</sub> <sup>-</sup>	75.0	$2.5 \times 10^{-2}$	38%	7 <sup>b</sup>
0.406	2.0 CH <sub>3</sub> C <sub>6</sub> H <sub>4</sub> CH <sub>3</sub>	75.0	$3.3 \times 10^{-2}$	25%	7 <sup>b</sup>
0.390	2.2 CH <sub>3</sub> C <sub>6</sub> H <sub>4</sub> CH <sub>3</sub>	75.0	$8.8 \times 10^{-2}$	15%	7 <sup>b</sup>
0.385	49.7 CH <sub>3</sub> C <sub>6</sub> H <sub>4</sub> SO <sub>3</sub> <sup>-</sup>	75.0	$2.60 \times 10^{-2}$	26%	7 <sup>b</sup>
0.386	2.2 CH <sub>3</sub> C <sub>6</sub> H <sub>4</sub> NO <sub>2</sub>	75.0	$2.4 \times 10^{-2}$	23%	7 <sup>b</sup>
<i>Ethylbenzene</i>					
0.211	2.93	45.0	$3.11 \times 10^{-2}$	13%	7 <sup>b</sup>
0.109	1.47	45.0	$3.54 \times 10^{-2}$	10%	7 <sup>b</sup>
0.219	2.15	75.0	$1.43 \times 10^{-1}$	13%	7 <sup>b</sup>
0.110	1.44	75.0	$1.51 \times 10^{-1}$	10%	7 <sup>b</sup>
0.110	1.43	85.0	$2.38 \times 10^{-1}$	15%	7 <sup>b</sup>

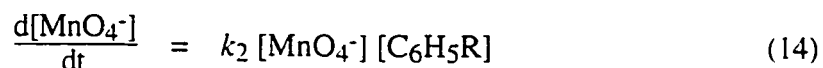
**Table 5.** (continued)

<i>Cumene</i>					
0.108	1.15	45.0	$1.74 \times 10^{-2}$	<i>g</i>	<i>7b</i>
0.202	1.15	55.0	$3.49 \times 10^{-2}$	<i>g</i>	<i>7b</i>
0.228	1.15	65.0	$5.74 \times 10^{-2}$	<i>g</i>	<i>7b</i>
0.190	1.15	75.0	$9.09 \times 10^{-2}$	<i>g</i>	<i>7b</i>

<sup>a</sup> Range of four rate constants derived from analysis of a single kinetics run (see Experimental Section and Appendix A). <sup>b</sup> pH as measured, except for those listed as pH 7 which were prepared as for the solutions whose pH was found to be 6.87, but their pH values were never specifically measured. <sup>c</sup> The buffer solution was sparged with O<sub>2</sub> for 15 minutes before being sealed in the reaction vessel. The O<sub>2</sub> concentration is calculated to be 0.79 mM at 70 °C, under 1 atm of O<sub>2</sub> pressure.<sup>40</sup> <sup>d</sup> Data analysis for these reactions produced only estimates for rate constants because of the spectroscopic complexity of the reaction solutions, which contained permanganate, manganate, and manganese dioxide. <sup>e</sup> These pH values were calculated from the hydroxide concentration, so they are only estimates. <sup>f</sup> KH<sub>2</sub>PO<sub>4</sub>/K<sub>2</sub>HPO<sub>4</sub> in D<sub>2</sub>O. <sup>g</sup> These values have not yet been calculated, but appear to be similar in magnitude to the errors calculated for the toluene and ethylbenzene reactions.

16), indicating first order dependence on  $[\text{MnO}_4^-]$ . The observed rate constants are proportional to the toluene concentration, demonstrating a first order dependence on the toluene concentration. Second-order rate constants  $k_2 (= k_{\text{obs}}/[\text{C}_7\text{H}_8])$  are independent of the starting toluene and permanganate concentrations (Table 5). An Eyring plot utilizing  $k_2$  values determined over the temperature range 20 to 95 °C (Figure 17) yields the activation parameters  $\Delta H^\ddagger = 12.7 (\pm 0.2)$  kcal/mol and  $\Delta S^\ddagger = -30 (\pm 1)$  e.u.  $d_8$ -Toluene reacts much more slowly, giving an isotope effect of 9.7 at 20 °C. At higher temperatures, the reaction with  $\text{C}_7\text{D}_8$  is also quite slow and concurrent coagulation and precipitation of the colloid prevents the accurate determination of rate constants.

Ethylbenzene and cumene are oxidized more rapidly than toluene by permanganate, but otherwise the reactions are similar. The experiments with cumene were carried out by Linda Kuehnert.<sup>93</sup> The solubility of these substrates is less than that of toluene but still sufficient to carry out the kinetics under pseudo-first order conditions. The first order plots are linear without induction periods and doubling the ethylbenzene concentration approximately doubled the observed rate constant. The data indicate that the reactions of toluene and ethylbenzene follow the simple bimolecular rate law (eq 14). The solubility of cumene in water is insufficient to allow its concentration to be varied, but a first order dependence is assumed on the basis of the toluene and ethylbenzene results. Rate constants for ethylbenzene and cumene oxidations are presented in Table 5. Activation parameters for ethylbenzene were determined by studying the reaction over the temperature range 45 to 85 °C.  $\Delta H^\ddagger = 10.4 (\pm 0.4)$  kcal/mol and  $\Delta S^\ddagger = -33 (\pm 2)$  e.u. The Eyring plot is presented in Figure 18. The activation parameters for cumene are similar, given in Table 6.



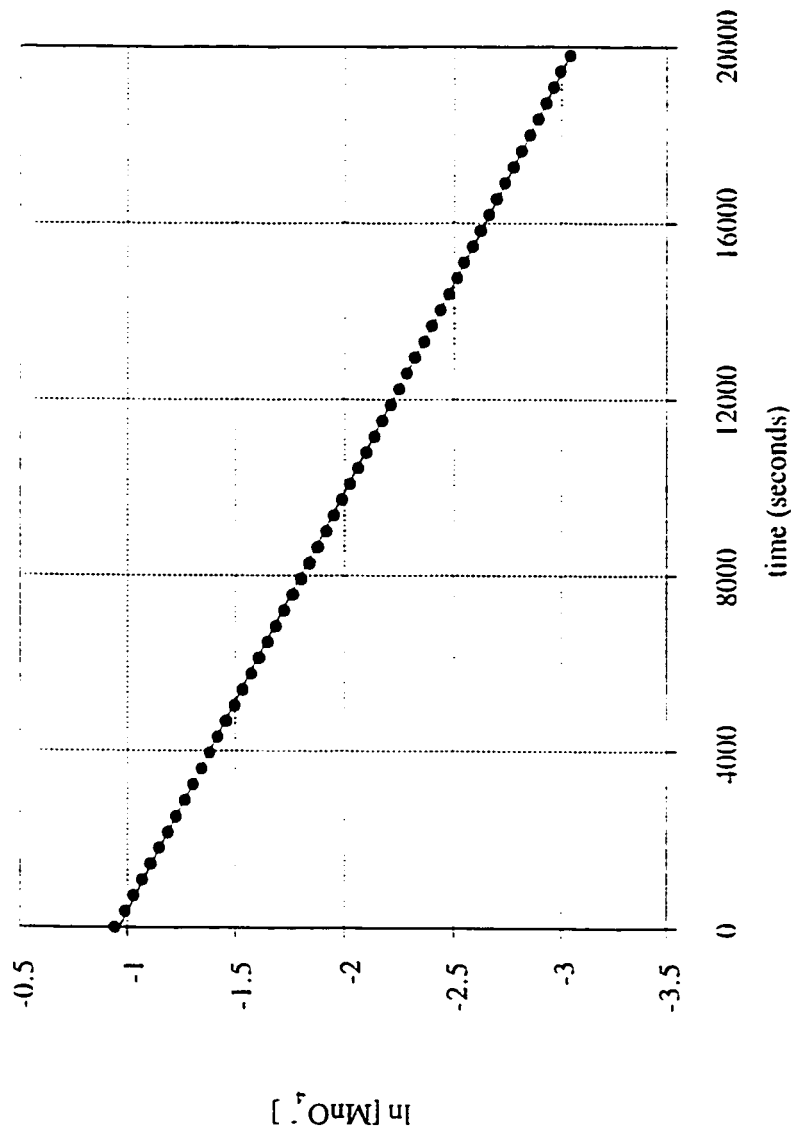


**Figure 16.** A plot of  $\ln [\text{MnO}_4^-]$  vs. time for the reaction of toluene with  $\text{KMnO}_4$  in aqueous solution, pH 7, at 75 °C.

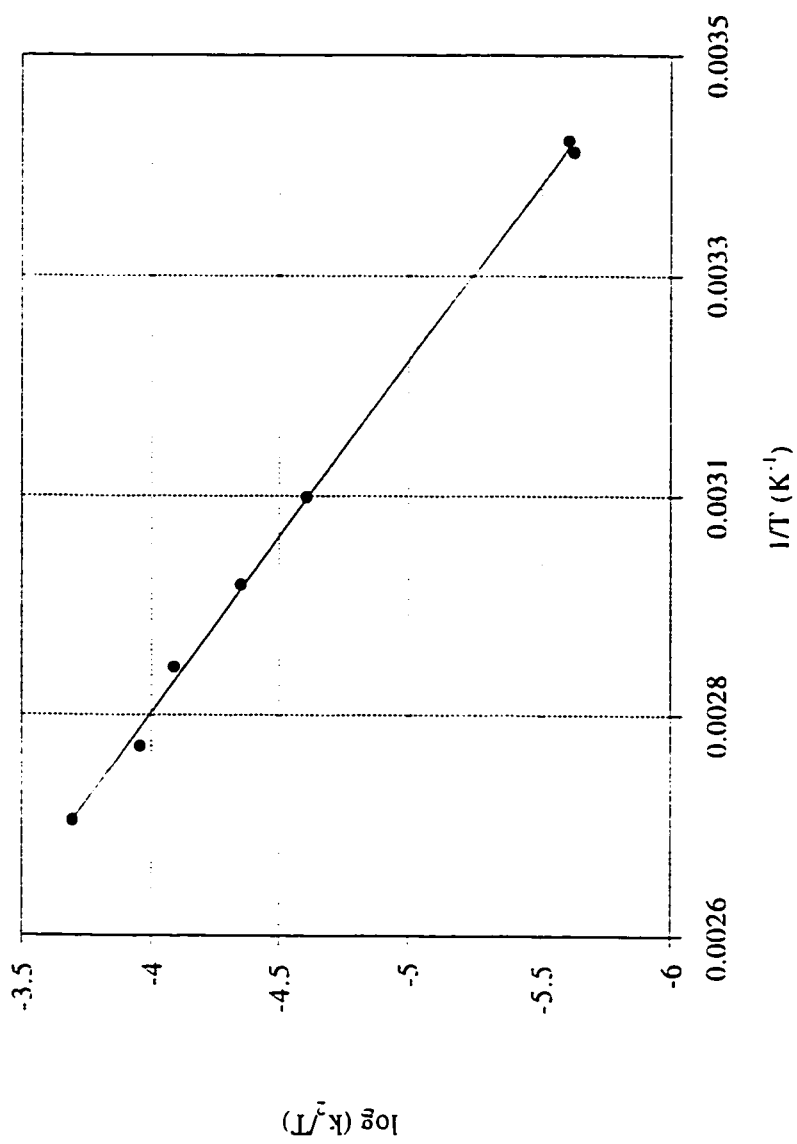


**Figure 17.** An Eyring plot,  $\log(k_2/T)$  vs.  $1/T$ , for the reaction of toluene with  $\text{KMnO}_4$  in aqueous solution, pH 7, over the temperature range 20 to 95 °C.

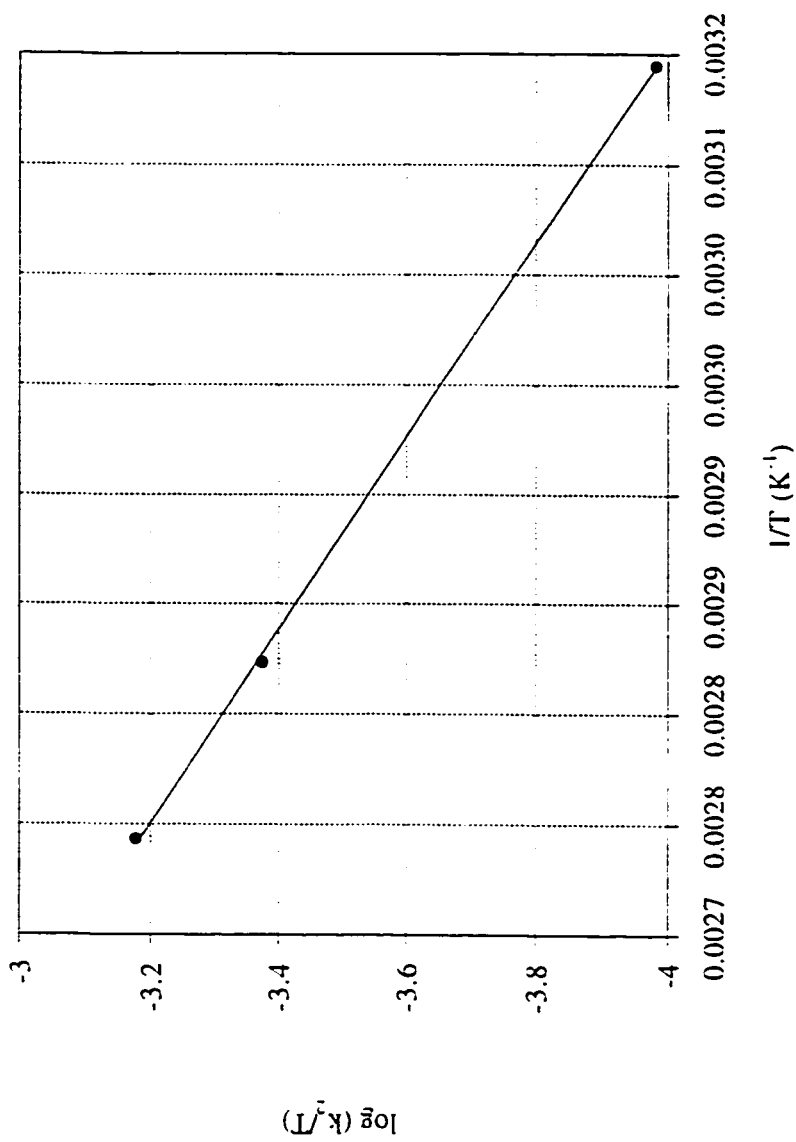


**Figure 18.** An Eyring plot,  $\log(k_2/T)$  vs.  $1/T$ , for the reaction of ethylbenzene with  $\text{KMnO}_4$  in aqueous solution, pH 7, over the temperature range 45 to 85 °C.

The pH dependence of the toluene oxidation was examined over the range pH 6 - 14, using phosphate buffers for pH 6 to 8, a  $\text{HCO}_3^-/\text{CO}_3^{2-}$  buffer from 9 to 11, and NaOH above pH 13. The rate constants are included in Table 5 and presented graphically in Figure 19. The rate constant is independent of the pH over the range 6 - 11, within the experimental error. This also demonstrates that the rate constant is independent of buffer type. Below pH 5 and above pH 12 the reactions were much faster, in agreement with other permanganate kinetics studies.<sup>7-10,89b</sup> In fact, a benzoate buffered permanganate solution (pH ~ 4), without added substrate, is not stable at room temperature, decomposing within a few hours. This suggests that at low pH, ring attack becomes a viable reaction pathway, possibly through the formation of  $\text{MnO}_3^+$ <sup>8</sup> or  $\text{HMnO}_4$ <sup>89b</sup>, as proposed by others. Above pH 11, the second order rate constants increased dramatically. There appears to be a dependence on  $\text{OH}^-$  concentration, but an exact value is difficult to obtain as the kinetics at high pH are not well-behaved and the spectra are very complicated.<sup>94</sup>

Deuteration of the solvent ( $\text{D}_2\text{O}$ ) had no measurable effect on the second order rate constant. A qualitative comparison also found no difference in the rate of permanganate disappearance when the buffer concentration was increased one order of magnitude. A quantitative comparison could not be made because the high phosphate concentration caused precipitation of the  $\text{MnO}_2$  over the course of the reaction. A Hammett study was carried out using a series of *para*-substituted toluenes,  $\text{CH}_3\text{C}_6\text{H}_4\text{X}$  where  $\text{X} = \text{COO}^-$ ,  $\text{SO}_3^-$ ,  $\text{Cl}$ ,  $\text{CH}_3$ , and  $\text{NO}_2$  (Table 5). Care was taken to choose substrates which did not have substituents, other than the methyl group, which could be oxidized by permanganate. Substitution on the ring has little effect on the rate constant. An electron withdrawing *para*-nitro group, for example, reduces the rate constant by only 20%. A Hammett  $\rho^+$  value of -0.2 is found vs.  $\sigma^+$  values,<sup>44</sup> which give the best fit to the data (Figure 20).

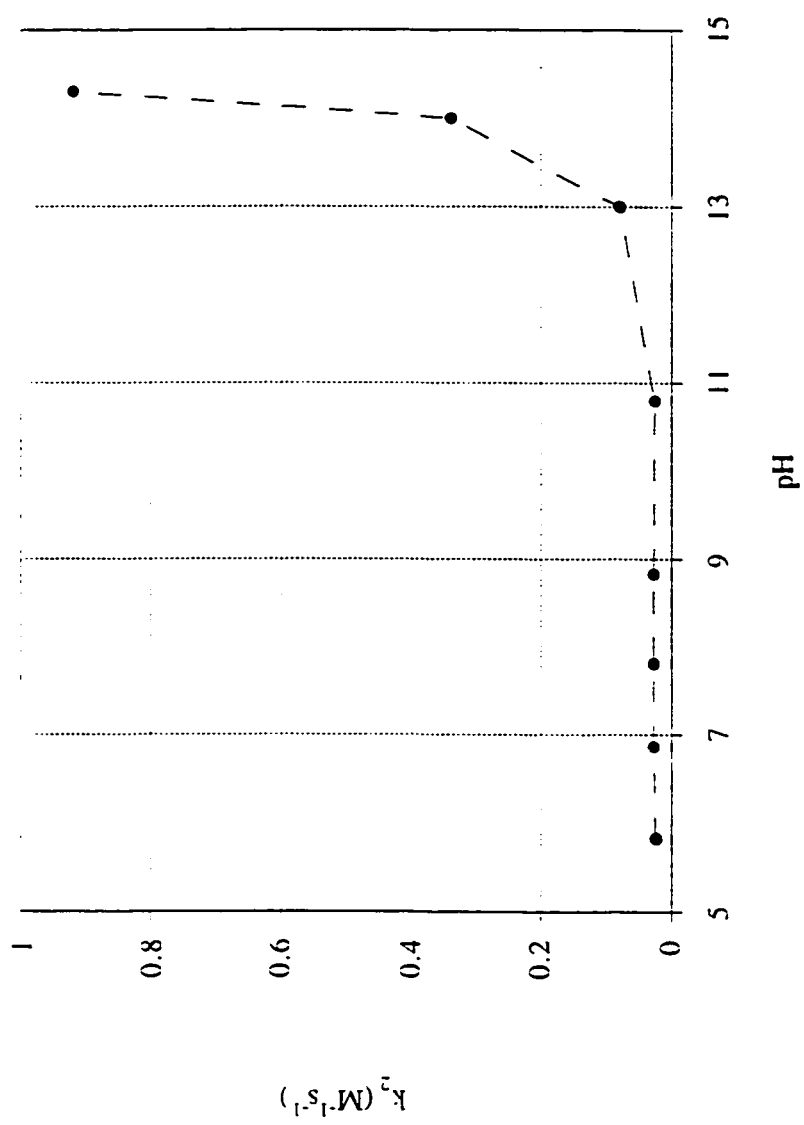


**Figure 19.** A plot of  $k_2$  vs. pH for the reaction of toluene with  $KMnO_4$  in aqueous solution over the pH range 6 to 14.3.

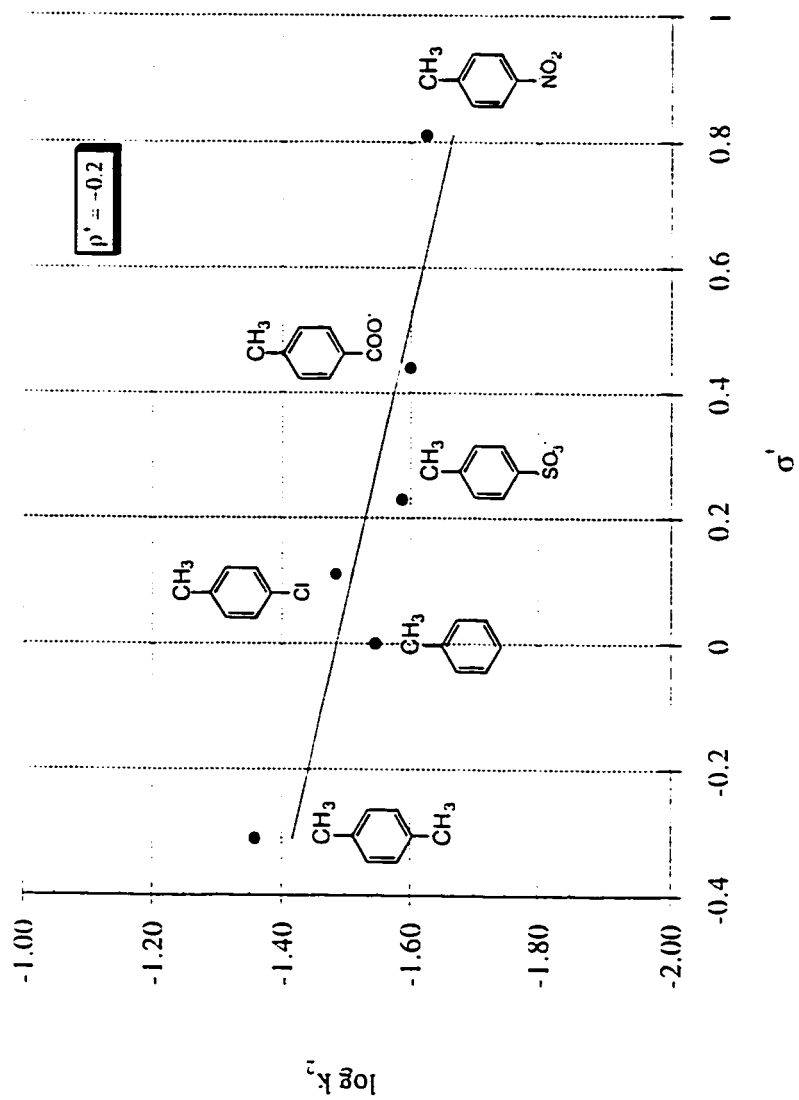


**Figure 20.** A plot of  $\log k_2$  vs.  $\sigma'$  for a Hammett study of *para*-substituted toluenes reacting with  $\text{KMnO}_4$  in aqueous solution, pH 7, at  $75^\circ\text{C}$ .

To test for the presence of radical intermediates, the influence of added oxygen on the rate of the reaction was explored. All other experiments were performed with careful exclusion of air. More common radical traps such as  $\text{CBrCl}_3$  are problematic in this system as the expected products (*i.e.* benzyl bromide) react with water, to give benzyl alcohol, which is further oxidized. Reductive radical traps, such as 9,10-dihydroanthracene or  ${}^n\text{Bu}_3\text{SnH}$ , are clearly not compatible with aqueous permanganate.  $\text{O}_2$  reacts with radicals at near the diffusion limit,<sup>38</sup> as does permanganate.<sup>39</sup> Thus, for  $\text{O}_2$  to compete with permanganate as a radical trap it must be present in equal or larger concentration. Qualitatively, the rate of reaction at room temperature does not appear to change in the presence of added  $\text{O}_2$ . The reaction of toluene with permanganate in water, however, is very sensitive to such variables as head space above the reaction solution due to non-ideal behavior of the solution. To insure that the apparent independence of reaction rate was not an artifact of the reaction vessel, a kinetics experiment was also run in the special cuvette. The  $\text{O}_2$  pressure was slightly greater than 1 atm, which gives  $[\text{O}_2] = 0.79$  mM at 70 °C,<sup>40</sup> larger than the 0.404 mM  $\text{MnO}_4^-$  concentration. The presence of  $\text{O}_2$  had no effect on the rate of the reaction, strongly suggesting that a radical mechanism is not operational in this system. It is unclear whether  $\text{O}_2$  should cause an acceleration or a deceleration of the reaction, but it is highly unlikely that if benzyl radicals were present, the reaction would proceed at the same rate with and without added oxygen. In contrast, a similar experiment with cumene, performed by Linda Kuehnert, showed an acceleration of permanganate disappearance when  $\text{O}_2$  was present. The reaction of permanganate with cumene in water at room temperature was complete in approximately a day in the presence of  $\text{O}_2$  and took several days to reach completion in the absence of  $\text{O}_2$ . The reaction of ethylbenzene with permanganate has the most intriguing results upon addition of  $\text{O}_2$ . Initially, side by side room temperature reactions of ethylbenzene with permanganate in water with and without  $\text{O}_2$  show no difference in rate of permanganate disappearance.

After almost one half life (four hours), however, the reaction with O<sub>2</sub> accelerates noticeably.

The final optical spectra of the toluene, ethylbenzene, and cumene reactions all indicate formation of colloidal MnO<sub>2</sub>, the typical product of permanganate reactions in this pH range.<sup>41</sup> Confirming this assignment, the final average manganese oxidation state was determined to be  $4.10 \pm 0.09$  by iodometric titration of a toluene reaction solution.<sup>29</sup> No manganese (or other) intermediates were detected spectroscopically. Mn(III) has been frequently invoked as the active oxidant in permanganate reactions,<sup>7c,10a</sup> but is apparently not formed in this reaction as addition of F<sup>-</sup>, which rapidly complexes with Mn<sup>3+</sup>, to a reaction solution did not cause a significant change in the apparent rate of reaction.<sup>95</sup>

The organic products were quantified by HPLC analysis. Since the colloidal MnO<sub>2</sub> is known to bind some of the oxidation products,<sup>30</sup> it was reduced to Mn<sup>2+</sup> prior to analysis by addition of NaHSO<sub>3</sub> or KI/HCl. In toluene reactions run at 75 °C, benzoic acid ( $42.3 \pm 2.7\%$ ) and benzaldehyde ( $0.6 \pm 0.2\%$ ) are observed; yields are reported as moles of product per mole of permanganate. Together these products account for  $85 \pm 6\%$  of the permanganate oxidizing equivalents consumed, assuming quantitative conversion of permanganate to MnO<sub>2</sub>. This result agrees well with the yield obtained for the same reaction in slightly acidic solution.<sup>89a</sup> The fate of the remaining oxidizing equivalents is not readily apparent. No benzyl alcohol was detected (< 12% yield based on oxidizing equivalents of MnO<sub>4</sub><sup>-</sup>). Permanganate is not reduced by free benzoate at pH 7, although complete oxidation of a very small amount of colloid-bound benzoic acid could account for the “missing” oxidizing equivalents. This was suggested in a similar system.<sup>89a</sup>

In the oxidation of ethylbenzene, the only detectable product is acetophenone. This accounts for  $74 \pm 5\%$  of the manganese oxidizing equivalents consumed (assuming complete conversion to MnO<sub>2</sub>) when the reaction is run at 76 °C. No benzoic acid (< 3.1% yield) or *sec*-phenethyl alcohol (< 3.9% yield) were observed. Oxidation of cumene

forms mainly cumyl alcohol with a trace of acetophenone. Benzoic acid is not found (< 2.3% yield). Based on oxidizing equivalents for  $\text{MnO}_4^-$  to  $\text{MnO}_2$ , acetophenone accounts for 2% and cumyl alcohol for 102% for a combined yield of 104 ( $\pm$  13) %.

In aqueous permanganate reactions performed in the absence of  $\text{O}_2$ , the oxygen incorporated into the organic product can either come from the solvent ( $\text{H}_2\text{O}$ ) or the oxidant ( $\text{MnO}_4^-$ ). Of the substrates studied, the simplest is cumene since it gains only one oxygen atom in forming the observed product, cumyl alcohol. Additionally, the oxygen atom in this product is unlikely to exchange with the solvent at neutral pH. Three experiments were performed. First, cumyl alcohol was placed in 70%  $^{18}\text{O}$  labelled water for 72 hours at 24 °C. Analysis of the solution by GCMS showed no incorporation of the label into the cumyl alcohol. Second, a reaction of cumene with 10%  $^{18}\text{O}$  labelled  $\text{KMnO}_4$  in pH 7 buffered aqueous solution was performed. The reaction took 72 hours at 24 °C to reach completion. The temperature was kept low to minimize exchange of the permanganate oxygen atoms with the solvent. At room temperature, this rate of exchange has been measured and found to be 0.5% per hour.<sup>21</sup> Once complete, the solution was analyzed by GCMS. A sample injected directly, prior to reduction of the colloidal  $\text{MnO}_2$ , showed no  $^{18}\text{O}$  incorporation into the product (< 8%, within experimental error). A portion of solid  $\text{NaHSO}_3$  was added to the sample and a second analysis performed. The results were the same. The cumyl alcohol  $\text{M}^+$  peak is quite small in the mass spectrum, so that even if the oxygen in the cumyl alcohol were coming exclusively from  $\text{MnO}_4^-$ , the peak would barely have been detectable. To be more certain about the origin of the oxygen in the product, a third experiment was performed using unlabelled  $\text{KMnO}_4$  and 70% enriched  $^{18}\text{O}$  labelled water. The solution was again analyzed before and after reduction of the  $\text{MnO}_2$ . The cumyl alcohol produced in this reaction contained only 8%  $^{18}\text{O}$  label, suggesting that less than 15% of the oxygen incorporated in the product had come from the solvent. Destruction of the  $\text{MnO}_2$  with  $\text{NaHSO}_3$  slightly increased the

apparent extent of  $^{18}\text{O}$  label to 10%, possibly as a result of exchange of the oxygen atom of the alcohol with the water upon acidification. This suggests that over 85% of the oxygen incorporated into cumyl alcohol is from  $\text{MnO}_4^-$ , but that some of the oxygen does come from the solvent as well.

## Discussion

In Chapter 1, permanganate's ability to react with arylalkanes via a one electron pathway, hydrogen atom transfer, was established. The literature of permanganate oxidation of organic compounds, however, contains many examples where slight changes in reaction conditions cause dramatic differences in reactivity or mechanism, as discussed in the introduction.<sup>96</sup> It is not surprising then, that in changing from toluene as a solvent to water, the reaction of toluene or ethylbenzene with permanganate is different.

**Comparison with Reactions in Organic Solvent.** For the aqueous reactions, the first order plots are linear over three half lives with no induction period, establishing a first order dependence on permanganate concentration and indicating that permanganate is the active oxidant in the system. This is in contrast to an earlier study of aqueous permanganate oxidation of toluene which proposed that  $\text{Mn}^{3+}$  was the active oxidant.<sup>10a</sup> The conclusion that permanganate is the active oxidant is reinforced by the finding that addition of  $\text{F}^-$ , a known scavenger of  $\text{Mn}^{3+}$ , causes no change in the apparent rate of the reaction. The aqueous reactions also show a first order dependence of  $k_{obs}$  on the toluene concentration, establishing a second order rate law for the overall reaction.

Regardless of the solvent used for the reaction of toluene with permanganate, there is a significant primary isotope effect. In aqueous solution,  $k_{\text{H}}/k_{\text{D}}$  is larger, approximately 9.7, but in both cases, the effect clearly indicates that the rate determining step in either solvent involves cleavage of a toluene C-H bond.

The other similarity that the aqueous reactions of arylalkanes with permanganate share with their counterparts in toluene solution are the products and their distribution. The oxidation of toluene produces mainly benzoic acid with a trace of benzaldehyde in both solvent systems. This result is not, perhaps, that surprising since most reactions of toluene with permanganate reportedly form benzoic acid.<sup>4,10a,65,89</sup> More unexpected is the product of the oxidation of ethylbenzene. In water, as for the reaction in toluene, acetophenone is the only detected product. In terms of synthetic utility, it is generally accepted that permanganate oxidation of any arylalkane results in the formation of benzoic acid with the remainder of the alkane chain being cleaved and converted to carbon dioxide.<sup>4</sup> The reaction of ethylbenzene in toluene and in water under these conditions is unusual since it stops at acetophenone without being further oxidized.

Despite these similarities, the reactions of arylalkanes in water and toluene have several important differences which suggest that the mechanisms are not the same. At room temperature, the second order rate constant for the reaction of toluene in water is more than three orders of magnitude larger than the corresponding rate constant for the reaction in toluene. An equivalent difference is seen in the ethylbenzene reactions. The values are given for comparison in Table 6. The activation parameters for the reactions in the different solvents also highlight how dissimilar the reactions are. In aqueous solution, the enthalpy of activation for toluene oxidation is 8 kcal/mol less than in toluene, 21.0 kcal/mol in toluene compared to 12.7 kcal/mol in water. An enthalpy barrier ( $\Delta H^\ddagger$ ) of only 13 kcal/mol would be difficult to understand in terms of a hydrogen atom transfer mechanism since the enthalpy ( $\Delta H^\circ$ ) for such a reaction is calculated to be +9 kcal/mol (see the Discussion section in Chapter 1). The entropy of activation also shows marked differences. In water, the entropy is much more unfavorable than in toluene, increasing from -18 e.u. in toluene to -32 e.u. in water. All of this evidence strongly suggests that

the mechanism of arylalkane oxidation by permanganate changes in going from non-polar toluene to highly polar water.

**The Rate Determining Step.** While a large number of experiments have been performed in an attempt to elucidate the rate determining step of arylalkane oxidation by permanganate in aqueous solution, the results do not lead to a single well-defined mechanism at this point. The majority of the results are for the reaction of toluene with permanganate, so that reaction will be discussed first, followed by a section where the results of the reactions of ethylbenzene and cumene are compared.

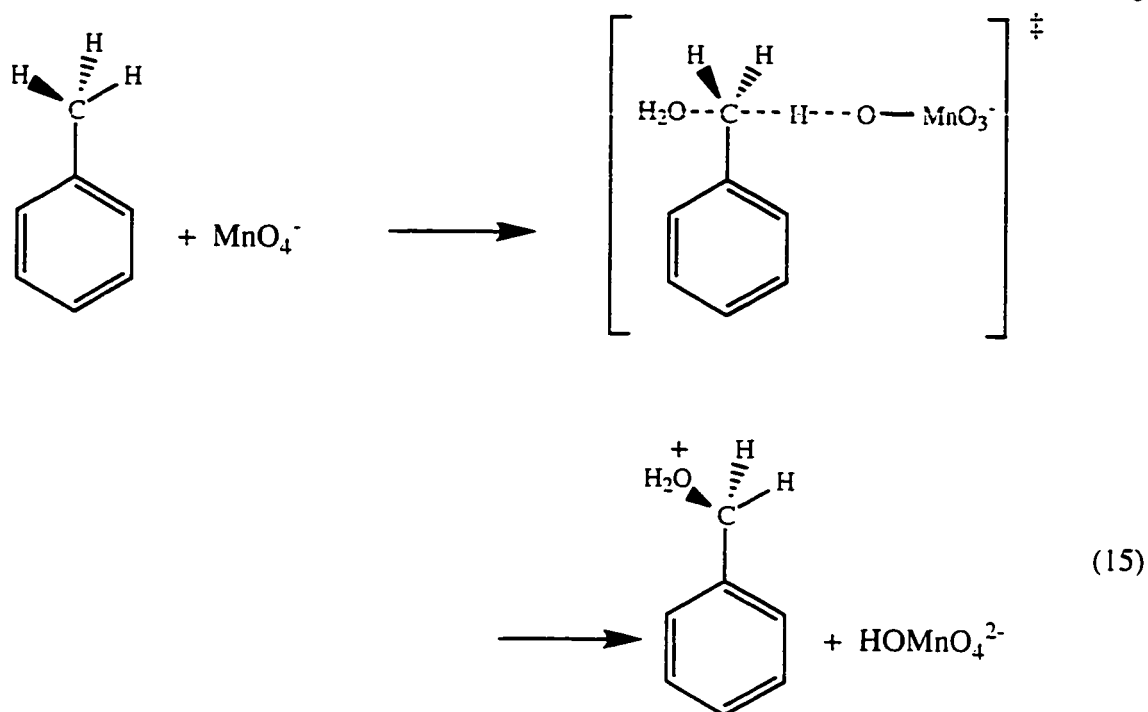
Solely on the basis of the reaction of toluene and *para*-substituted toluenes with  $\text{KMnO}_4$  in water at neutral pH, it is possible to propose a reasonable rate determining step which fits with experimental results. The appearance of an isotope effect and the formation of benzoic acid as the predominant product indicates that the rate determining step is attack of the benzylic C-H bond. As discussed earlier, the species responsible is permanganate. There are two possible ways for permanganate to break the C-H bond--homolytically or heterolytically. If bond cleavage were homolytically, benzylic radicals would be produced and addition of oxygen should have an effect on the rate of permanganate disappearance. There is no apparent dependence of the rate of reaction on the oxygen concentration, leading to the conclusion that the C-H bond is broken heterolytically. Cleavage of the C-H bond heterolytically and transfer of a hydride to an oxo group of permanganate would that substitution of either electron donating or withdrawing groups had little effect on the reaction rate. This apparent discrepancy can be explained by postulating a mechanism in which a hydride is transferred from toluene to an oxo group of the permanganate with stabilization of the incipient carbocation by a water molecule (eq 15).

**Table 6.** Comparison of Arylalkane Reactivity with  $\text{MnO}_4^-$  in Water and Toluene.<sup>a</sup>

substrate	aqueous <sup>b</sup>	organic <sup>c</sup>
toluene	$k = 1.7 \times 10^{-4} \text{ M}^{-1}\text{s}^{-1}$ $\Delta H^\ddagger = 12.7 \text{ kcal/mol}$ $\Delta S^\ddagger = -32 \text{ e.u.}$	$k = 1.4 \times 10^{-7} \text{ M}^{-1}\text{s}^{-1}$ $\Delta H^\ddagger = 21.0 \text{ kcal/mol}$ $\Delta S^\ddagger = -18 \text{ e.u.}$
ethylbenzene	$k = 3.9 \times 10^{-3} \text{ M}^{-1}\text{s}^{-1}$ $\Delta H^\ddagger = 10.4 \text{ kcal/mol}$ $\Delta S^\ddagger = -34 \text{ e.u.}$	$k = 3.3 \times 10^{-6} \text{ M}^{-1}\text{s}^{-1}$ $\Delta H^\ddagger = 20.8 \text{ kcal/mol}$ $\Delta S^\ddagger = -13 \text{ e.u.}$
cumene <sup>d</sup>	$k = 7.7 \times 10^{-3} \text{ M}^{-1}\text{s}^{-1}$ $\Delta H^\ddagger = 11.0 \text{ kcal/mol}$ $\Delta S^\ddagger = -31 \text{ e.u.}$	

<sup>a</sup> All values are at 25 °C, on a per H basis. The rate constants are also corrected to account for the stoichiometry and have been extrapolated from the respective Eyring plots.

<sup>b</sup> These experiments were performed in aqueous solution, pH 7. This is the work described in this Chapter and in reference 6. <sup>c</sup> These experiments were performed in toluene solution. This is the work described in Chapter 1 of this dissertation. <sup>d</sup> This work was performed by Linda Kuehnert.



The developing positive charge is then delocalized onto the oxygen atom, removing it from a position adjacent to the arene ring where resonance stabilization by *para*-substituted electron donating groups would have been possible. This type of mechanism was proposed by Thompson and Meyer in the reaction of arylalkanes with  $(\text{trpy})(\text{bpy})\text{RuO}^{2+}$ .<sup>97</sup> Their evidence was more conclusive as they were able to demonstrate a dependence of the rate constant on the concentration of added nucleophile. A preliminary report on only the toluene oxidation reactions touted this mechanism.<sup>6</sup> prior to completion of the ethylbenzene and cumene experiments.

While this mechanism fits the experimental results for the oxidation of toluene, it is not clear that the same mechanism is satisfactory for the reactions of ethylbenzene and cumene with permanganate. There are two pieces of experimental evidence from the ethylbenzene and cumene studies which cast doubt on this mechanism as the rate determining step in the reaction. First, these reactions show a dependence of the

disappearance of permanganate on the presence of oxygen, which is not predicted by the mechanism of the rate determining step described above. Second, this rate determining step predicts that the oxygen incorporated into the organic product in the reaction of cumene should come exclusively from the solvent. Experimentally, however, it is found that the oxygen is supplied primarily by the oxidant ( $\text{MnO}_4^-$ ) and to a less extent, by the solvent. There are a number of possible explanations for these observations. Each will be explored in turn and suggestions made, when possible, of experiments that might be used to prove or disprove these theories.

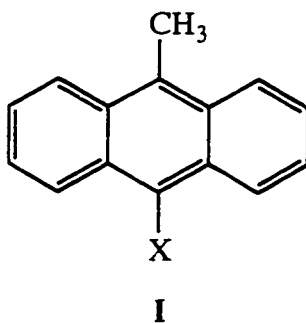
A classic test for organic radical intermediates in a reaction is a change in rate upon addition of oxygen.<sup>1b,98</sup> The acceleration of the rate of permanganate disappearance in the reactions of ethylbenzene and cumene when oxygen is present clearly demonstrates that radicals have been produced, but little other information is revealed. For example, it is unclear whether permanganate or another manganese species has generated the radicals. In fact, the rate of reaction of ethylbenzene in the presence of oxygen appeared to be independent of the oxygen for approximately the first half life before accelerating, suggesting that the radicals are produced later in the reaction. Possibly, the reactions of ethylbenzene and cumene result in the generation of an intermediate valence manganese species which is capable of generating radical intermediates. For example, the toluene reaction shows no evidence that  $\text{Mn}^{3+}$  is an active oxidant, but in the reactions of cumene and ethylbenzene, perhaps  $\text{Mn}^{3+}$  is formed and is able to generate radicals. A similar discrepancy was reported in studies of toluene and ethylbenzene oxidations by permanganate in acidic aqueous solution.<sup>10a,c</sup> The possible involvement of  $\text{Mn}^{3+}$  in these reactions could be tested by running the reactions of ethylbenzene and cumene with permanganate in the presence of  $\text{F}^-$ . If  $\text{Mn}^{3+}$  is playing a role in these reactions, the addition of  $\text{F}^-$  should complex the  $\text{Mn}^{3+}$  and slow the rates of the reactions. A negative

result for that experiment, however, may simply mean that another intermediate valence manganese species is responsible for this effect.

The presence of intermediate valence manganese species may also explain the results of the  $^{18}\text{O}$  labelling studies in the reaction of cumene. The proposed mechanism, solvent assisted hydride transfer, predicts that all of the oxygen in the organic product should come from the solvent. However, experimentally, as others have found for neutral aqueous permanganate reactions of benzaldehyde,<sup>21</sup> the product formed contains oxygen from both the permanganate and the solvent. Stewart and Wiberg found that the extent of incorporation of oxygen into benzoic acid from the solvent actually increased at longer reaction times.<sup>21</sup> They attributed this to formation of an intermediate valence manganese species able to rapidly exchange oxygen atoms with the solvent before undergoing disproportionation to permanganate and a lower valence manganese species. Intermediate valence manganese species are likely in these reactions, but exact identification is not usually possible. An experiment examining the origins of the oxygen incorporated into the product in the oxidation of toluene is unlikely to prove useful. Benzaldehyde is probably an intermediate of the reaction since it was observed in the products, and studies of its oxidation under these conditions found scrambling of the label and a time dependence as described above.<sup>21</sup>

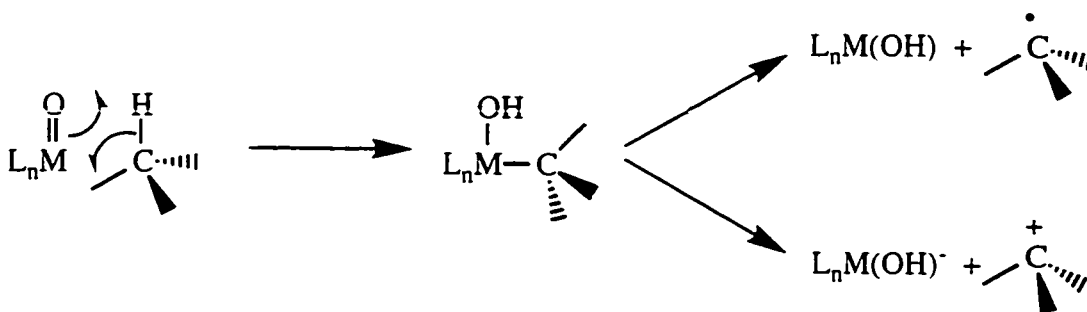
If nucleophile assisted hydride transfer is the correct mechanism for the rate determining step in these reactions, the best evidence would be to demonstrate a dependence of the rate constant on the concentration of water or other added nucleophile. This experiment requires a solvent which is miscible with water, but less reactive than toluene with permanganate. Preliminary work on acetonitrile and pyridine are described in Appendix C, but both solvents were found to be too reactive for this work. The only apparent way in which to do this study is to work with a more reactive substrate than toluene. However, the substrate should still contain a primary C-H bond susceptible to

oxidation as more sterically hindered substrates would be less likely to proceed through the five coordinate intermediate proposed. Most primary C-H bonds are fairly strong unless adjacent to an arene ring. For example, the C-H bond strength in toluene is 88 kcal/mol,<sup>84</sup> and in 9-methylantracene (**I**, X = H), is reportedly 82 kcal/mol.<sup>86,99</sup>



The C-H bond of 9-methylantracene is weak enough that studies in acetonitrile should be possible, but substitution in the 10 position is necessary to improve its solubility in polar solvents such as acetonitrile and water. For example, if X = NO<sub>2</sub>, Cl, COOH, or SO<sub>3</sub>H in **I**, the solubility should be sufficient for the reaction to be studied in water or acetonitrile.<sup>100</sup> These compounds are not commercially available, but they can be synthesized by literature methods.<sup>99</sup>

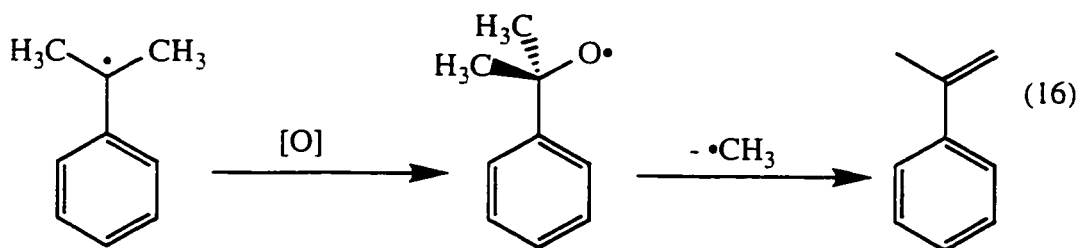
There remains the possibility that the mechanism discussed so far is simply incorrect for the oxidations of cumene and ethylbenzene or for all three substrates. One mechanism which cannot be completely ruled out for these reactions is that proposed by Lee for oxidations of alcohols and hydrocarbons by all high valent metal oxo species-- [2+2] addition. On the basis of theoretical calculations of CrO<sub>2</sub>Cl<sub>2</sub> oxidations of hydrocarbons and alcohols.<sup>13</sup> Lee suggested that all of these reactions proceed by addition of a metal oxo bond to either a C-H or O-H bond followed by either homolytic or heterolytic cleavage of the putative C-M bond (Scheme 3).<sup>12</sup>



**Scheme 3.** [2+2] Addition of a C-H bond to a M=O bond with subsequent homolytic or heterolytic cleavage of the M-C bond.

In Chapter 1, this mechanism was argued against on the basis that it requires expansion of the manganese coordination sphere to five coordinate, which is highly unlikely for such a small cation. That same argument is also applicable here. Nonetheless, the entropy of activation is much more unfavorable, as predicted for such a highly ordered transition state,<sup>12</sup> and the enthalpy of activation is very low. If a [2+2] addition does occur in the rate determining step for all of the substrates, the subsequent cleavage of the C-Mn bond may vary depending on the substrate.<sup>12,101</sup> In the case of toluene, where no radicals were implicated, the cleavage may indeed be heterolytic. For ethylbenzene and cumene, there may be homolytic cleavage of the C-Mn bond instead of or in addition to heterolytic cleavage. Other evidence indicates, however that this is probably not the correct mechanism. The isotope effect suggests that the transition state is linear, which is contrary to this mechanism.<sup>24,102</sup> While the entropy of activation is low for oxidation of a hydrocarbon, it is higher than might be predicted for a rate determining step where bonds are both broken and formed.<sup>12</sup> Unfortunately, there is no clear way to either implicate or disprove this mechanism. The tests used by Lee to "prove" this mechanism for other oxidations seem less than convincing,<sup>12</sup> but such a mechanism cannot be fully eliminated from consideration.

Possibly the most likely scenario for these reactions is a mixed mechanism involving competing pathways. For example, there may be both radical (i.e.  $\text{H}\cdot$  transfer) and ionic mechanisms (i.e. solvent assisted  $\text{H}^-$  transfer) operating. In proceeding from toluene to ethylbenzene to cumene, the steric congestion around the carbon center increases, increasing the probability of a radical mechanism being favored over an ionic mechanism which requires a five coordinate intermediate. The presence of a radical component to the mechanism is also supported by the observation of acetophenone in the oxidation of cumene. This requires cleavage of a C-C bond which is known to be facile for the cumyloxy radical by loss of  $\cdot\text{CH}_3$  (eq 16).<sup>103</sup>



The unresolved issue, if a radical mechanism is occurring, is why the rate of a hydrogen atom transfer reaction in water would be so much faster than the corresponding reaction in organic solvent. Typically, the rate constants for reactions involving hydrogen atom transfer and formation of organic radicals are independent of solvent. For example, the rate constant for cumyloxy radical abstracting a hydrogen atom from cyclohexane only increases by 21% when the reaction is run in acetic acid rather than chlorobenzene.<sup>64</sup> One possible explanation of the difference in rate constants for the reactions is involvement of the counterion. In order to study the reactions of hydrocarbons in organic solvent, the cation also had to be changed. Non-polar solvents force tight ion pairing of the cation with permanganate.<sup>42</sup> In water, however, the cation and anion are solvated with a larger distance between them. Perhaps it is this coupling in organic solvent which reduces

permanganate's ability to react by hydrogen atom transfer in organic solvent, slowing the reaction. The reaction of toluene in *o*-dichlorobenzene, a much more polar solvent with less ion pairing, should have been faster than the analogous reaction in toluene if this is true, but was not. Still, counterion effects have been observed in other related reactions<sup>22g</sup> (see dihydroanthracene reactions in Chapter 1 and Appendix C). To completely rule out the counterion influence, studies should be done with other counterions. As with the suggested experiments in other solvents, this requires the use of different solvents and hence, different substrates.

## Conclusions

Despite the execution of a well-planned series of experiments involving the oxidation of toluene and ethylbenzene, permanganate has again demonstrated its complex and adaptable nature. Toluene, ethylbenzene, and cumene, in neutral aqueous solution, react with permanganate forming predominantly benzoic acid, acetophenone, and cumyl alcohol, respectively. At 25 °C, the rate constants for the reactions of toluene and ethylbenzene are three orders of magnitude larger than for the comparable reactions in toluene. The aqueous reactions are first order with respect to oxidant and substrate and show no induction periods. Toluene has a large isotope effect, indicating C-H bond cleavage in the rate determining step and a linear transition state. At high and low pH, the reaction with toluene accelerates dramatically. Electron donating and withdrawing substituents in the *para* position of the aryl ring have little influence on the rate of reaction. The three substrates show differences, however, in the response of the rate of disappearance of permanganate upon addition of O<sub>2</sub>, a classic test for radical intermediates. The reaction of toluene is independent of the presence of O<sub>2</sub>, while the reactions of ethylbenzene and cumene accelerate when O<sub>2</sub> is added.

For the reaction of toluene, a mechanism for the rate determining step involving hydride transfer from the methyl group to an oxo of permanganate with stabilization of the incipient carbocation by solvent is in accord with the experimental evidence. This mechanism involves a five coordinate transition state for the carbon center, which is less favorable for the secondary and tertiary carbon centers in ethylbenzene and cumene due to steric crowding. There are several possible explanations for the differences observed in the toluene reaction relative to the ethylbenzene and cumene reactions: (1) All three proceed by initial hydride transfer with nucleophilic assistance, but the reactions of ethylbenzene and cumene result in the formation of intermediate valence manganese species capable of generating radicals. (2) The rate determining step of the reaction is actually [2+2] addition of a Mn=O bond to a benzylic C-H bond for all of the substrates studied. (3) The reaction involves both radical and ionic components to the mechanism and as the steric crowding around the carbon center increases, the radical pathway is increasingly favored. None of these explanations are wholly satisfactory, but it is clear that further work is needed to distinguish between these possibilities.

## REFERENCES

---

1. (a) Olah, G. A.; Molnár, Á. *Hydrocarbon Chemistry*; Wiley-Interscience: New York, 1995. (b) Sheldon, R. A.; Kochi, J. K. *Metal-Catalyzed Oxidations of Organic Compounds*; Academic Press: New York, 1981. (c) *Activation and Functionalization of Alkanes*; Hill, C. L., Ed.; Wiley-Interscience: New York, 1989.
2. Haggin, J. *Chem. and Eng. News* **1995**, *73*, 20-23.
3. (a) *Cytochrome P-450: Structure, Mechanism, and Biochemistry*; Ortiz de Montellano, P. R. Ed.; Plenum: New York, 1985. (b) Watanabe, Y.; Groves, J. T. in *The Enzymes*, 3rd ed.; Academic Press: New York, 1992, Volume XX, p. 405-452.
4. March, J. *Advanced Organic Chemistry*, 3rd ed.; Wiley-Interscience: New York, 1985.
5. (a) Cook, G. K.; Mayer, J. M. *J. Am. Chem. Soc.* **1994**, *116*, 1855-1868 and (b) correction, *ibid.* **1994**, *116*, 8859. (c) Cook, G. K.; Mayer, J. M. *J. Am. Chem. Soc.* **1995**, *117*, 7139-7156.
6. A preliminary report on this work has appeared Gardner, K. A.; Mayer, J. M. *Science* **1995**, *269*, 1849-1851.
7. (a) Waters, W. A. *Quart. Rev. (London)* **1958**, 277-300. (b) Carrington, A.; Symons, M. C. R. *Chem. Rev.* **1963**, *63*, 443-460. (c) Stewart, R. in *Oxidation in Organic Chemistry Part A*; K. B. Wiberg, Ed.; Academic Press: New York, 1965, p. 1-68. (d) Stewart, R. *Oxidation Mechanisms*; Benjamin: New York, 1964. (e) Fatiadi, A. J. *Synthesis (Stuttgart)* **1987**, 85-127. (f) Kochi, J. K. in *Comprehensive Organic Synthesis*, Vol. 7 (Oxidation); Trost, B. M., Ed.; Pergamon: New York, 1991.
8. Stewart, R.; Spitzer, U. A. *Can. J. Chem.* **1978**, *56*, 1273-1279.

- 
9. (a) Brauman, J. I.; Pandell, A. J. *J. Am. Chem. Soc.* **1970**, *92*, 329-335. (b) Wiberg, K. B.; Fox, A. S. *J. Am. Chem. Soc.* **1963**, *85*, 3487-3491.
  10. (a) Cullis, C. F.; Ladbury, J. W. *J. Chem. Soc.* **1955**, 555-560. (b) Cullis, C. F.; Ladbury, J. W. *J. Chem. Soc.* **1955**, 1407-1412. (c) Cullis, C. F.; Ladbury, J. W. *J. Chem. Soc.* **1955**, 2850-2854. (d) Cullis, C. F.; Ladbury, J. W. *J. Chem. Soc.* **1955**, 4186-4190.
  11. Stewart, R. *J. Am. Chem. Soc.* **1957**, *79*, 3057-3061.
  12. (a) Lee, D. G.; Chen, T. *J. Am. Chem. Soc.* **1993**, *115*, 11231-11236. (b) Lee, D. G.; Chen, T. *J. Org. Chem.* **1991**, *56*, 5341-5345. (c) Lee, D. G.; Congson, L. N. *Can. J. Chem.* **1990**, *68*, 1774-1779. (d) Lee, D. G.; Gai, H. *Can. J. Chem.* **1993**, *71*, 1394-1400.
  13. Rappé, T.; Goddard, W. A. III *J. Am. Chem. Soc.* **1982**, *104*, 3287-3294.
  14. This chapter has been adapted with revision from Gardner, K. A.; Kuehnert, L. L.; Mayer, J. M. submitted to *J. Am. Chem. Soc.* for publication.
  15. Karaman, H.; Barton, R. J.; Robertson, B. E.; Lee, D. G. *J. Org. Chem.* **1984**, *49*, 4509-4518.
  16. Martinsen, A.; Songstad, J. *Acta Chem. Scand. A* **1977**, *31*, 645-650.
  17. Sala, T.; Sargent, M. V. *J. Chem. Soc., Chem. Commun.* **1978**, 253-254.
  18. (a) Radtke, R.; Hessing, A. *Chem. Ber.* **1990**, *123*, 621-626. (b) Poulouse, A.; Croteau, R. *J. Chem. Soc. Chem. Commun.* **1979**, 243-244.
  19. Herriot, A. W.; Picker, D. *Tetrahedron Lett.* **1974**, *16*, 1511-1514.
  20. Vepřek-Šiška, J.; Ettel, V.; Regner, A. *J. Inorg. Nucl. Chem.* **1964**, *26*, 1476-1477.
  21. Wiberg, K. B.; Stewart, R. *J. Am. Chem. Soc.* **1955**, *77*, 1786-1795.

- 
22. (a) Lee, D. G.; Brown, K. C. *J. Am. Chem. Soc.* **1982**, *104*, 5076-5081. (b) Lee, D. G.; Perez-Benito, J. F. *Can. J. Chem.* **1985**, *63*, 1275-1279. (c) Perez-Benito, J. F.; Lee, D. G. *J. Org. Chem.* **1987**, *52*, 3239-3243. (d) Lee, D. G.; Chen, T. *J. Am. Chem. Soc.* **1989**, *111*, 7534-7538. (e) Perez-Benito, J. F.; Lee, D. G. *Can. J. Chem.* **1985**, *63*, 3545-3550. (f) Perez-Benito, J. F.; Lee, D. G. *J. Org. Chem.* **1988**, *53*, 5725-5728. (g) Lee, D. G.; Brown, K. C.; Karaman, H. *Can. J. Chem.* **1986**, *64*, 1054-1059. (h) Freeman, F.; Kappos, J. C. *J. Org. Chem.* **1989**, *54*, 2730-2734.
23. (a) Leddy, B P.; McKervey, M. A.; McSweeney, P. *Tetrahedron Lett.* **1980**, *21*, 2261-2264. (b) Schmidt, H.-J.; Schäfer, H. *J. Angew. Chem., Int. Ed. Engl.* **1979**, *18*, 68-69.
24. Radtke, R.; Heesing, A. *Chem. Ber.* **1990**, *123*, 621-626.
25. Perrin, D. D.; Armarego, W. L. F.; Perrin, D. R. *Purification of Laboratory Chemicals*, 2nd ed.; Pergamon Press: Oxford, 1980.
26. Rakus, K.; Verevkin, S. P.; Schätzer, J.; Beckhaus, H.-D.; Rüchardt, C. *Chem. Ber.* **1994**, *127*, 1095-1103.
27. Diphenylmethane has a melting point between 22 and 24 °C. The commercially available material is a liquid, but after sublimation is a soft, crystalline solid at room temperature.
28. The author wishes to thank Tom Crevier for providing a sample of *d*<sub>12</sub>-dihydroanthracene, prepared by a procedure described in Crevier, T. J.; Mayer, J. M. manuscript in preparation.
29. Harris, D. C. *Quantitative Chemical Analysis*; Freeman: New York, 1982, p. 383.

- 
30. Fieser, L. F.; Fieser, M. *Reagents for Organic Synthesis*, Vol. 1; Wiley: New York, 1967, p. 943.
  31. The HPLC systems used were graciously loaned to the author by the Gouterman and Sasaki research groups of the University of Washington Chemistry Department.
  32. The extinction coefficient for permanganate in all solvents at 25 °C is approximately constant at 526 nm. See reference 15 and references therein.
  33. The  $pK_a$  of benzoic acid is 4.2,<sup>34</sup> so at a pH of 9, essentially only benzoate is present.
  34. *CRC Handbook of Chemistry and Physics*, 62nd ed.; Weast, R. C., Ed.; CRC Press: Boca Raton, FL, 1982, p. D-142.
  35. Previous studies suggest that  ${}^n\text{Bu}_4\text{NMnO}_4$  is not reactive with pyridine;<sup>17</sup> however, under our conditions, it seems to react at approximately the same rate as toluene. This is discussed in more detail in Appendix C. Benzene was deemed unacceptable as a solvent because when a saturated solution of  ${}^n\text{Bu}_4\text{NMnO}_4$  in benzene was passed through a frit, the salt began crystallizing out of solution.
  36. The concentration of 4-methylbenzophenone in *o*-dichlorobenzene at 55 °C was calculated assuming a density of 1 g/mL for 4-methylbenzophenone.
  37. Based on work done by Linda Kuehnert, the initial rate constant for the oxidation of toluene by  ${}^n\text{Bu}_4\text{NMnO}_4$  in *o*-dichlorobenzene was shown to be first order with respect to toluene concentration. Within experimental error, the second order rate constant for toluene oxidation by  ${}^n\text{Bu}_4\text{NMnO}_4$  was the same in toluene and *o*-dichlorobenzene. For further details, see reference 14.
  38. Maillard, B.; Ingold, K. U.; Scaiano, J. C. *J. Am. Chem. Soc.* **1983**, *105*, 5095.

- 
39. Steenken, S.; Neta, P. *J. Am. Chem. Soc.* **1982**, *104*, 1244-1248.
40. Stephen, H.; Stephen, T. *Solubilities of Inorganic and Organic Compounds*, Volume I Binary Systems, Part 1; MacMillan: New York, 1963, p. 573.
41. Perez-Benito, J. F.; Arias, C. *J. Colloid Interface Sci.* **1992**, *152*, 70-84.
42. Sam, D. J.; Simmons, H. E. *J. Am. Chem. Soc.* **1972**, *94*, 4024-4025.
43. *o*-Dichlorobenzene, when very pure, is fairly inert to oxidation by  ${}^n\text{Bu}_4\text{NMnO}_4$ , allowing it to be used as a solvent for permanganate oxidations of hydrocarbons. The rate of solvent oxidation, however, is very sensitive to water content and light exposure, so careful purification of the solvent is necessary. The procedure for this is described in the Experimental section. The exposure of *o*-dichlorobenzene to fluorescent light results in the generation of a number of new organic species. Robinson, G. E.; Vernon, J. M. *Chem. Commun.* **1969**, 977-980. Fox, M.-A.; Nichols, W. C., Jr.; Lemal, D. M. *J. Am. Chem. Soc.* **1973**, *95*, 8164-8166.
44. Exner, O. *Correlation Analysis in Chemistry*; Chapman, N. B., Shorter, J., Eds.; Plenum: New York, 1978, 439-540.
45. Exner, O. *Advances in Linear Free Energy Relationships*; Chapman, N. B., Shorter, J., Eds.; Plenum Press: London, 1972, p. 20.
46. No data are available for the solubility of  $\text{O}_2$  in *o*-dichlorobenzene, but the concentration of  $\text{O}_2$  in chlorobenzene at 20 °C under 1 atm  $\text{O}_2$  is 8.3 mM.<sup>40</sup> The solubility of  $\text{O}_2$  in toluene at 20 °C under 1 atm  $\text{O}_2$  is 5.7 mM.<sup>40</sup>
47. The oxidation of *t*-butylbenzene by  ${}^n\text{Bu}_4\text{NMnO}_4$  in *o*-dichlorobenzene was studied and the details are included in reference 14. The rate of oxidation of a solution that was one-third *t*-butylbenzene by volume was actually slower than the rate of oxidation of neat *o*-dichlorobenzene, so only an estimate of the actual rate constant for the oxidation of *t*-butylbenzene could be made. This observation is in

- 
- agreement with the trend in C-H bond strength since *t*-butylbenzene has no benzylic C-H bonds and therefore, should have relatively strong C-H bonds.
48. The correction for reaction stoichiometry is necessary, but it is not very accurate because products are not quantitatively formed (~ 60% yield of benzoic acid from toluene). If the remainder of the  $\text{MnO}_4^-$  is consumed in production of benzyl alcohol or benzaldehyde, then the idealized correction is too big, but if they are consumed in overoxidation of benzoic acid or counterion oxidation, then the correction is too large. The correction does not influence the  $\Delta H^\ddagger$  values in Table 3, as long as it is constant over the temperature range studied.
49. Reference 4, p. 1072.
50. Anthracene has a vibrational progression between 300 and 400 nm, the most intense band of which is at 380 nm. The molar absorptivity of  $8.5 \text{ mM}^{-1}\text{cm}^{-1}$ <sup>51</sup> was used to calculate the amount of anthracene in the solution.
51. *UV Atlas of Organic Compounds*, Vol. 2; Butterworths: London, 1966, p. E2/T1.
52. The oxidation of cumene by  ${}^n\text{Bu}_4\text{NMnO}_4$  in *o*-dichlorobenzene was studied by Linda Kuehnert. The kinetics were irreproducible and the observed rate constants did not seem to correlate with the cumene concentration.
53. The first order plots for the oxidation of cumene by  ${}^n\text{Bu}_4\text{NMnO}_4$  in toluene were almost sigmoidal in shape, possibly indicative of autocatalytic behavior, as described in reference 10a and references therein. The shape of the first order plot and the slope at a particular time seemed to be independent of the cumene concentration at 25 °C. This is described in detail in Appendix C.
54. (a) Wallis, J. M.; Kochi, J. K. *J. Am. Chem. Soc.* **1988**, *110*, 8207-8223. (b) Mulliken, R. S.; Person, W. B. *Molecular Complexes*; Wiley-Interscience: New

- 
- York, 1969. (c) Foster, R. *Organic Charge-Transfer Complexes*; Academic Press: New York, 1969.
55. Reference 5c and references therein.
  56. Murray, J. W. *J. Colloid Interface Sci.* **1974**, *46*, 357-371.
  57.  $E^\circ$  for aqueous  $MnO_4^-$  taken from Latimer, W. M. *The Oxidation States of the Elements and Their Potentials in Aqueous Solution*, 2nd ed.; Prentice Hall: New York, 1952.
  58. See, for instance, Traylor, T. G.; Nakano, T.; Miksztal, A. R.; Dunlap, B. E. *J. Am. Chem. Soc.* **1987**, *109*, 3625. Ostrovic, D. Bruice, T. C. *Acc. Chem. Res.* **1992**, *25*, 314-320. Kim, T.; Mirafzal, G. A.; Liu, J.; Bauld, N. L. *J. Am. Chem. Soc.* **1993**, *115*, 7653. Gross, Z.; Nimri, S. *J. Am. Chem. Soc.* **1995**, *117*, 8021.
  59. Reference 7f, p. 849-855.
  60. A difference of 0.4 V in oxidation potential between *p*-xylene and toluene translates to  $\Delta\Delta G$  of 9 kcal/mol.
  61. Schaller, C. P.; Cummins, C. C.; Wolczanski, P. T. *J. Am. Chem. Soc.* **1996**, *118*, 591-611 and references therein.
  62. Haight, G. P., unpublished results (personal communication, 1996).
  63. Thompson, M. S.; Meyer, T. J. *J. Am. Chem. Soc.* **1982**, *104*, 5070-5076.
  64. Avila, D. V.; Brown, C. E.; Ingold, K. U.; Luszyk, J. *J. Am. Chem. Soc.* **1993**, *115*, 466-470.
  65. Radhakrishnamurti, P. S.; Mahapatro, S. N. *Indian J. Chem.* **1975**, *13*, 1294-1296.
  66. Howard, J. A.; Chenier, J. H. B. *J. Am. Chem. Soc.* **1973**, *95*, 3054-3055.

- 
67. References 1,3 (a) Stubbe, J.; Kozarich, J. W. *Chem. Rev.* **1987**, *87*, 1107-1136. (b) Hecht, S. M. *Acc. Chem. Res.* **1986**, *19*, 383-391. (c) Tian, G.; Berry, J. A.; Klinman, J. P. *Biochemistry* **1994**, *33*, 226-234. (d) Simons, Th. G. J.; Verheijen, E. J. M.; Batist, Ph. A.; Schuit, G. C. A. in *Oxidation of Organic Compounds Vol. II*; F. R. Mayo, Ed.; Adv. Chem. Ser. #76, American Chemical Society, Washington, D.C., 1968, p. 262-275 and references therein.
68. Ballhausen, C. J.; Gray, H. B. *Coordination Chemistry*, Vol. I; Martell, A. E., Ed.; Van Nostrand Rheingold: New York, 1971, p. 3-83.
69. (a) Rüchardt, C.; Gerst, M.; Nölke, M. *Angew. Chem., Int. Ed. Engl.* **1992**, *31*, 1523-1525. (b) For earlier discussions of the formation of organic radicals from diamagnetic precursors, see: Pryor, W. A. in *Organic Free Radicals*; Pryor, W. A., Ed.; ACS Symposium Series #69, 1978, Washington D.C., pp. 33-62; Harmony, J. A. K. *Methods in Free Radical Chemistry* **1974**, *5*, 101-176.
70. (a) Theopold, K. H.; Detrich, J. L.; Reinaud, O. M.; Turner, J. F. C. *J. Am. Chem. Soc.* **1995**, *117*, 11745-11748 (b) Spin-crossover in transition metal complexes typically occurs very rapidly and with very low barriers: McKusker, J. K.; Reingold, A. L.; Hendrickson, D. N. *Inorg. Chem.* **1996**, *35*, 2100-2112 and references therein.
71. For leading references see (a) Bordwell, F. G.; Cheng, J.-P.; Ji, G.-Z.; Satish, A. V.; Zhang, X. *J. Am. Chem. Soc.* **1991**, *113*, 9790-9795. (b) Bordwell, F. G.; Cheng, J.-P.; Harrelson, J. A., Jr. *J. Am. Chem. Soc.* **1988**, *110*, 1229-1231. Zhang, X.-M.; Bordwell, F. G. *J. Am. Chem. Soc.* **1992**, *114*, 9787-9792. (c) Parker, V. D. *J. Am. Chem. Soc.* **1992**, *114*, 7458-7462; and correction: Parker, V. D. *J. Am. Chem. Soc.* **1993**, *115*, 1201. (d) For application to the calculation of metal hydride bond strengths see: Tilset, M.;

- 
- Parker, V. D. *J. Am. Chem. Soc.* **1989**, *111*, 6711-6717; and correction: Tilsted, M.; Parker, V. D. *J. Am. Chem. Soc.* **1990**, *112*, 2843.
72. The recently revised  $pK_a$  of  $\text{HMnO}_4^-$  is 7.4 as reported by: Rush, J. D.; Bielski, B. H. *Inorg. Chem.* **1995**, *34*, 5832-5838.
73. The previously accepted  $pK_a$  of  $\text{HMnO}_4^-$ , 10.5, was taken from the following sources: Lister, M. W.; Yoshino, Y. *Can. J. Chem.* **1960**, *38*, 2342-2348. Heckner, K.-H.; Landsberg, R. *J. Inorg. Nucl. Chem.* **1967**, *19*, 423-430.
74. There is an error in the calculation of the free energy value for  $\text{H}\cdot + \text{MnO}_4^-$  in the Scheme reported in reference 5b (in addition to the use of the older  $pK_a$  value<sup>72,73</sup>). This Scheme used an incorrect reference state for  $\Delta G_{\text{solv}}(\text{H}_2)$ , unit mole fraction instead of 1 M. We thank Professors John Brauman (Stanford) and Neil Bartlett (Berkeley) for bringing this to our attention (personal communications, January 1995).
75. The value of  $\Delta H^\circ \{\text{H}\cdot(\text{g}) \rightarrow 1/2 \text{H}_2(\text{g})\} = -1/2 \text{BDE}(\text{H}_2(\text{g}))$  is  $-52.1 \text{ kcal/mol}$ .<sup>76</sup> Solvation of  $\text{H}_2$  is typically used as a good model for solvation of  $\text{H}\cdot$  (see discussion in reference 71 including corrections), so  $\Delta H^\circ \{\text{H}\cdot(\text{g}) \rightarrow \text{H}\cdot(\text{aq})\} \cong \Delta H^\circ \{\text{H}_2(\text{g}) \rightarrow \text{H}_2(\text{aq})\} = -1.0 \text{ kcal/mol}$ .<sup>77</sup> Entropy terms involving  $\text{H}\cdot$  (g or aq) cancel and therefore, do not appear in the constant. The only remaining entropy term,  $S\{\text{H}_2(\text{g})\} = 31.2 \text{ e.u.}$  is taken from reference 76, Vol. 2, p. 1260. Overall, the constant is calculated to be  $-55.8 \text{ kcal/mol}$  for the thermodynamic cycle in water, referenced to NHE. This agrees well with constants calculated by others for similar cycles.<sup>71</sup>
76. *JANAF Thermochemical Tables*, 3rd ed.; *J. Phys. Chem. Ref. Data* **1985**, *14*, Supplement #1.

- 
77. *Solubility Data Series*; Young, C. L., Ed.; Pergamon: New York, 1981; Vol. 5/6, p. 2.
78. Values for phenol taken from: Lind, J.; Shen, X.; Eriksen, T. E.; Merényi, G. *J. Am. Chem. Soc.* **1990**, *112*, 479-482. Values for aniline taken from: Jonsson, M.; Lind, J.; Eriksen, T. E.; Merényi, G. *J. Am. Chem. Soc.* **1994**, *116*, 1423-1427.
79. (a)  $D(\text{HO-H}) = 119.2$  kcal/mol,  $D(\text{H-Br}) = 87.4$  kcal/mol,  $D(\text{H-I}) = 71.4$  kcal/mol derived from data in reference 76. (b)  $D(^t\text{BuO-H}) = 104.8$ ,  $D(\text{MeO-H}) = 104.4$  and  $D(^t\text{BuOO-H}) = 89.4$  kcal/mol from Colussi, A. J. in *Chemical Kinetics of Small Organic Radicals*; Alfassi, Z. B., Ed.; CRC Press: Boca Raton, FL, 1988, p. 33.
80. Buxton, G. V.; Greenstock, C. L.; Helman, W. P.; Ross, A. B. *J. Chem. Phys. Ref. Data* **1988**, *17*, 513.
81. Howard, J. A.; Scaiano, J. C. *Oxyl-, Peroxyl- and Related Radicals*. In *Radical Reaction Rates in Liquids*; Landolt-Börnstein New Series; Fischer, H., Ed.; Springer Verlag: New York, 1984, Vol. 13, subvol. d.
82. (a) Ingold, K. U. Chapter 2, p. 69ff in (b) Vol. 1 of *Free Radicals*; Kochi, J. K., Ed.; Wiley: New York, 1973. (c) Russell, G. A. Chapter 7, Vol. 1 of reference 82b, pp. 283-293. (d) Knox, J. H. in reference 67d p. 1-22. The correlation of rates with driving force holds for similar kinds of radicals, when polar effects are not significant.<sup>82c,e</sup> (e) Tedder, J. M. *Angew. Chem., Int. Ed. Engl.* **1982**, *21*, 401-410. (f) A discussion of free energy relationships in radical reactions is also given in: Korzekwa, K. R.; Jones, J. P.; Gillette, J. R. *J. Am. Chem. Soc.* **1990**, *112*, 7042-7046.

- 
83. A recent re-evaluation of C-H bond strengths has resulted in a 3-4 kcal/mol upward revision. The C-H bond strengths for toluene, ethylbenzene, and diphenylmethane (88.0, 85.4, and 84 kcal/mol, respectively) have been taken from a review done after the revision.<sup>84</sup> A more current analysis of hydrocarbon bond strengths cites 88.5 ( $\pm 1.5$ ) kcal/mol for the C-H bond in toluene,<sup>85</sup> which within the error bars, is the same as the value we have chosen to use. The bond strengths for xanthene and dihydroanthracene (78 and 75.5 kcal/mol, respectively) have been taken from another recent article which uses the toluene bond strength of 88.0 kcal/mol as the reference.<sup>86</sup> The C-H bond strength for triphenylmethane is not well-defined. Older literature cites a bond strength which is 6 kcal/mol less than diphenylmethane<sup>87</sup> while more recent work claims that the difference should be less based on saturation and steric effects and calculates a difference of only 1 kcal/mol.<sup>71a</sup> While the recent values are for solution phase, the argument that the difference in bond strength between diphenylmethane and triphenylmethane should be less than 6 kcal/mol seems reasonable, so the bond strength that we are using for triphenylmethane, 81 kcal/mol, reflects an average of these two differences, relative to the revised diphenylmethane bond strength.
84. McMillen, D. F.; Golden, D. M. *Ann. Rev. Phys. Chem.* **1982**, *33*, 493-532.
85. Berkowitz, J.; Ellison, G. B.; Gutman, D. *J. Phys. Chem.* **1994**, *98*, 2744-2765.
86. Stein, S. E.; Brown, R. L. *J. Am. Chem. Soc.* **1991**, *113*, 787-793.
87. Korcek, S.; Chenier, J. H. B.; Howard, J. A.; Ingold, K. U. *Can. J. Chem.* **1972**, *50*, 2285-2297.
88. (a) Wang, K.; Mandell, M.; Mayer, J. M., work in progress. (b) Adkins, J.; Crevier, T. C.; Mayer, J. M., work in progress.

- 
89. (a) Lobachev, V. L.; Rudakov, E. S. *Kinet. Katal.* **1994**, *35*, 198-202. (b) Lobachev, V. L.; Rudakov, E. S. *Kinet. Katal.* **1994**, *35*, 203-210.
90. Electrospray ionization mass spectrometry was performed by Ann Hunter of the University of Washington Medicinal Chemistry Department using on a VG Fisons QUATTRO II triple quadrupole mass spectrometer. The mobile phase was 80% acetonitrile, 20% water at a flow rate of 20  $\mu\text{L}/\text{min}$ . The probe voltage was 3.4 KV and the cone voltage was 23 V.
91. Lau, T.-C.; Wang, J.; Siu, K. W. M.; Guevremont, R. *J. Chem. Soc., Chem. Commun.* **1994**, 1487-1488.
92. Harris, D. C. *Quantitative Chemical Analysis*; Freeman: New York, 1982, p. 383.
93. This is work in progress.
94. The first order plots are not linear, possibly showing signs of autocatalysis.<sup>10a</sup>
95. Accurate rate constants could not be determined for the F<sup>-</sup>-added experiments because the addition of large quantities of ionic compounds interferes with the colloid formation, causing precipitation during the course of the reaction and preventing accurate data analysis.
96. Compare, for example, the studies of toluene oxidation in references 8, 10a, 65, and 89a. All four cite different active oxidants and dramatically different rate constants and one cites very different products. Other examples in the literature include the oxidation of alcohols and fluoro-alcohols and the oxidation of aldehydes in neutral and basic aqueous solution.<sup>7</sup>
97. Thompson, M. S.; Meyer, T. J. *J. Am. Chem. Soc.* **1982**, *104*, 5070-1076.
98. Parshall, G. W. *Homogeneous Catalysis*; Wiley-Interscience: New York, 1980.

- 
99. Zhang, X.-M.; Bordwell, F. G.; Bares, J. E.; Cheng, J.-P.; Petrie, B. C. *J. Org. Chem.* **1993**, *58*, 3051-3059.
100. A substrate concentration of 5 mM should be great enough to be able to easily study these reactions, so even the chloro- or nitro- substitution should increase the solubility of 9-methylanthracene sufficiently.
101. In reference 12, Lee repeatedly relies on examination of the products of the oxidation of cyclobutanol to determine if the reaction of a particular oxidant with alcohols results in the formation of radicals or ionic species. The basis for this distinction is that cyclobutanol is known to ring open if a hydrogen atom is abstracted. It has clearly been shown by others, Scott, S. L.; Bakac, A.; Espenson, J. H. *J. Am. Chem. Soc.* **1992**, *114*, 4205-4213, that cyclobutanol may not react with a given oxidant by the same pathway as other alcohols do.
102. See reference 24 and references therein. Also, Melander, L.; Saunders, W. H., Jr. *Reaction Rates of Isotopic Molecules*; Wiley-Interscience: New York, 1980, p. 154.
103. A closely related example is given in Baciocchi, E.; d'Acunzo, F.; Galli, C.; Ioele, M. *J. Chem. Soc., Chem. Commun.* **1995**, 429-431. This paper examines the oxidation of cumene by a high valent iron-oxo species. The reaction appears to proceed by a radical pathway. Rates for methyl loss from cumyloxy radical can be found in reference 81 of this paper.
104. The vapor pressure data for toluene and water were taken from the following sources. Smith, B. D.; Srivastava, R. *Thermodynamic Data for Pure Compounds*, Part A; Elsevier: Amsterdam, 1986, p. 576-577. *Thermodynamic Properties of Inorganic Substances*, 2nd ed., Vol. I; Knacke, O., Kubaschewski, O., Hesselmann, K., Eds.; Springer-Verlag: New York, 1991, p. 810.

## **Appendix A**

### **Analysis of Kinetic Data for Permanganate Reactions Monitored Spectroscopically**

For almost all of the kinetic experiments performed, the reaction was followed by monitoring the disappearance of  $\text{MnO}_4^-$  and the formation of colloidal  $\text{MnO}_2$  spectroscopically, over the range 400 to 640 nm. The colloidal  $\text{MnO}_2$  exhibits a broad absorbance in this region which is due to both scattering and absorbance by the colloidal particles. The development of isosbestic points over the course of the reaction suggests that the colloid is well-behaved spectroscopically, obeying Beer's law, given generically in eq 17.

$$A = \epsilon bc \quad (17)$$

where A = absorbance

$\epsilon$  = molar absorptivity

b = path length

(1 cm for all experiments discussed)

c = concentration of absorbing species

In this spectral region, the absorbance at a given wavelength,  $\lambda$ , during the course of the reaction has components due to both  $\text{MnO}_4^-$  and the colloid (eq 18).

$$A_x = [\text{MnO}_4^-] \epsilon_{\text{MnO}_4^-,x} + [\text{MnO}_2] \epsilon_{\text{MnO}_2,x} \quad (18)$$

Since neither  $[\text{MnO}_2]$  nor  $\epsilon_{\text{MnO}_2}$  is well-defined, the concentration of  $\text{MnO}_4^-$  is calculated from the absorbance at two different wavelengths,  $x$  and  $y$ , which relies only on the relative  $\text{MnO}_2$  absorbance,  $Q$ , at these wavelengths (eqs 19, 20).

$$[\text{MnO}_4^-] = \frac{A_y - Q A_x}{\epsilon_{\text{MnO}_4^-,y} - Q \epsilon_{\text{MnO}_4^-,x}} \quad (19)$$

$$\text{where } Q = \frac{\epsilon_{\text{MnO}_2;y}}{\epsilon_{\text{MnO}_2;x}} = \frac{A_{\text{MnO}_2;y}}{A_{\text{MnO}_2;x}} \quad (20)$$

While the colloid is well-behaved in general, toward the end of most reactions, it begins to change spectroscopically due to coagulation, so that a final spectrum cannot be used to calculate the ratio,  $Q$ . Instead, the ratio is calculated earlier in the reaction.

Colloidal  $\text{MnO}_2$  has a smooth, broad absorbance over the spectral region of interest. The absorbance in the ranges 438 - 478 nm and 598 - 638 nm is due almost entirely to  $\text{MnO}_2$  over the course of the reaction, with essentially no contribution from  $\text{MnO}_4^-$  (Figure 21). A third order polynomial is fit to the absorbance over both these ranges after 2 - 3 half lives (Figure 21). The fit is typically quite good,  $R > 0.9999$  usually. From the polynomial equation generated, the absorbance due to  $\text{MnO}_2$  at any wavelength may be calculated, hence giving the ratio,  $Q$ , of absorbances for any two wavelengths.

Four wavelengths were used to calculate the concentration of  $\text{MnO}_4^-$  at time  $t$  from eq 3. Two of the wavelengths were absorbance maxima for permanganate ( $\lambda_{\text{max}} = 526$  and 546 nm). The other two were wavelengths where  $\text{MnO}_2$  strongly absorbs ( $\lambda = 450$  and 494 nm). Each permanganate  $\lambda_{\text{max}}$  was analyzed with respect to each of the wavelengths where  $\text{MnO}_2$  absorbance dominates, yielding four different  $[\text{MnO}_4^-]_t$  data

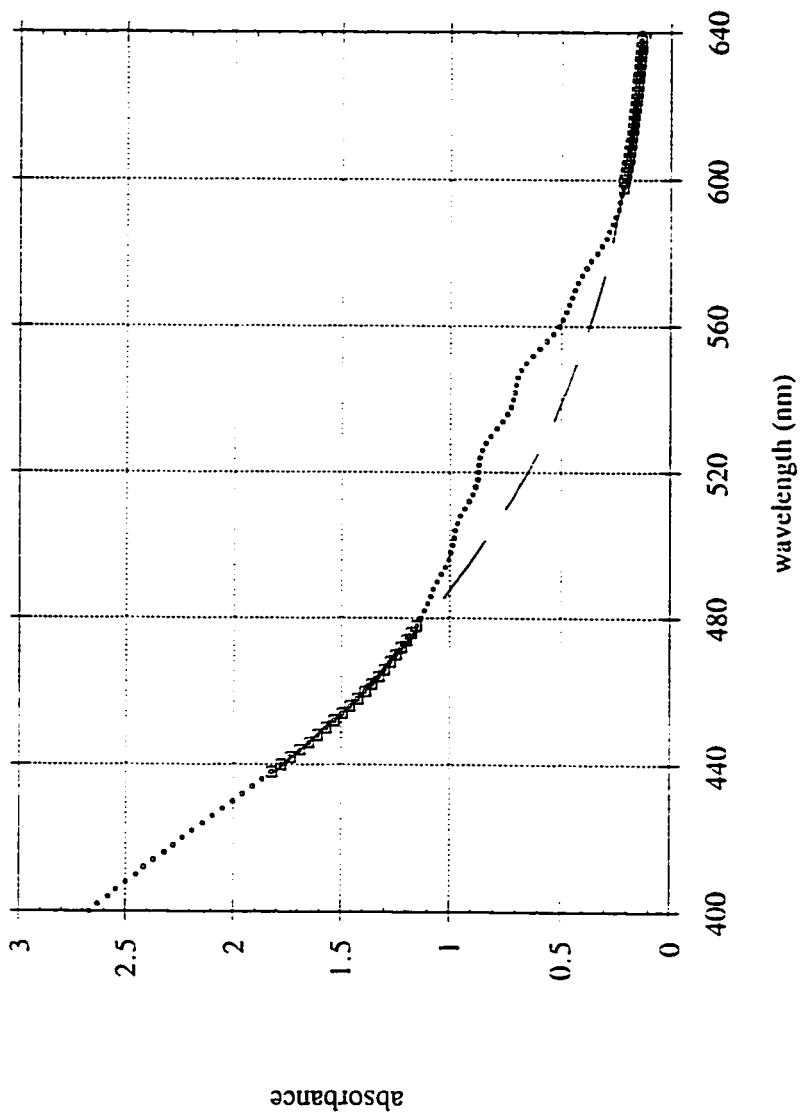


**Figure 21.** UV/vis spectrum of the solution for the reaction of  $\text{KMnO}_4$  and toluene in water after 2 half-lives. The small dots are the full UV/vis spectrum, the large squares are the segments used to model the  $\text{MnO}_2$ , and the dashed line is the third order polynomial fit.

sets and four apparent rate constants for each kinetics experiment (526 vs. 450; 546 vs. 450; 526 vs. 494; 546 vs. 494). The rate constants reported are the average of the four values for each experiment. Errors reflect three  $\sigma$ , reported as a percentage of the average rate constant.

For the aqueous reactions,  $Q$  varied little so long as the  $\text{MnO}_2$  modelling was done after one half-life. The modelling for these reactions was fairly accurate because the  $\text{MnO}_2$  absorbance/scattering was comparable to the permanganate absorbance, so small deviations in the baseline or curve fitting did not have an effect on  $Q$ . For the reactions performed in organic solvent, however, the absorbance/scattering due to  $\text{MnO}_2$  is smaller relative to the permanganate absorbance. The net result is that, for reactions in organic solvent, the calculated ratio,  $Q$ , is highly dependent on where the  $\text{MnO}_2$  modelling is performed. This is of significance because the ratios have an influence on the appearance of the first order plots. Figure 22 shows first order plots generated by  $\text{MnO}_2$  modelling at three different times during the course of a single reactions. The initial slopes are all the same within experimental error, but the curvature later in the reaction is dramatically different between the three models. This suggests that for all of the reactions in organic solvent, initial rate constants are valid, but no other firm conclusions can be drawn from the shape of the first order plots later in the reaction.

Most of the  $\text{MnO}_2$  modelling was performed fairly late in the reaction for those run in organic solution. While this decreased errors in  $Q$  due to baseline or modelling problems, this meant that the modelling was done at a time where the nature of the colloid had already begun to change. The curvature for most of the first order plots was not severe, resulting in a doubling of the apparent slope from the beginning of the reaction to the end. While the curvature is likely an artifact of the calculation of the ratio,  $Q$ , it may also be caused by a buildup of an organic intermediate under conditions where the steady

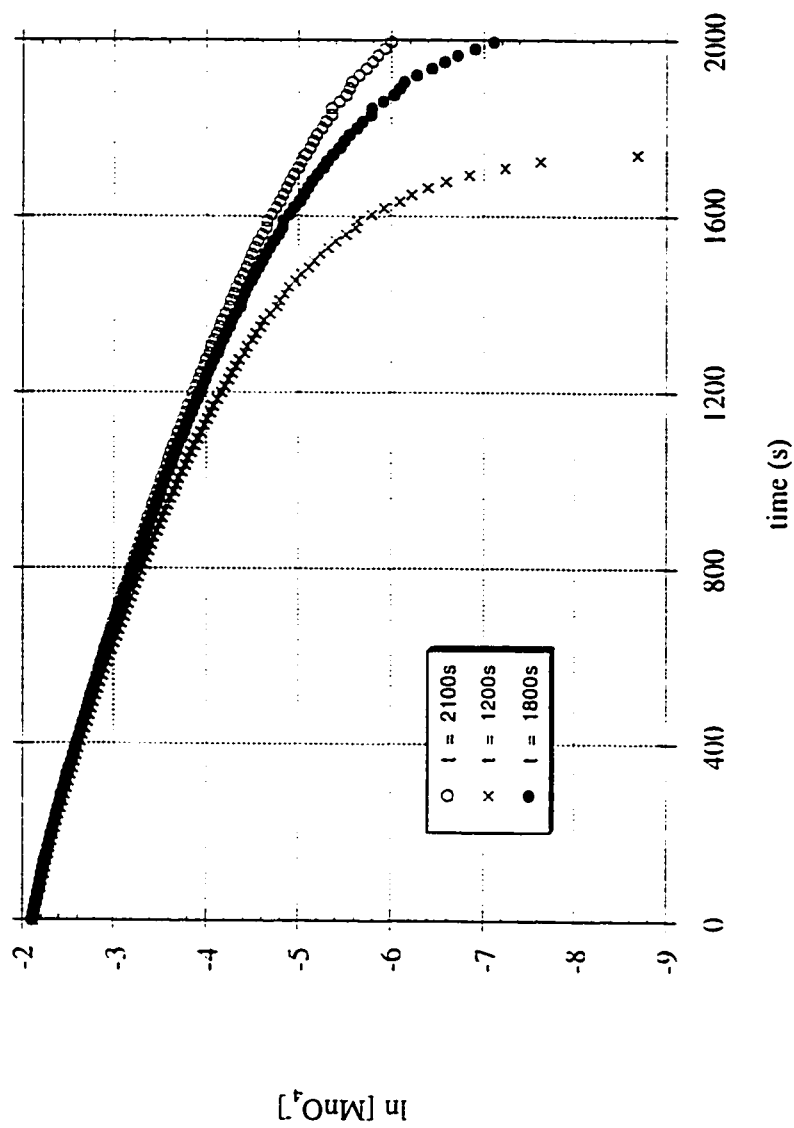


**Figure 22.** A plot of  $\ln [\text{MnO}_4^-]$  vs. time for the reaction of triphenylmethane with  ${}^t\text{Bu}_4\text{NMnO}_4$  in toluene at  $55\text{ }^\circ\text{C}$ . The curves arise from modelling the  $\text{MnO}_2$  scattering/absorbance at 1200s (crosses), 1800s (filled circles), and 2100s (open circles).

state concentration is never attained. To obtain the initial rate constant, the first order plots were fit with a third order polynomial and the slope at  $t = 0$  calculated (Figure 2).

In many of the reactions studied, the first order plots had another feature which complicated the analysis. Hydrocarbons are much less reactive with permanganate than other organic species such as alkenes, alcohols, and aldehydes (likely impurities in the substrates studied), so trace amounts of impurities were found to cause an initial fast segment in the first order plot (Figure 23). While in most cases, this portion accounted for less than 5% of the reaction (based on permanganate lost), diphenylmethane reactions at low temperature ( $< 25\text{ }^{\circ}\text{C}$ ) had first order plots which showed longer fast reactions, accounting for up to 45% of one half-life. To account for these contaminants, the fast portion of the reaction was removed from the first order plots and the remaining data fit with a third order polynomial and the fit extrapolated back to  $t = 0$ .

The final aspect of data analysis which should be addressed involves solvent oxidation. In the reaction of other hydrocarbons in toluene, the correction made to the observed rate constant used the rate constant for toluene oxidation adjusted to account for the lower toluene concentration, when necessary. In all cases, the correction due to solvent oxidation accounts for 20% or less (usually less than 10%) of the total observed rate constant. In doing this, the assumption has been made implicitly that in neat toluene, the only reaction which occurs is between permanganate and toluene. This is probably not completely correct as the toluene reaction does not have complete mass balance and there is evidence that counterion oxidation does occur. Based on the yield of products from the toluene reaction however, counterion oxidation accounts for less than 40% of the oxidative equivalents of permanganate, so the error in the corrected rate constant for any reaction would be less than 8%. This error is less than the run-to-run reproducibility, so for these purposes, it is negligible.

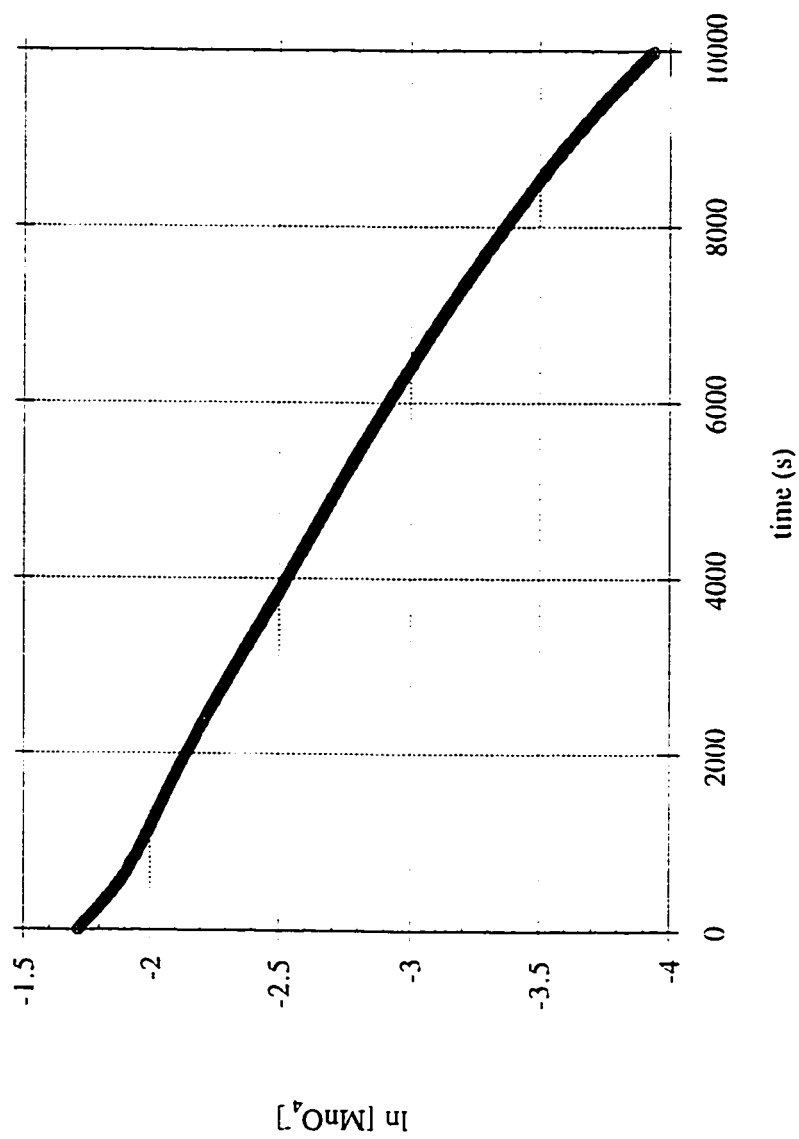


**Figure 23.** A plot of  $\ln[\text{MnO}_4^-]$  vs. time for the reaction of diphenylmethane with  ${}^n\text{Bu}_4\text{NMnO}_4$  in toluene at 35 °C.

For reactions run in *o*-dichlorobenzene, the data have been treated in an analogous fashion, although it is unclear that this is the proper way to handle this correction. *o*-Dichlorobenzene is a very polar solvent compared with toluene, probably resulting in greater ion pair separation of  ${}^n\text{Bu}_4\text{NMnO}_4$  in *o*-dichlorobenzene. When toluene, or another non-polar hydrocarbon, constitutes a high proportion of the total solution volume, ion-pairing may increase (compared to neat *o*-dichlorobenzene), causing an increase in counterion oxidation while the correction to the observed rate constant neglects this. The problems with reproducibility for reactions in *o*-dichlorobenzene however, result in a much greater error than introduced by this data analysis, therefore, since a better method is not yet apparent, this technique has been applied for all data analyses.

To illustrate the data manipulations described, a sample calculation is given for a kinetics experiment of the reaction of triphenylmethane with  ${}^n\text{Bu}_4\text{NMnO}_4$  in toluene at 25 °C. The average of the initial slopes for the first order plots (eq 21) is calculated and the standard deviation of the average determined (eq 22).

$$\text{average slope} = \bar{k}_{\text{obs}} = 5.152 \times 10^{-5} \text{ s}^{-1} \quad (21)$$

$$\sigma = 5.7 \times 10^{-7} \quad (22)$$

The error is reported as  $3\sigma$ , as a percentage of  $\bar{k}_{\text{obs}}$  (eq 23).

$$\text{error} = \frac{3(5.7 \times 10^{-7})}{5.152 \times 10^{-5}} = 3.3\% \quad (23)$$

From the Eyring plot for oxidation of neat toluene by  ${}^n\text{Bu}_4\text{NMnO}_4$ , the second order rate constant at 25 °C is predicted to be  $8.92 \times 10^{-7} \text{ M}^{-1}\text{s}^{-1}$ . The concentration of neat toluene at this temperature is 9.37 M. Relative to the toluene concentration, the triphenylmethane concentration (26.9 mM) is negligible, so the toluene concentration is assumed to be the

same as neat toluene. The pseudo-first order rate constant for toluene oxidation under these conditions,  $k_{\text{corr}}$ , is calculated in eq 24.

$$\begin{aligned}k_{\text{corr}} &= [\text{PhCH}_3] k_2 = (9.37 \text{ M})(8.92 \times 10^{-7} \text{ M}^{-1}\text{s}^{-1}) \\ &= 8.36 \times 10^{-6} \text{ s}^{-1}\end{aligned}\quad (24)$$

The observed rate constant for the oxidation of triphenylmethane is then corrected for solvent oxidation and converted to a second order rate constant by dividing by substrate concentration (eq 25).

$$\begin{aligned}k &= \frac{k_{\text{obs}} - k_{\text{corr}}}{[\text{Ph}_3\text{CH}]} \\ &= \frac{(5.152 \times 10^{-5} - 8.36 \times 10^{-6}) \text{ s}^{-1}}{26.9 \text{ mM}} \\ &= 1.61 \times 10^{-3} \text{ M}^{-1}\text{s}^{-1}\end{aligned}\quad (25)$$

The calculation of a second order rate constant is valid for all substrates studied as the corrected observed rate constants show a first order dependence on the substrate concentration as discussed in Chapters 1 and 2.

## Appendix C

### Miscellaneous Related Reactions

During the course of this work, there were a large number of experiments which were performed, but not included in the body of this dissertation. Most often, this was a result of reproducibility problems. These experiments and their results are briefly summarized here.

#### Experimental

The general experimental techniques described in Chapters 1 and 2 were also followed here. The preparation and purification of  $\text{KMnO}_4$ ,  ${}^n\text{Bu}_4\text{NMnO}_4$ , toluene, cumene, and 9,10-dihydroanthracene were described previously (Chapters 1 and 2). Fluorene was obtained from two sources (Aldrich, 98%; Fluka, 99%) and used as received since all attempted purifications resulted in increasing the concentration of the impurities. These techniques included recrystallization, sublimation, and chromatography on alumina. Acetonitrile (Baker, 100.0%) and pyridine (Aldrich, 99.99%) were dried over  $\text{CaH}_2$  and vacuum transferred prior to use.

Kinetic data was obtained by monitoring the disappearance of the  $\text{MnO}_4^-$  spectrum and the appearance of the  $\text{MnO}_2$  scattering/absorbance over the range 400 to 640 nm. Details of the data collection are given in Chapters 1 and 2 and data analysis in Appendix A. All of the rate constants reported are the average of four rate constants calculated for each kinetics experiment. The errors are  $3\sigma$  of that average, reported as a percentage of the average rate constant. The solutions for kinetic experiments were prepared in the

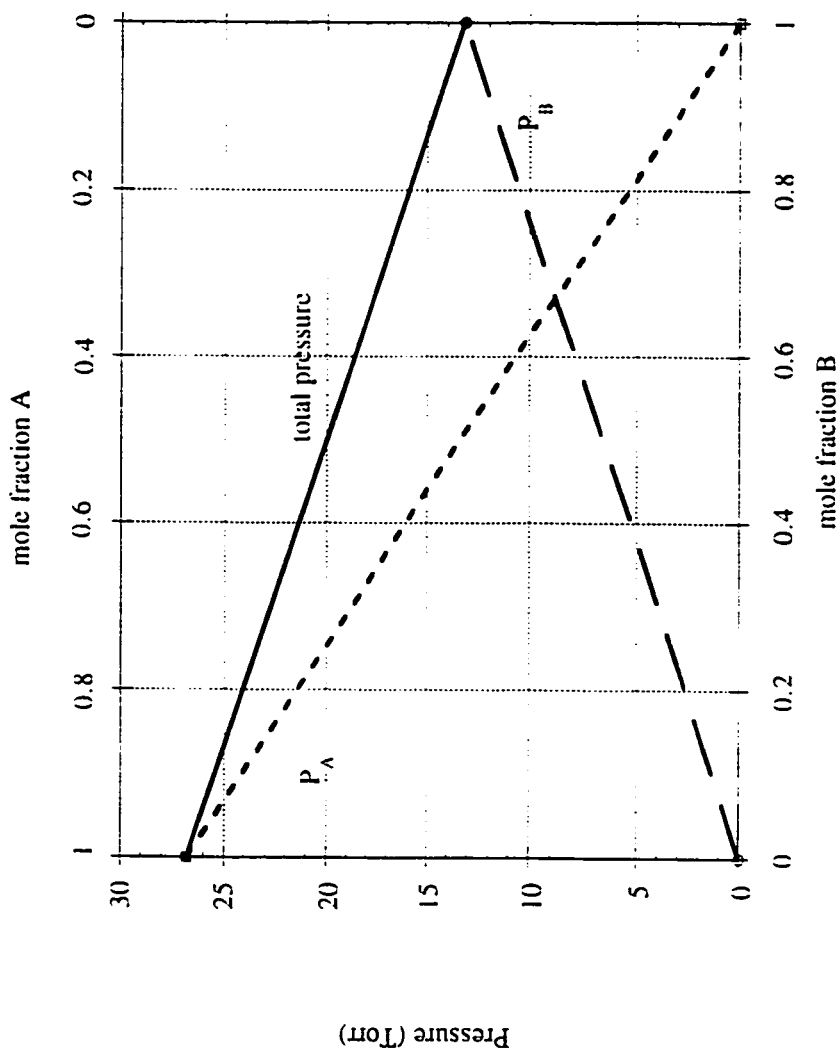


**Figure 24.** A plot of vapor pressure vs. mole fraction for an ideal solution of two volatile liquids. The solid line is the total vapor pressure, the dotted line is the vapor pressure of component A, and the dashed line is the vapor pressure of component B. 104

molecules in each of the neat solutions. A solution of toluene in water is very non-ideal as water is polar and capable of hydrogen bonding while toluene is very non-polar. The result is a strong positive deviation from Raoult's law. The toluene placed into water in a sealed container preferentially partitions itself into the vapor phase, leaving an unknown quantity of toluene actually dissolved.

The simplest solution to this problem is to eliminate the headspace of the reaction vessel, thus forcing essentially all of the toluene placed in the system into solution. The reactions were followed spectroscopically at temperatures usually above room temperature (generally 45 to 95 °C), so the reaction vessel had to be a cuvette which could be sealed and maintain the seal to reasonably high temperatures (relative to the boiling point of water). Furthermore, the cuvette had to allow the addition of the  $\text{KMnO}_4$  solution after it had been sealed and equilibrated at the desired temperature. No commercially available cell was found to meet these needs, so a new cuvette was designed and built. The cuvette portion is constructed from an ordinary glass, 10 mm pathlength, cell. To the top was fused the thread portion of a Fischer-Porter needle valve. A glass disk was fashioned between the cuvette and the glass valve with a small hole in the center. The Teflon portion of the valve was cut off and a thin channel drilled through the center. The seal between the Teflon valve and glass seat was maintained by a 8 mm red rubber septum which was Teflon coated on one side. Figure 25 is a diagram of the cuvette. The septum was found to be sufficient to seal the system. Additions to the cuvette could be made by syringe through the channel.

For a kinetics experiment, the cuvette was filled to within 0.2 mL of its total capacity, the organic substrate was added, the system sealed, and heated until the solution had equilibrated. Visually, the solution was inspected to insure that all of the organic substrate had dissolved and that there were no "bubbles" of organic. The background was

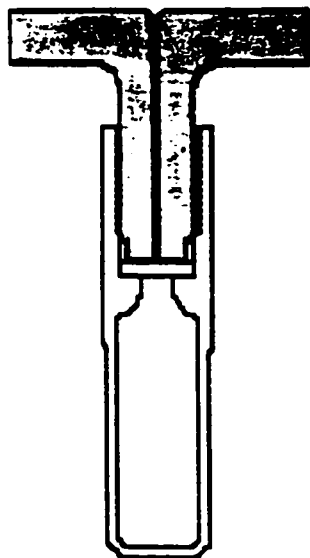


**Figure 25:** Cross-section of cuvette.

taken, then a small portion of concentrated  $\text{KMnO}_4$  solution was added by syringe. At higher temperatures (85 °C and above) if the cuvette had been weakened from stress, the cuvette occasionally burst. For this reason, the permanganate solution was always injected while the cuvette was in the cell holder. This contained the explosion and prevented injury. After each catastrophic failure, the cell was rebuilt, resulting in a slightly different total volume each time.

## Appendix B

### **Spectroscopic Cell for Studying Aqueous Solutions of Hydrocarbons**

Toluene has a slight solubility in water--approximately 5 mM at room temperature. This concentration is sufficient to study the reaction of toluene with permanganate in water under pseudo-first order conditions with an excess of toluene, following the disappearance of permanganate spectroscopically. According to Raoult's law (eq 26), in the vapor above a solution of containing two volatile species, A and B, the fraction of each should be proportional to its mole fraction in solution.

$$P_{\text{TOTAL}} = \chi_A P^{\circ}_A + \chi_B P^{\circ}_B \quad (26)$$

where  $P_{\text{TOTAL}}$  = total vapor pressure

$P^{\circ}_A$  = vapor pressure of neat A

$P^{\circ}_B$  = vapor pressure of neat B

$\chi_A$  = mole fraction of A in solution

$\chi_B$  = mole fraction of B in solution

This suggests that for a 5 mM solution of toluene in water, very little toluene should be in the vapor phase. This is depicted graphically in Figure 24 where A represents toluene and B represents water. Raoult's law however, only applies to ideal solutions where the interaction between the two components in solution is similar to the interactions between

manner described in Chapter 1 for reactions in organic solvent and in Chapter 2 for reactions in water.

## Results and Discussion

### I. Reactions of cumene and fluorene with $n\text{Bu}_4\text{NMnO}_4$ in toluene.

In Chapter 1, oxidations of arylalkanes by permanganate were studied in toluene solvent. Besides the substrates studied and reported in detail in there, there are two others with similar, known C-H bond strengths. Cumene (isopropylbenzene) has a tertiary benzylic C-H bond, leading to a very weak bond of 84.4 kcal/mol.<sup>84</sup> The bond strength of fluorene, 80 kcal/mol,<sup>71a,86</sup> is even weaker. Both seem reasonable substrates to include in a study of permanganate oxidations. Despite repeated efforts, however, studies of both substrates were plagued by reproducibility problems.

Cumene was extensively purified and stored in the dark in a glovebox. By GC, the purity was determined to be 99.96%. Kinetics experiments were performed over the temperature range 35 to 65 °C. The data are summarized in Table 7. Some reproducibility is seen if the cumene concentration is held constant (see, for example, the data at 65 °C), but changes in the cumene concentration cause unpredictable changes in the observed rate constant. For example, at 55 °C, a 33% increase in the cumene concentration produced no change in the observed rate constant, while at 45 °C, a similar increase resulted in a 42% increase in the observed rate constant. Reproducibility problems are a hallmark of radical chain reactions. While it is difficult to envision such a pathway for these reactions, one experiment was performed where cumene was passed through a column of activated alumina in the glovebox prior to use. This technique had been used successfully previously to remove radical chain initiators.<sup>5a</sup> In this case, however, treatment of the cumene with alumina had no effect on the kinetics.

**Table 7.** Rate Constants for the Reaction of Cumene with  $n\text{Bu}_4\text{NMnO}_4$  in Toluene.

$[\text{MnO}_4^-]$ (mM)	[cumene] (M)	T (°C)	$k_{\text{obs}}$ (s <sup>-1</sup> )	$k_2$ (M <sup>-1</sup> s <sup>-1</sup> ) <sup>a</sup>	data analysis error <sup>b</sup>
0.111	3.55	35.0	$8.95 \times 10^{-5}$	$2.14 \times 10^{-5}$	4.1%
0.0926	3.50	45.0	$2.29 \times 10^{-4}$	$5.40 \times 10^{-5}$	2.5%
0.0451	4.66	45.0	$3.27 \times 10^{-4}$	$6.44 \times 10^{-5}$	1.7%
0.100	3.46	55.0	$6.35 \times 10^{-4}$	$1.51 \times 10^{-4}$	2.9%
0.0875	4.61	55.0	$6.01 \times 10^{-4}$	$1.14 \times 10^{-4}$	6.0%
0.0852	4.63	65.0	$9.45 \times 10^{-4}$	$1.60 \times 10^{-4}$	1.8%
0.0954	4.63	65.0	$9.84 \times 10^{-4}$	$1.68 \times 10^{-4}$	2.8%

<sup>a</sup> Second order rate constants have been calculated and included since other substrates show a first order dependence on the substrate concentration. The data presented here do not necessarily support such a relationship. <sup>b</sup> Range of four rate constants derived from analysis of a single kinetics run (see Appendix A).

Reactions of fluorene with  ${}^n\text{Bu}_4\text{NMnO}_4$  in toluene suffered from similar problems. The reactions were analogous to those of 9,10-dihydroanthracene described in Chapter 1. There was an initial slow reaction which lasted an unpredictable length of time (from 260s to greater than 2 hours at 25 °C) followed by an almost instantaneous reaction to form an apparent charge transfer complex. The kinetic data are summarized in Table 8. Although all of the experiments were performed under nearly identical conditions (temperature and substrate concentration), the second order rate constants differ by nearly a factor of three! The only known variable in these reactions, the permanganate concentration, does not seem to correlate with the rate constants either. Table 8 additionally lists the duration of the slow reaction. This varies greatly, in one case not forming in over two hours. There is no apparent relationship between any of the reaction conditions and the timing of the occurrence of the fast reaction.

**II. Reactions in other organic solvents.** The results presented in this dissertation raise a number of intriguing questions about the role of solvation in permanganate reactions. For example, to substantiate the mechanism proposed for the oxidation of arylalkanes in Chapter 2, the observed rate constant should be shown to be dependent on the concentration of added nucleophile. Such an experiment requires a solvent which is miscible with water and less reactive with permanganate than the substrate to be studied. The literature suggests two possible solvents--acetonitrile and pyridine. Both forms of permanganate studied here-- $\text{KMnO}_4$  and  ${}^n\text{Bu}_4\text{NMnO}_4$ --are sufficiently soluble in these solvents to perform kinetics experiments.

**Acetonitrile.** Permanganate does react with acetonitrile, although slowly. At room temperature, a solution of either  ${}^n\text{Bu}_4\text{NMnO}_4$  or  $\text{KMnO}_4$  in acetonitrile decomposes completely to  $\text{MnO}_2$  over several days, comparable to the reactivity of  ${}^n\text{Bu}_4\text{NMnO}_4$  with

**Table 8.** Rate Constants for the Reaction of Fluorene with  ${}^n\text{Bu}_4\text{NMnO}_4$  in Toluene.

[MnO <sub>4</sub> <sup>-</sup> ] (mM)	[fluorene] (mM)	T (°C)	k <sub>2</sub> (M <sup>-1</sup> s <sup>-1</sup> ) <sup>a</sup>	data analysis error <sup>b</sup>	breakpoint (s) <sup>c</sup>
0.214	1.07	25.0	0.141	4.1%	435
0.165	1.07	25.0	0.0779	6.0%	1005
0.0960	1.07	25.0	0.0786	7.3%	2300
0.0876	1.07	25.0	0.0753	3.7%	1350
0.0757	1.04	25.0	0.171	4.2%	1800
0.0652	1.07	25.0	0.154	10%	550
0.143	1.11	25.0	0.125	14%	270
0.154	1.11	25.0	0.140	7.2%	1230
0.173	1.11	25.0	0.113	12%	260
0.191	1.11	25.0	0.0746	2.3%	1640
0.146	1.09	25.0	0.0608	2.3%	— <sup>d</sup>

<sup>a</sup> Second order rate constants are reported so that a comparison can be made to other substrates. The substrate concentration was not varied in these experiments, so it is unclear whether this is valid. <sup>b</sup> Range of four rate constants derived from analysis of a single kinetics run (see Appendix A). <sup>c</sup> The breakpoint in the reaction is defined as the point at which the fast reaction takes place. <sup>d</sup> A fast reaction never occurred in this experiment, over the time span of 7200s. This may have been caused by contamination of the glovebox atmosphere by O<sub>2</sub>.

neat toluene. This makes acetonitrile a suitable solvent only for substrates that are much more reactive than toluene.

The first reaction examined was of  ${}^n\text{Bu}_4\text{NMnO}_4$  with 9,10-dihydroanthracene. In Chapter 1, this experiment was discussed briefly. The reaction proceeds in a similar fashion to the analogous reaction in toluene with two notable exceptions. First, the charge transfer complex which forms has maxima at 530 and 494 nm. This is a shift of approximately 30 nm to shorter wavelength relative to the complex in toluene, probably as a result of the difference in solvent, as discussed in Chapter 1. The second feature of this reaction which differs from the reaction in toluene is the concurrent disappearance of  $\text{MnO}_4^-$  and formation of the charge transfer complex. In toluene, the charge transfer complex did not form until all of the  $\text{MnO}_4^-$  had been depleted. The lack of isosbestic points suggests that  $\text{MnO}_2$  or another absorbing species may also be present in solution when the reaction is run in acetonitrile. The complexity of the spectra render the data useless in terms of determining rate constants. As a result, no further experiments were performed under these conditions.

The second group of reactions examined were of  $\text{KMnO}_4$  with dihydroanthracene in acetonitrile. Over the range of temperatures studied (10 to 35 °C), the rate constant for solvent oxidation is less than 5% of the observed rate constant, so solvent oxidation was considered negligible. The data from the kinetic experiments is compiled in Table 9. As the observed rate constants demonstrate, there are serious problems with these results. The data show no apparent dependence on temperature over this temperature range and the observed rate constants do not show a dependence on substrate concentration. Although these experiments failed to yield any useful kinetic data, they do provide an interesting result. During the entire course of the reaction, there is no evidence of charge transfer complex formation. The only difference between this reaction and the previous one is the

**Table 9.** Rate Constants for the Reaction of 9,10-Dihydroanthracene with  $\text{KMnO}_4$  in Acetonitrile.

$[\text{MnO}_4^-]$ (mM)	$[\text{DHA}]^a$ (mM)	T (°C)	$k_{\text{obs}}$ ( $\text{s}^{-1}$ )	$k_2$ ( $\text{M}^{-1}\text{s}^{-1}$ ) <sup>b</sup>	data analysis error <sup>c</sup>
0.194	2.81	10.0	$1.26 \times 10^{-3}$	0.449	8.2%
0.273	2.95	10.0	$3.98 \times 10^{-4}$	0.135	5.8%
0.447	2.79	15.0	$1.01 \times 10^{-3}$	0.361	15%
0.353	2.76	20.0	$1.64 \times 10^{-3}$	0.596	20%
0.408	2.74	25.0	$7.83 \times 10^{-4}$	0.286	21%
0.0891	1.41	25.0	$8.96 \times 10^{-4}$	0.635	10%
0.394	2.88	25.0	$1.00 \times 10^{-3}$	0.348	7.6%
0.0861	1.48	25.0	$7.83 \times 10^{-4}$	0.529	2.0%
0.122	1.83	35.0	$2.26 \times 10^{-3}$	1.23	11%

<sup>a</sup> DHA is used as the abbreviation for 9,10-dihydroanthracene. <sup>b</sup> Second order rate constants are calculated on the basis of the results of the reaction of  ${}^n\text{Bu}_4\text{NMnO}_4$  with 9,10-dihydroanthracene in toluene. The data presented here do not necessarily support a first order dependence of the observed rate constant on the substrate concentration, but the second order rate constants are presented nonetheless for comparison purposes. <sup>c</sup> Range of four rate constants derived from analysis of a single kinetics run (see Appendix A).

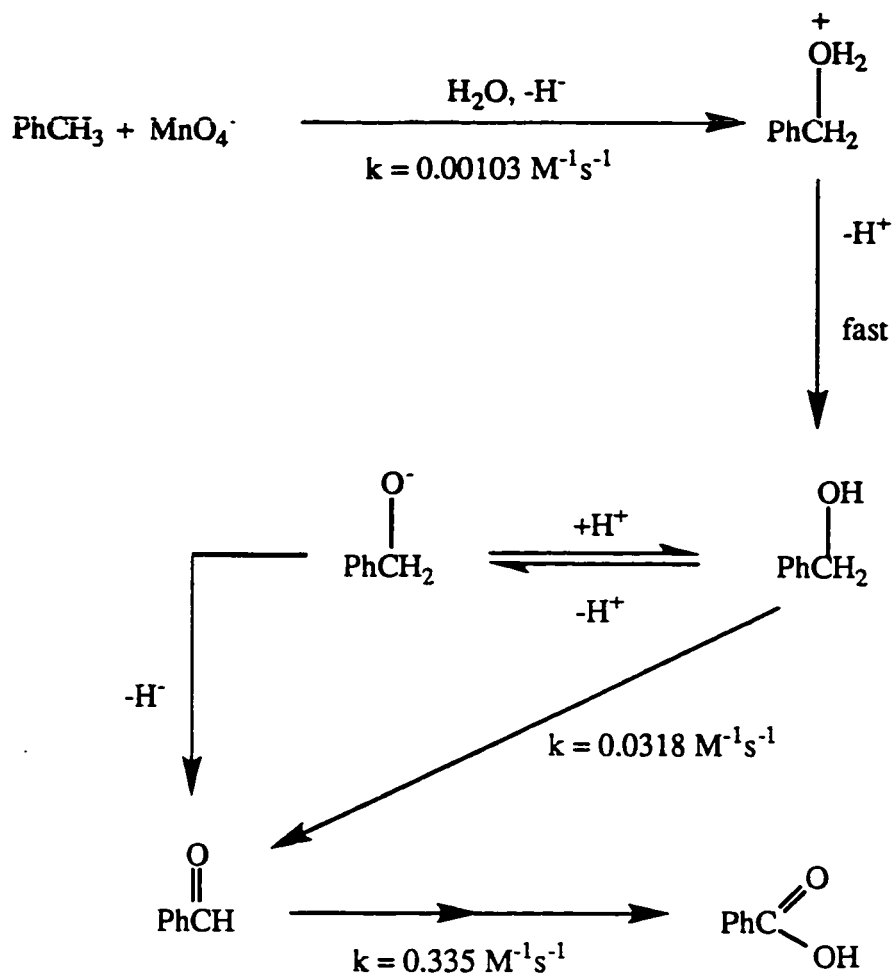
counterion for permanganate. This seems to suggest that the counterion,  ${}^n\text{Bu}_4\text{N}^+$ , is a necessary component in the charge transfer complex. Such a possibility is in agreement with the hypothesis that the surface of the colloid is involved in charge transfer complex formation. The colloid surface can be negatively charged, so a close association of the cation is reasonable.

**Pyridine.**  ${}^n\text{Bu}_4\text{NMnO}_4$  is reportedly stable in pyridine at room temperature for days, suggesting that pyridine is resistant to oxidation by permanganate.<sup>17</sup> In order to study the oxidation of toluene in pyridine, however, this reaction must be slower than the reaction with toluene. To avoid the counterion oxidation which is believed to occur with  ${}^n\text{Bu}_4\text{NMnO}_4$ ,  $\text{KMnO}_4$  was used as the permanganate source.  $\text{KMnO}_4$  has a slight solubility in pyridine, enough to permit a spectroscopic study. The reaction of  $\text{KMnO}_4$  with pyridine was examined at 55 °C. The observed rate constant was calculated to be  $6.76 \times 10^{-4} \text{ s}^{-1}$ , which is approximately three times larger than the observed rate constant for the reaction of permanganate with toluene in organic solvent at 55 °C. Thus, while pyridine might be a suitable solvent for more reactive hydrocarbons, its oxidation by permanganate is too fast to be used as a solvent for studies of toluene oxidation.

**III. Reactions of Possible Intermediates.** For the reactions in aqueous and organic solution, a number of species were considered reasonable reaction intermediates. For example, benzaldehyde and/or benzyl alcohol are possible intermediates in the oxidation of toluene by permanganate. In an attempt to evaluate their competence as intermediates, several kinetics experiments were performed on species related to the substrates studied in order to measure the rate constants for their oxidation under similar reaction conditions. The goal was to use these numbers in computer simulations of the kinetics, however, it was subsequently found that kinetic modelling was not useful, as discussed in Appendix A. The results of these experiments, nonetheless, may eventually prove useful.

In Chapter 2, the rate determining step in the oxidation of toluene by permanganate in aqueous solution was hydride transfer from the benzylic carbon to an oxo of permanganate with stabilization of the incipient carbocation with solvent. If this mechanism is correct, deprotonation seems the inevitable fate of the carbocation formed. Benzyl alcohol is the product from deprotonation, making it a likely intermediate in the reaction if the mechanism has been correctly assigned. Benzaldehyde is also a likely intermediate in the oxidation of toluene to benzoic acid, since some was found in solution at the end of the reaction. The rate of benzyl alcohol and benzaldehyde oxidation by permanganate was measured under the same conditions as toluene oxidation to test their competence as intermediates (Table 10). At 25 °C, benzyl alcohol reacts approximately thirty times faster than toluene and benzaldehyde reacts an order of magnitude faster than that (in agreement with previous work<sup>21</sup>).

If the mechanism for the rate determining step proposed in Chapter 2 for the oxidation of toluene is taken to be correct, an assessment can be made of the validity of benzyl alcohol and benzaldehyde as intermediates in the reaction. Assuming that toluene is converted sequentially to benzyl alcohol, benzaldehyde, and benzoic acid (Scheme 4, the mechanism shown for the oxidation of benzyl alcohol by permanganate is based on previous studies of similar species<sup>7d,11</sup>), and applying the steady state approximation, the expected concentrations can be calculated.



**Scheme 4.** Proposed mechanistic pathway for the reaction of toluene with  $\text{MnO}_4^-$ , proceeding through the intermediates benzyl alcohol and benzaldehyde.

The steady state concentration of benzyl alcohol is estimated to be 0.1 mM (at 25 °C, [toluene] = 4 mM). The HPLC, which operates with a UV detector, is very insensitive to benzyl alcohol, with a detection limit of 0.25 mM. Under these conditions then, even the maximum expected yield would go undetected. Additionally, the predicted steady state concentration of benzyl alcohol is very large relative to the permanganate concentration, typically 0.4 to 0.6 mM, suggesting that the steady state concentration of benzyl alcohol

may never be reached. To explore the potential effect this situation would have on first order kinetic plots, the kinetics were simulated using the program KINSIM and the rate constants given in Scheme 3. The data from the program show that the steady state is never reached, leading to a slight downward curvature, at least initially, in the first order plots ( $\ln [\text{MnO}_4^-]$  vs. time). The analysis of the kinetics data for these reactions, however, leads to some uncertainty in the curvature or linearity of the first order plots, as discussed in Appendix A. The curvature expected in reaching steady state may in fact be present, but masked by the data analysis. Benzaldehyde is the only detected potential intermediate in this system. Assuming that the reaction of toluene proceeds through benzyl alcohol and benzaldehyde as given in Scheme 3, the steady state concentration of benzaldehyde is estimated to be 0.01 mM (at 25 °C, [toluene] = 4 mM). The observed concentration is less, but of the same magnitude, confirming that benzaldehyde is a competent intermediate in the reaction of toluene to permanganate.

The mechanism of the reaction of ethylbenzene with permanganate in aqueous solution is not clear at this time. However, for the oxidation of ethylbenzene, *sec*-phenethylalcohol was examined under these conditions as a possible intermediate. Two experiments were performed, at 25 °C and 55 °C. The data are given in Table 10. An approximation can then be made of the activation parameters for the reaction-- $\Delta H^\ddagger \sim 10$  kcal/mol and  $\Delta S^\ddagger \sim -30$  e.u. These values are similar to those for ethylbenzene under the same conditions and the rate constants are within an order of magnitude, as reported in Chapter 2.

In neat toluene, the oxidation of benzyl alcohol and benzaldehyde at 25 °C were studied. Rate constants for both are summarized in Table 10. Benzyl alcohol reacted very quickly, so the rate constant given is only an estimate. The first order plots were strongly

**Table 10.** Rate Constants for Reactions with  $\text{MnO}_4^-$  of Species Related to Substrates Studied.

$[\text{MnO}_4^-]$ (mM)	[substrate] (mM)	T (°C)	$k_2$ ( $\text{M}^{-1}\text{s}^{-1}$ )	reaction conditions
<i>sec-Phenethylalcohol</i>				
0.231	2.24	25.0	0.0213	aq. solution, pH 7, $\text{KMnO}_4$
0.309	2.23	55.0	0.112	aq. solution, pH 7, $\text{KMnO}_4$
<i>Benzyl alcohol</i>				
0.381	4.39	25.0	0.0318	aq. solution, pH 7, $\text{KMnO}_4$
0.269	1.61	25.0	0.9 <sup>a</sup>	toluene, ${}^n\text{Bu}_4\text{NMnO}_4$
<i>Benzaldehyde</i>				
0.381	4.47	25.0	0.335	aq. solution, pH 7, $\text{KMnO}_4$
0.295	1.64	25.0	0.200	toluene, ${}^n\text{Bu}_4\text{NMnO}_4$

<sup>a</sup> This value is estimated. See the text for details.

curved downward, a trend also reflected in the spectroscopic data, indicating that the reaction accelerated as it progressed. Benzaldehyde was oxidized much more slowly and the first order plots were well-behaved. The second order rate constant,  $0.200 \text{ M}^{-1}\text{s}^{-1}$ , is very similar to the second order rate constant for oxidation of benzaldehyde in neutral aqueous solution based on the work described above and previous reports.<sup>21</sup> This may possibly suggest a similar mechanism for the reaction under these extremely different conditions, although further experiments would be necessary.

## VITA

Kimberly Annette Lott was born on the 9<sup>th</sup> of July, 1967 in Moscow, Idaho. She was raised in Maryville, Missouri, graduating from Maryville R-II High School in May of 1985. In the fall of that year, she entered the University of Idaho in Moscow, where she graduated with a B.S. degree in chemistry in May of 1989. She continued her education at the University of Idaho and, under the guidance of Professor Thomas E. Bitterwolf, finished a M.S. degree in Inorganic Chemistry in December of 1990. In April of the following year, she began graduate studies at the University of Washington in Seattle, working with the supervision of Professor James M. Mayer. In July of 1991, she married Jeff Gardner, becoming Kimberly Annette Gardner. She completed a Ph.D. in Inorganic Chemistry in June of 1996.